



**Universiteit  
Leiden**  
The Netherlands

## **Mechanisms of mtDNA segregation and mitochondrial signalling in cells with the pathogenic A3243G mutation**

Jahangir Tafrechi, R.S.

### **Citation**

Jahangir Tafrechi, R. S. (2008, June 5). *Mechanisms of mtDNA segregation and mitochondrial signalling in cells with the pathogenic A3243G mutation*. Retrieved from <https://hdl.handle.net/1887/12961>

Version: Corrected Publisher's Version

License: [Licence agreement concerning inclusion of doctoral thesis in the Institutional Repository of the University of Leiden](#)

Downloaded from: <https://hdl.handle.net/1887/12961>

**Note:** To cite this publication please use the final published version (if applicable).

**MECHANISMS OF mtDNA SEGREGATION AND MITOCHONDRIAL  
SIGNALING IN CELLS WITH THE PATHOGENIC A3243G MUTATION**

Proefschrift

ter verkrijging van  
de graad van Doctor aan de Universiteit van Leiden,  
op gezag van de Rector Magnificus Prof. Mr. P. F. van der Heijden,  
volgens besluit van het College der Promoties  
te verdedigen op 5 juni 2008  
klokke 15:00 uur

door

**Roshan Sakineh Jahangir Tafrechi**

geboren te Heemstede

in 1974

## Promotiecommissie

Promotores	Prof. Dr. A. K. Raap Prof. Dr. J. A. Maassen
Co-Promotor	Dr. G. M. C. Janssen
Referent	Dr. H. J. M. Smeets (Universiteit van Maastricht)
Overige leden	Prof. Dr. P. de Knijff Prof. Dr. L. H. F. Mullenders

The cover shows electron microscopic images of mitochondria in the cells used in this thesis. Wild type cells show mitochondria with linear cristae and mutant cells show mitochondria with aberrant circular and concentric ring patterns. The images were taken by courtesy of the Section Electron Microscopy.

<b>Contents</b>	<b>Page</b>
Chapter 1: General introduction	5
Chapter 2: Single cell A3243G mitochondrial DNA mutation load assays for mtDNA segregation analyses	19
Chapter 3: Suppressed and quantal mtDNA segregation in heteroplasmic cell cultures	33
Chapter 4: Distinct nuclear gene expression profiles in cells with mtDNA depletion and homoplasmic A3243G mutation	47
Chapter 5: Effects of mtDNA variants on the nuclear transcription profile and the cytosolic protein synthesis machinery	61
Chapter 6: General discussion	77
Summary	87
Samenvatting	91
Samenvatting voor de leek	95
Curriculum Vitae with list of publication	97

---



# 1

General introduction



## Introduction

Cells consume energy for basic household tasks and specialized functions. Biosynthesis of proteins and nucleic acids, transport of ions across membranes for electric activity, intracellular transport of proteins, RNAs and organelles, locomotive and contractile processes are prominent examples of energy consuming events. Also in the cybernetics of a cell, that is, the control of gene expression and signaling, a small but significant amount of energy is continuously invested.

Carbohydrates and lipids are the main chemical sources of cellular energy. Amino acids in protein may also be used as energy source. Nutrient molecules are taken up by the cell from the environment through dedicated transport systems. Once in the cell they serve in anabolic processes as building blocks for macromolecular constituents or as precursors of intermediate metabolites. The majority of the energy content of especially fatty acids and glucose is, however, transformed in catabolic pathways to a high-energy compound called adenosine 5'-triphosphate, abbreviated as ATP. ATP may be considered as the universal energy currency of cells: virtually all energy demanding processes use ATP directly or indirectly as an energy source by hydrolyzing it to ADP and inorganic phosphate.

Oxidative phosphorylation, often abbreviated as OXPHOS, is the catabolic pathway responsible for most ATP production. Glycolysis also produces ATP but its ATP yield is only about 1/18th of oxidative phosphorylation.

OXPHOS uses energy contained in reduced cofactors called NADH and FADH<sub>2</sub> to convert ADP to ATP and in the process reduces dioxygen (O<sub>2</sub>) to water. Most of the NADH and FADH<sub>2</sub> is produced in the tricarboxylic acid cycle (also called TCA-, Krebs or Citric Acid cycle) and fatty acid  $\beta$ -oxidation. The doorway to the TCA cycle for all fuel-molecules: sugars, fat and proteins, is acetyl coenzyme A and both the TCA cycle and fatty acid  $\beta$ -oxidation and OXPHOS itself take place in the mitochondria.

Evidently, mitochondria take a central position in energy metabolism and often they

are referred to as the powerhouse of the cell (1). Obviously, failure of the powerhouse is detrimental to the cell. It inevitably leads to loss of cell function and death.

This truism is rightfully used to explain late cellular events in diseases with a mitochondrial etiology. Also in physiological aging, failure of the cell's powerhouse is alleged as etiological. The truism, however, gives no insight in the molecular processes that initiate and amplify mitochondrial dysfunction, nor does it pinpoint leads for therapeutic intervention.

Mitochondria are involved in multiple other processes besides energy production, such as apoptosis through an intricate regulation of cytochrome c release by pro- and anti-apoptotic factors, the regulation of cytosolic calcium concentrations, metabolism of fatty acids and some amino acids, iron homeostasis and cholesterol/steroid biosynthesis (2). The undermining of the various processes involving mitochondrial functions may lead to disease.

In contrast to the other cytoplasmic organelles, mitochondria contain their own DNA in multiple copies. This mitochondrial DNA (mtDNA) is essential for OXPHOS function and mutations in mtDNA can lead to disease. Diseases with mtDNA mutation in their etiology are remarkable in that they display a high phenotypical diversity. This is counter intuitive when realizing that all pathogenic mtDNA mutations lead to respiratory defects at some point, it might therefore be expected that their phenotypical presentation would be similar. A point in case is made by the A3243G mtDNA mutation. This is a mutation in the mitochondrial tRNA<sup>(UUR)</sup>-leucine gene (*MTTL- $\lambda$* ) that is associated with syndromic and non-syndromic phenotypes with as many as 61 clinical manifestations documented (3).

To explain the wide spectrum of clinical expression, mtDNA mutation accumulation by segregation as well as dominant-negative effects of aberrant mtDNA products on the mitochondrial-nuclear crosstalk have been proposed, but the mechanisms remain essentially undisclosed.



This thesis attempts to contribute to disclosing such mechanisms by investigating segregation mechanisms and identifying nuclear genes that alter expression under A3243G mutational mitochondrial dysfunction. Starting off with a brief view on origin of mitochondria, a number of aspects of mitochondrial genetics, disease and cell biology of relevance for the experimental chapters of this thesis are briefly highlighted in the next paragraphs.

## Origin of mitochondria

It is a well accepted evolutionary view that mitochondria result from a prokaryotic symbiosis of a fermenting cell producing ATP only by substrate level phosphorylation as in glycolysis and a cell capable of much more efficient ATP production by coupling respiration to ADP phosphorylation. The former is envisioned to have engulfed the latter by an endocytotic process. The double membrane appearance of mitochondria upon electron microscopical examination, presence of DNA, sensitivity of mitochondrial protein synthesis to prokaryotic translation inhibitors, similarities of the mitochondrial inner membrane lipid composition and bacterial membranes are among the popular arguments for the endosymbiotic view (4), which is confirmed by modern comparative genomics (5;6). Comparative mtDNA genomics across eukaryotes presents the view of mtDNA being structurally very diverse, but well-conserved and limited in genetic function. It contributes invariably to mitochondrial protein synthesis and oxidative phosphorylation and occasionally to transcription and protein import (7).

The origin and evolution of the mitochondrial protein content is under active study. The proteome of the ancestral endosymbiont appears to have undergone major changes in protein content by extensive losses and gains as assessed by comparative, mass-spectrometry based proteomics (8). It is remarkable that in the evolutionary process of shaping eukaryotic mitochondria a tiny fraction of the ancestral genome with very limited and universally conserved functions resisted elimination.

## Mitochondrial DNA

The double stranded, circular mitochondrial human mtDNA of 16.569 basepair is densely packed with genetic information (figure 1) and occurs in 100s to 1000s of copies per cell. The only non-coding part of ~ 1 kb (the D-loop) is highly polymorphic and the target of demographic and forensic mtDNA studies. mtDNA encodes 13 proteins of the ~90 that make up the 5 protein Complexes of the oxidative phosphorylation system (figure 2).

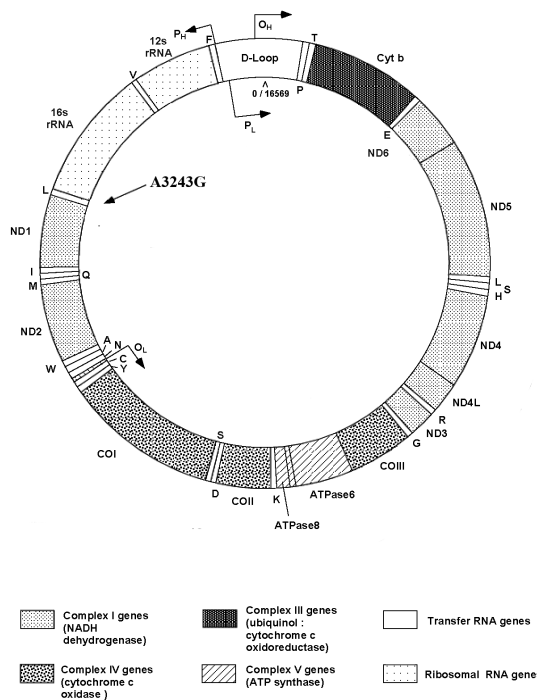


Figure 1: Mitochondrial DNA. The mitochondrial DNA is a circular, double stranded molecule of 16,569 basepairs, most of which are coding. Next to the 13 OXPHOS protein genes it contains the sequences for 2 rRNAs and 22 tRNAs as indicated. The A3243G mutation is located in the tRNA leucine (UUR) gene, note that there is a second tRNA leucine gene present (CUN). The D-loop is the only non-coding part of the mtDNA, which is highly variable and contains the center of origin for replication of the heavy chain ( $O_H$ ) and the transcription start sites of both the heavy and light chain ( $P_H$  and  $P_L$ ).

Noteworthy, only Complex II is fully encoded by the nuclear genome. mtDNA also codes 22 tRNAs and 2 rRNAs which function in translation of the mtDNA encoded proteins. All other OXPHOS proteins and factors needed for mitochondrial protein synthesis are nuclear encoded and imported from the cytoplasm. The same holds true for factors involved in mtDNA replication and transcription. It is beyond the scope of this thesis to review mtDNA transcription (9), translation (10), repair (11) and replication (12). However it is of importance to note that mtDNA replication is relaxed, that is, it occurs independent of the nuclear DNA synthesis phase and that it is in constant turnover (13). In post-mitotic cells also extensive mtDNA turnover occurs and based on available half life data of 2 – 10 days (14;15), it can be calculated that in a lifetime of a neuron or cardiomyocyte its mtDNA content is refreshed approximately 1500 to 15.000 times.

Due to inefficient mtDNA repair mechanisms (11) and a mutagenic oxidative environment constituted by the nearby location of the respiratory chain, mtDNA experiences high mutation rates. mtDNA mutation rates are on average 5-10 times higher compared to nuclear DNA, but hotspots exist. Today there are hundreds of point mutations, deletions and rearrangements in mtDNA known, many of them associated with disease (see [www.mitomap.org](http://www.mitomap.org)).

As said a cell may contain hundreds to thousands copies of mtDNA and a sequence variant (or mutant form) can therefore co-exist with the original sequence. The occurrence of both wild type and mutant mtDNA in one cell is called heteroplasmy as opposed to homoplasmy. The (pathogenic) mutation load can reach percentages up to 80 percent or more without any perceptible malfunction of the cell (16;17), although the actual threshold varies per cell type and mutation. Thus wild type mtDNAs can compensate mutants to a large extent. The importance of understanding mechanisms that lead to mtDNA mutation accumulation resulting in failure of oxidative phosphorylation will be evident.

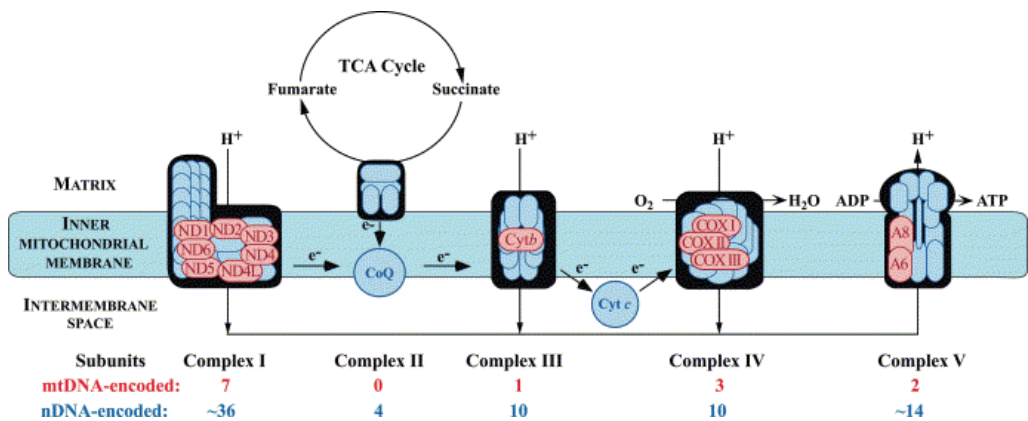


Figure 2: Scheme of oxidative phosphorylation

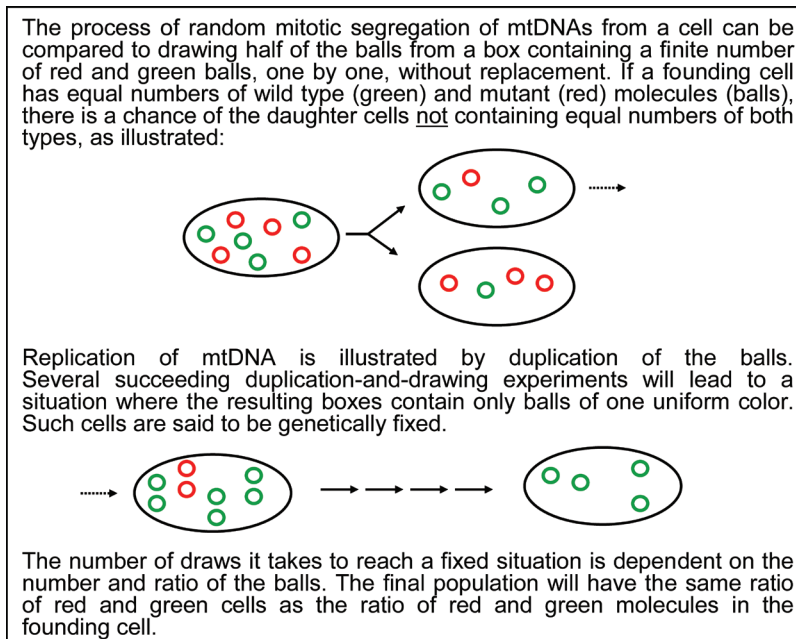
Oxidative phosphorylation can be divided in two parts, electron transport through the respiratory chain and parallel proton pumping, and the formation of a high-energy bond by phosphorylation of ADP to ATP employing the energy contained in the electrochemical proton gradient. The respiratory chain consists of 4 complexes which contain multiple subunits, most of which are nuclear encoded. Note that complex II does not contain any mitochondrial DNA encoded subunits. The mitochondrial encoded proteins are indicated in the figure as is the flow of electrons and hydrogen ions through the different complexes. The generation of ATP takes place in complex V.

## Maternal inheritance and random segregation in germ line and soma

Sperm mtDNA is rapidly eliminated after fertilization (19). Consequently, mtDNA inheritance is indeed maternal in virtually all conceptions (20). Because of the absence of a paternal partner recombination of mtDNA does not occur in the germ line. When a female transmits two mtDNA variants to the zygote, the cells descending from the heteroplasmic primordial germ cell that differentiate to primary oocytes undergo random segregation of the maternal mtDNA alleles. Along with a reduction in mtDNA copy number this is assumed to lead to a large increase in the variance of heteroplasmy in the mature oocytes and consequently offspring (21). This mtDNA genetic bottleneck elegantly explains why in the mammalian population homoplasmy is the norm and heteroplasmy rare. It leads to fixation of either of the mtDNA alleles in only a few or even one organismal generation, contributing to characteristic demographic distribution of mtDNA haplogroups and exposing new non-neutral sequence variants homogenously to evolutionary forces (22).

Non-neutral mtDNA mutations are under positive or negative selection. Positive selection may contribute to climatic adaptation. Conversely, negative selection eliminates deleterious mutations from the population. It is thus random mitotic mtDNA segregation (see box) and negative selection that is assumed to purge deleterious mtDNA, with rate of random segregation (and purging) being primarily determined by mtDNA copy number in the female germ line. Recently it has become clear however, that in the germ line of mice mtDNA segregation may not go hand in hand with strong copy number reduction (23). Thus, other mechanisms than random mtDNA segregation may underlie rapid generational mtDNA variant changes.

Also in the soma, random (mitotic) segregation is thought to be the norm. However, a multitude of clinical investigation and heteroplasmy mouse model studies with naturally occurring neutral mtDNA mutations, unambiguously show that there are notable exceptions to the presumed rule of random segregation in somatic cells (24;25).



Box: Illustration of random segregation; the hypergeometric distribution

### mtDNA is organized in nucleoids

In recent years it has become evident that mtDNA does not occur in mitochondria as naked molecules (26). Several mtDNA molecules form a complex with a set of proteins, of which mitochondrial transcription factor A (TFAM) is the most abundant and, next to its role as a transcription factor, seems to function in a similar way as the histones do for nuclear DNA in that it packages mtDNA (27). Other proteins in the mtDNA-protein complexes known as nucleoids are identified and include mitochondrial single-stranded DNA-binding protein (mtSSB), polymerase  $\gamma$  and the DNA helicase Twinkle (28). The number of mtDNA molecules and the actual shape and molecular composition of the nucleoids remain uncertain. Two publications give an indication for the number of mtDNAs per nucleoid: it should be around 2 to 10 in human cells (29;30).

At the next higher level of mtDNA genome organization may reside the mitochondrial compartment. Its morphological appearance as many fragmented mitochondria, as a single tubular reticulum or intermediates, is highly dynamic and dictated by the balance of the activities of nuclear encoded mitochondrial fusion and fission genes (see page 14).

In conclusion, it is not a collection of freely diffusing single mtDNA molecules that constitute the mtDNA segregation unit. Rather, there appear two levels of organizational complexity of mtDNA genome segregation, the nucleoid and the dynamic mitochondrial compartment.

### mtDNA and disease

Mitochondrial diseases afflict ~1 in 5000 of the human population (31), part of which are caused by inherited mitochondrial DNA mutations. In addition, healthy individuals acquire mtDNA mutations during life, contributing to such common ageing phenomena as muscle weakness and neuro-degeneration.

Since all pathogenic mtDNA mutations lead to respiratory defects at some point, it might be expected that their phenotypical representation would be similar. On the contrary, however,

there is great clinical variance among mtDNA diseases, with many characterized by tissue-specific defects (32). An important feature of mitochondrial DNA disease is the threshold effect: a biochemical defect e.g. as measured by oxygen consumption becomes overt only after the percentage of mutation exceeds a given threshold. Typically, the consumption of oxygen, which is an indication for the amount of ATP produced by the mitochondria, decreases tenfold if the cells carry over approximately 80 percent mutated mtDNA (16), though actual thresholds may vary.

Understanding the molecular mechanisms which control the level of mutant mtDNA and the ensuing pathobiochemistry obviously is an important aspect to understanding mitochondrial and ageing diseases, as far as mtDNA is involved in the latter. Spreading and accumulation of mtDNA mutations by segregation in cells and tissues may underlie mtDNA disease variability, but mechanisms are elusive.

Segregation leading to mutation accumulation above threshold and loss of OXPHOS may as such be able to explain mtDNA diseases with a heteroplasmy degree exceeding the 80-90% threshold, as for instance in patients with the phenotype of mitochondrial myopathy, encephalopathy, lactic acidosis, and stroke-like episodes (MELAS; OMIM 540000) in which the A3243G mutation studied in this thesis was first discovered (33;34). Segregation however fails to explain pathogenesis of the maternally inherited diabetes and deafness phenotype of the A3243G mutation (MIDD; OMIM 520000). MIDD is a type of diabetes (contributing ~5%) which resembles mostly type II diabetes without the obese appearance. It is a maternally transmitted disease with an average age-of-onset of 38 years and the glucose intolerance is caused by impaired insulin secretion of the pancreas, but the relevant tissue, pancreatic  $\beta$ -cells, contains only moderate levels of mutation load (35), far from the ~80 % threshold levels required for mitochondrial OXPHOS dysfunction. A dominant negative gain-of-function would explain the lack of threshold

effect seen in this case. The tRNA<sup>(UUR)</sup>-leucine mutation could lead to dominantly acting, qualitative translation defects like amino acid mis-incorporation or premature translation termination products directing synthesis of a set of aberrant translation products (36). Such dominant acting factors could by e.g. reprogramming the nuclear transcriptional program, lead to  $\beta$ -cell dysfunction.

### **mtDNA and aging**

The phenotypes of mitochondrial DNA diseases often resemble diseases of the elderly (deafness, muscle weakness, diabetes, neurodegeneration, cardiomyopathy), implying mtDNA mutation in aging. For many decades the vicious circle theory of somatic accumulation of mtDNAs has dominated the mtDNA aging literature. It states that a first somatically acquired mtDNA mutation ignites a self-amplifying process of mitochondrial ROS generation, oxidative mtDNA mutation and deleterious oxidative protein modification. It predicts that in a single cell, random mtDNA mutations will accumulate exponentially with age. Formally never proven and lingering in scientific literature, recent experimental evidence now strongly defy this view.

First, single cell analyses of mitotic and post-mitotic tissues of healthy, aged individuals show that in individual (Cytochrome c oxidase negative) cells of a given tissue (brain (37;38), muscle (39), colon mucosa (40), kidney (41), cardiomyocytes (42), accumulation of unique, not random, mtDNA mutations occurs. Second, model system studies with the mtDNA mutator mice (mice with proofreading-deficient polymerase  $\gamma$ ), which dramatically and prematurely replicates physiological aging, do not show exponential mtDNA accumulation (43;44). They do show increased apoptosis (45), in line with notion of reduction of organ function with aging. What transpires is that clonal accumulation of unique mtDNA mutations acquired early in development through mtDNA replication errors or mitochondrial ROS, appears to be a significant contributor to physiological aging.

### **Morphological dynamics of mitochondria**

By light microscopy mitochondria can be observed in unstained living cells as filamentous or grain like structures. These appearances underlie their etymology. The word mitochondrion is derived from the Greek words for thread (mito) and grain (chondro). Major developments in fluorescence microscopy and in vivo staining nowadays enables a much more detailed view on organelle dynamics and motility of molecular constituents. Particularly the use of lipophilic, cationic fluorescent dyes (which accumulate in well functioning mitochondria due to the electrochemical proton gradient) and expression of mitochondrially targeted auto-fluorescent proteins in combination with sophisticated fluorescence microscopy techniques, led to the contemporary view that the mitochondrial compartment is dynamic, not only in terms of shape, size, motion and number of mitochondria, but also in terms of fusion and fission and mobility of intra-mitochondrial molecules. It is overtly clear now that the balance between the activity of fusion and fission proteins determines the actual morphology of the mitochondrial compartment. Depending on cell type and stage, many distinct, individual mitochondria, a single continuous mitochondrion of filamentous shape and any intermediate state can thus be found (46). The mitochondrial GTPases Mitofusin 1 and 2 and Opa1 are now well established as mediators of mitochondrial fusion (47). Mitochondrial fission is mediated by Drp1, another mitochondrial GTPase of the dynamin family

Microscopic Fluorescence Recovery After Photobleaching (FRAP) experiments permit to analyze diffusion parameters of macromolecules in living cells. Such experiments with mitochondrially targeted auto-fluorescent proteins showed their extensive intra-mitochondrial diffusion (48).

It follows naturally from the above that cells have the potential to homogenize their mitochondrial compartments among which is mtDNA.



Indeed, cells deprived of mitochondrial fusion genes do not mix their reporter contents as shown by elegant cell fusion experiments with *mfn*<sup>-/-</sup> and *mfn*<sup>+/+</sup> embryonic mouse cells differentially labeled with permanent mitochondrial markers (49). By sampling synchronized cells in time, the morphology of mitochondria has been found to oscillate between the reticular and fragmented state in a cell cycle dependent manner (50). Mitochondria of cells in mid-interphase appear as a tubular network (figure 3), whereas shortly before, during and after mitosis the mitochondrial mass is fragmented. It is this fragmentation that ensures that daughter cells get their share of mitochondria, including mtDNA.

Electron microscopy and conventional electron microscopical contrast techniques provide a view that is quite familiar to many researchers. Healthy mitochondria viewed through an electron microscope look at first sight like oval-

shaped forms, grain-like indeed, which appear covered with stripes. On detailed inspection, a two membrane system becomes usually obvious. What is well known as the outer membrane lines the oval shape, whereas the heavily folded inner membrane is responsible for the stripes, known as cristae. The two membranes clearly define sub-mitochondrial compartments: the inter membrane space and the mitochondrial matrix. Of note in normally functioning mitochondria, linear cristae are seen while aberrant patterns such as circular or concentric ring pattern are an indication of dysfunction. The popularity of electron microscopic images of mitochondria may have contributed to the long held, but incorrect view that they occur as distinct and individual organelles each containing their own mtDNA, instead of the dynamic network which the mitochondria actually form.

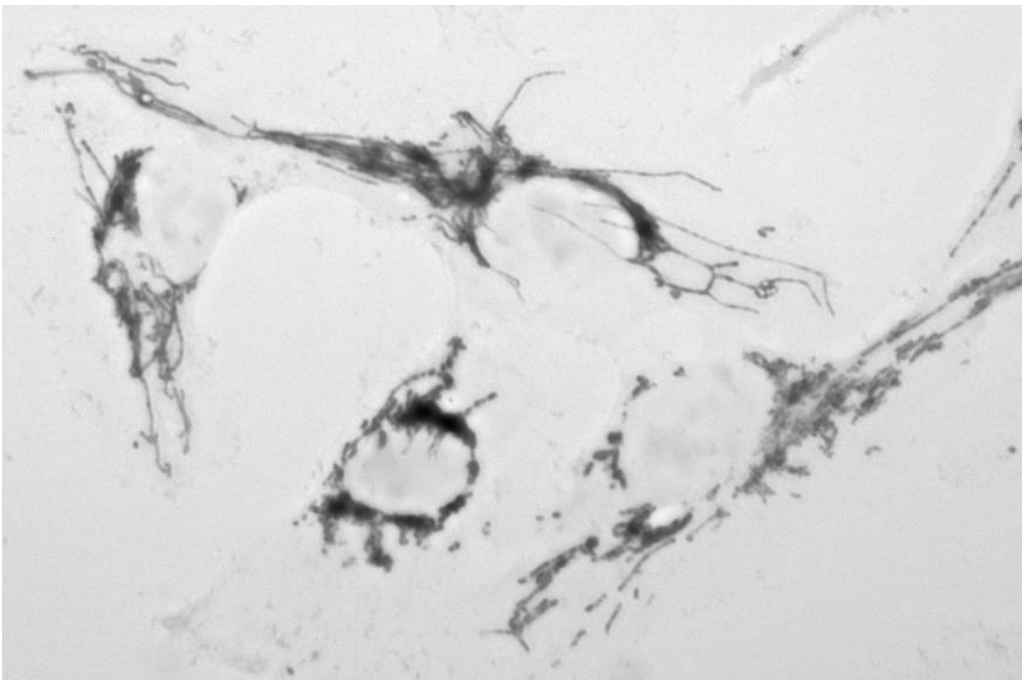


Figure 3: Mitochondrial morphology assessed by enzyme-cytochemical staining. Using exogenous cytochrome c as substrate, Cytochrome c oxidase (COX) in these fixed cells has converted diaminobenzidine tetrahydrochloride (DAB) into a brown reaction product which is visible. The shape of the functional mitochondria becomes visible, either as fragments or a tubular network.

## Scope of this thesis

In the Introduction of this thesis it is argued that tissue-specific mtDNA segregation and dominant negative effects of mtDNA mutations may underlie variable disease expression of A3243G mutant mtDNA. These two aspects have been investigated in the experimental chapters of this thesis. Chapters 2 and 3 deal with mtDNA segregation analysis. Specifically, Chapter 2 describes two methodologies that were key to the experiments of Chapter 3, where the role of nucleoids in segregation has been analyzed.

In Chapter 4 and 5, genome wide gene expression experiments are presented, analyzing the effect of mitochondria with an A3243G mutation or total DNA depletion ( $\rho^0$  cells) on nuclear gene expression, with the aim to uncover mutation-specific nuclear transcriptional responses. In Chapter 5 additional experiments are described to dissect the signaling of mitochondrial dysfunction to the cytosolic protein synthesis machinery. Chapter 6 discusses experimental results.

## Reference List

1. McBride,H.M., Neuspiel,M. and Wasiak,S. (2006) Mitochondria: more than just a powerhouse. *Curr. Biol.*, 16, R551-R560.
2. Maassen,J.A., Jahangir Tafrechi,R.S., Janssen,G.M., Raap,A.K., Lemkes,H.H. and 't Hart,L.M. (2006) New insights in the molecular pathogenesis of the maternally inherited diabetes and deafness syndrome. *Endocrinol.Metab Clin.North Am.*, 35, 385-3xi.
3. Finsterer,J. (2007) Genetic, pathogenetic, and phenotypic implications of the mitochondrial A3243G tRNA<sup>Leu</sup>(UUR) mutation. *Acta Neurol.Scand.*, 116, 1-14.
4. Margulis,L. (1981) *Symbiosis in Cell Evolution*. W.H.Freeman and Co., San Fransisco.
5. Gray,M.W., Lang,B.F., Cedergren,R., Golding,G.B., Lemieux,C., Sankoff,D., Turmel,M., Brossard,N., Delage,E., Littlejohn,T.G. et al. (1998) Genome structure and gene content in protist mitochondrial DNAs. *Nucleic Acids Res.*, 26, 865-878.
6. Castresana,J. (2001) Comparative genomics and bioenergetics. *Biochim.Biophys.Acta*, 1506, 147-162.
7. Burger,G., Gray,M.W. and Lang,B.F. (2003) Mitochondrial genomes: anything goes. *Trends Genet.*, 19, 709-716.
8. Gabaldon,T. and Huynen,M.A. (2004) Shaping the mitochondrial proteome. *Biochim.Biophys.Acta*, 1659, 212-220.
9. Asin-Cayuela,J. and Gustafsson,C.M. (2007) Mitochondrial transcription and its regulation in mammalian cells. *Trends Biochem.Sci.*, 32, 111-117.
10. Fernandez-Silva,P., Acin-Perez,R., Fernandez-Vizarra,E., Perez-Martos,A. and Enriquez,J.A. (2007) In vivo and in organello analyses of mitochondrial translation. *Methods Cell Biol.*, 80, 571-588.
11. Larsen,N.B., Rasmussen,M. and Rasmussen,L.J. (2005) Nuclear and mitochondrial DNA repair: similar pathways? *Mitochondrion.*, 5, 89-108.
12. Clayton,D.A. (2000) Transcription and replication of mitochondrial DNA. *Hum.Reprod.*, 15 Suppl 2, 11-17.
13. Birky,C.W., Jr. (1994) Relaxed and Stringent Genomes: Why Cytoplasmic Genes Don't Obey Mendel's Laws. *J Hered*, 85, 355-365.
14. Kai,Y., Takamatsu,C., Tokuda,K., Okamoto,M., Irita,K. and Takahashi,S. (2006) Rapid and random turnover of mitochondrial DNA in rat hepatocytes of primary culture. *Mitochondrion.*, 6, 299-304.
15. Gross,N.J., Getz,G.S. and Rabinowitz,M. (1969) Apparent turnover of mitochondrial deoxyribonucleic acid and mitochondrial phospholipids in the tissues of the rat. *J.Biol.Chem.*, 244, 1552-1562.
16. Chomyn,A., Martinuzzi,A., Yoneda,M., Daga,A., Hurko,O., Johns,D., Lai,S.T., Nonaka,I., Angelini,C. and Attardi,G. (1992) MELAS mutation in mtDNA binding site for transcription termination factor causes defects in protein synthesis and in respiration but no change in levels of upstream and downstream mature transcripts. *Proc.Natl.Acad.Sci.U.S.A*, 89, 4221-4225.

17. Janssen,G.M., Maassen,J.A. and van Den Ouweland,J.M. (1999) The diabetes-associated 3243 mutation in the mitochondrial tRNA(Leu)(UUR) gene causes severe mitochondrial dysfunction without a strong decrease in protein synthesis rate. *J.Biol.Chem.*, 274, 29744-29748.
18. DiMauro,S. (2004) Mitochondrial diseases. *Biochim.Biophys.Acta*, 1658, 80-88.
19. Sutovsky,P., Van Leyen,K., McCauley,T., Day,B.N. and Sutovsky,M. (2004) Degradation of paternal mitochondria after fertilization: implications for heteroplasmy, assisted reproductive technologies and mtDNA inheritance. *Reprod.Biomed.Online.*, 8, 24-33.
20. Bandelt,H.J., Kong,Q.P., Parson,W. and Salas,A. (2005) More evidence for non-maternal inheritance of mitochondrial DNA? *J Med.Genet.*, 42, 957-960.
21. Jenuth,J.P., Peterson,A.C., Fu,K. and Shoubridge,E.A. (1996) Random genetic drift in the female germline explains the rapid segregation of mammalian mitochondrial DNA. *Nat.Genet.*, 14, 146-151.
22. Wallace,D.C., Brown,M.D. and Lott,M.T. (1999) Mitochondrial DNA variation in human evolution and disease. *Gene*, 238, 211-230.
23. Cao,L., Shitara,H., Horii,T., Nagao,Y., Imai,H., Abe,K., Hara,T., Hayashi,J.I. and Yonekawa,H. (2007) The mitochondrial bottleneck occurs without reduction of mtDNA content in female mouse germ cells. *Nat. Genet.*, 39, 386-390
24. Chinnery,P.F., Zwijnenburg,P.J., Walker,M., Howell,N., Taylor,R.W., Lightowlers,R.N., Bindoff,L. and Turnbull,D.M. (1999) Nonrandom tissue distribution of mutant mtDNA. *Am.J.Med.Genet.*, 85, 498-501.
25. Jenuth,J.P., Peterson,A.C. and Shoubridge,E.A. (1997) Tissue-specific selection for different mtDNA genotypes in heteroplasmic mice. *Nat.Genet.*, 16, 93-95.
26. Capaldi,R.A., Aggeler,R., Gilkerson,R., Hanson,G., Knowles,M., Marcus,A., Margineantu,D., Marusch,M., Murray,J., Oglesbee,D. et al. (2002) A replicating module as the unit of mitochondrial structure and functioning. *Biochim.Biophys.Acta*, 1555, 192-195.
27. Kanki,T., Nakayama,H., Sasaki,N., Takio,K., Alam,T.I., Hamasaki,N. and Kang,D. (2004) Mitochondrial nucleoid and transcription factor A. *Ann.N.Y.Acad.Sci.*, 1011, 61-68.
28. Garrido,N., Griparic,L., Jokitalo,E., Wartiovaara,J., van der Bliek,A.M. and Spelbrink,J.N. (2003) Composition and dynamics of human mitochondrial nucleoids. *Mol.Biol.Cell*, 14, 1583-1596.
29. Iborra,F.J., Kimura,H. and Cook,P.R. (2004) The functional organization of mitochondrial genomes in human cells. *BMC.Biol.*, 2, 9.
30. Legros,F., Malka,F., Frachon,P., Lombes,A. and Rojo,M. (2004) Organization and dynamics of human mitochondrial DNA. *J.Cell Sci.*, 117, 2653-2662.
31. Schaefer,A.M., Taylor,R.W., Turnbull,D.M. and Chinnery,P.F. (2004) The epidemiology of mitochondrial disorders--past, present and future. *Biochim.Biophys.Acta*, 1659, 115-120.
32. Leonard,J.V. and Schapira,A.H. (2000) Mitochondrial respiratory chain disorders I: mitochondrial DNA defects. *Lancet*, 355, 299-304.
33. Kobayashi,Y., Momoi,M.Y., Tominaga,K., Momoi,T., Nihei,K., Yanagisawa,M., Kagawa,Y. and Ohta,S. (1990) A point mutation in the mitochondrial tRNA(Leu)(UUR) gene in MELAS (mitochondrial myopathy, encephalopathy, lactic acidosis and stroke-like episodes). *Biochem.Biophys.Res.Commun.*, 173, 816-822.
34. Goto,Y., Nonaka,I. and Horai,S. (1990) A mutation in the tRNA(Leu)(UUR) gene associated with the MELAS subgroup of mitochondrial encephalomyopathies. *Nature*, 348, 651-653.
35. Lynn,S., Borthwick,G.M., Charnley,R.M., Walker,M. and Turnbull,D.M. (2003) Heteroplasmic ratio of the A3243G mitochondrial DNA mutation in single pancreatic beta cells. *Diabetologia*, 46, 296-299.
36. Janssen,G.M., Hensbergen,P.J., van Bussel,F.J., Balog,C.I., Maassen,J.A., Deelder,A.M. and Raap,A. K. (2007) The A3243G tRNA(Leu)(UUR) mutation induces mitochondrial dysfunction and variable disease expression without dominant negative acting translational defects in complex IV subunits at UUR codons. *Hum.Mol.Genet.*, 16, 3472-3481.
37. Bender,A., Krishnan,K.J., Morris,C.M., Taylor,G.A., Reeve,A.K., Perry,R.H., Jaros,E., Hersheson,J.S., Betts,J., Klopstock,T. et al. (2006) High levels of mitochondrial DNA deletions in substantia nigra neurons in aging and Parkinson disease. *Nat.Genet.*, 38, 515-517.
38. Kraytsberg,Y., Kudryavtseva,E., McKee,A.C., Geula,C., Kowall,N.W. and Khrapko,K. (2006) Mitochondrial DNA deletions are abundant and cause functional impairment in aged human substantia nigra neurons. *Nat.Genet.*, 38, 518-520.



39. Bua,E., Johnson,J., Herbst,A., Delong,B., McKenzie,D., Salamat,S. and Aiken,J.M. (2006) Mitochondrial DNA-deletion mutations accumulate intracellularly to detrimental levels in aged human skeletal muscle fibers. *Am.J.Hum.Genet.*, 79, 469-480.
40. Taylor,R.W., Barron,M.J., Borthwick,G.M., Gospel,A., Chinnery,P.F., Samuels,D.C., Taylor,G.A., Plusa,S. M., Needham,S.J., Greaves,L.C. et al. (2003) Mitochondrial DNA mutations in human colonic crypt stem cells. *J.Clin.Invest*, 112, 1351-1360.
41. McKiernan,S.H., Tuen,V.C., Baldwin,K., Wanagat,J., Djamali,A. and Aiken,J.M. (2007) Adult-onset calorie restriction delays the accumulation of mitochondrial enzyme abnormalities in aging rat kidney tubular epithelial cells. *Am.J Physiol Renal Physiol*, 292, F1751-F1760.
42. Nekhaeva,E., Bodyak,N.D., Kraytsberg,Y., McGrath,S.B., Van Orsouw,N.J., Pluzhnikov,A., Wei,J.Y., Vijg,J. and Khrapko,K. (2002) Clonally expanded mtDNA point mutations are abundant in individual cells of human tissues. *Proc.Natl.Acad.Sci.U.S.A*, 99, 5521-5526.
43. Larsson,N.G., Wang,J., Wilhelmsson,H., Oldfors,A., Rustin,P., Lewandoski,M., Barsh,G.S. and Clayton,D.A. (1998) Mitochondrial transcription factor A is necessary for mtDNA maintenance and embryogenesis in mice. *Nat.Genet.*, 18, 231-236.
44. Trifunovic,A., Wredenberg,A., Falkenberg,M., Spelbrink,J.N., Rovio,A.T., Bruder,C.E., Bohlooly,Y., Gidlof,S., Oldfors,A., Wibom,R. et al. (2004) Premature ageing in mice expressing defective mitochondrial DNA polymerase. *Nature*, 429, 417-423.
45. Kujoth,G.C., Hiona,A., Pugh,T.D., Someya,S., Panzer,K., Wohlgemuth,S.E., Hofer,T., Seo,A.Y., Sullivan,R., Jobling,W.A. et al. (2005) Mitochondrial DNA mutations, oxidative stress, and apoptosis in mammalian aging. *Science*, 309, 481-484.
46. Dimmer,K.S. and Westermann,B. Solo or networked, mitochondria lead a complex life. *the elso gazette* (11). 2002.
47. Chen,H. and Chan,D.C. (2005) Emerging functions of mammalian mitochondrial fusion and fission. *Hum.Mol.Genet.*, 14 Spec No. 2, R283-R289.
48. Collins,T.J. and Bootman,M.D. (2003) Mitochondria are morphologically heterogeneous within cells. *J.Exp.Biol.*, 206, 1993-2000.
49. Chen,H., Detmer,S.A., Ewald,A.J., Griffin,E.E., Fraser,S.E. and Chan,D.C. (2003) Mitofusins Mfn1 and Mfn2 coordinately regulate mitochondrial fusion and are essential for embryonic development. *J.Cell Biol.*, 160, 189-200.
50. Margineantu,D.H., Gregory,C.W., Sundell,L., Sherwood,S.W., Beechem,J.M. and Capaldi,R.A. (2002) Cell cycle dependent morphology changes and associated mitochondrial DNA redistribution in mitochondria of human cell lines. *Mitochondrion.*, 1, 425-435.





# 2

## Single cell A3243G mitochondrial DNA mutation load assays for mtDNA segregation analyses

Roshan S. Jahangir Tafrechi\*, Frans M. van de Rijke\*, Amin Allallou‡, Chatarina Larsson°, Willem C.R. Sloos\*, Marchien van de Sande1, Carolina Wählby‡, George M.C. Janssen\* and Anton K. Raap\*

\* Department of Molecular Cell Biology, Leiden University Medical Center,  
P.O. Box 9503, 2300 RA Leiden, The Netherlands

° Department of Genetics and Pathology, The Rudbeck Laboratory, Uppsala, Sweden

‡ Center for Image Analysis, Uppsala University, Sweden

Published in the Journal of Histochemistry and Cytochemistry, 2007 Nov; 55 (11): 1159-66



## Abstract

Segregation of mtDNA is an important underlying pathogenic factor in mtDNA mutation accumulation in mitochondrial diseases and aging, but the molecular mechanisms of mtDNA segregation are elusive. Lack of high-throughput single cell mutation load assays lies at the base of the rareness of studies in which, at the single cell level, mitotic mtDNA segregation patterns have been analyzed. Here we describe development of a novel fluorescence-based, non-gel PCR-RFLP method for single cell A3243G mtDNA mutation load measurement. Results correlated very well with a quantitative in situ Padlock/Rolling Circle Amplification based genotyping method. In view of the throughput and accuracy of both methods for single cell A3243G mtDNA mutation load determination, we conclude that they are well suited for segregation analysis.

## Introduction

As a norm all mtDNA molecules in all cells of an individual have identical sequences, a situation referred to as homoplasmy (1). Due to lack of sophisticated DNA repair systems in the mitochondrial compartment, mutation rates of mtDNA are 5 to 10 times higher than nuclear DNA and deviation from the norm of homoplasmy will inevitably occur by acquisition of mtDNA mutation. Thus, invariably the situation arises where two mtDNA sequence variants are present within cells of individuals, a condition referred to as heteroplasmy. Whether inherited or acquired, as a consequence of segregation, deleterious mtDNA mutations can accumulate to a level (the critical threshold) at which too little compensation from the wild-type molecules occurs, accounting for cell and tissue failure and hence disease.

Studies with mice that are heteroplasmic for neutral mtDNA haplotypes contributed significantly to establishment of the germ line mitochondrial genetic bottleneck: reduction of the mtDNA copy number in early oogenesis in combination with random segregation leading to return to homoplasmy in one or only a few generations (2). Recently, however, it has been suggested that actual mtDNA copy numbers in early oogenesis are not compatible with the genetic bottle neck/random segregation mechanism (3). Also with heteroplasmic mice it has been shown that post-natally, tissue-specific non-random or directional segregation occurs (4). Furthermore, in human post-embryonic life non-random segregation of

inherited, pathogenic mtDNA mutations occurs (5;6). Gaining further knowledge of segregation mechanisms will thus contribute to better understanding of the nature of the mitochondrial genetic bottleneck and clonal accumulation of acquired mtDNA mutation with age, and how differences in pathogenic mtDNA mutation load among different tissues and organs are generated.

So-called transmitochondrial cybrids are created by fusion of enucleated cells carrying two different mtDNA sequence variants with a nucleated cell that has no mtDNA ( $\rho^0$  cells). Heteroplasmic cybrid cells have been a valuable source for experimental mitotic segregation studies. In the human situation, they have been particularly used to study segregation of the A3243G mtDNA sequence variants. This mutation causes a variety of disease phenotypes. It may be considered as exemplary for a central question in diseases with mtDNA mutation in their etiology: How can a single mutation causes variable phenotypes? Segregation is an obvious, but elusive factor (7).

By heteroplasmy analysis of bulk DNA of passages of cybrid clones carrying the A3243G pathogenic mutation stable various patterns have been found heteroplasmy and heteroplasmy shifts to either wild-type or mutant (for review, see Enriquez (1)). Of significance, stable heteroplasmy as measured on bulk DNA of cells in passages of cultured cybrid clone can be the result of random mitotic mtDNA segregation or non-segregation. Single

cell heteroplasmy determinations are needed to discriminate the two, but such studies are rare. Lehtinen *et al.* used limiting dilution to clone cells of late passages of continuously cultured A3243G cybrid founder cells. Following limited outgrowth, the mutation load of individual cells in the passages was assessed from bulk DNA using a PCR-RFLP method with gel electrophoresis to quantify mutant fractions (8).

The workload associated with the gel-based PCR-RFLP method for A3243G single cell heteroplasmy quantification after limited clonal expansion of cells in cybrid clone passages limits throughput. As an illustration, a total of 6 clones have been analyzed after 30 weeks of continuous culture with on average ~33 single cells analyzed (range 22-63) (8;9). We therefore sought to develop high-throughput A3243G mutation-load assays enabling analysis of hundreds of single cells in long term serial passages of multiple cybrid clones. This will enable analysis of heteroplasmy evolution longitudinally which is essential in mechanistically sorting out segregation processes that determine heteroplasmy.

Here we used two strategies for single cell A3243G mtDNA mutation load quantization: i) physical isolation of individual cells by single cell sorting, followed by closed-tube, real-time fluorescence PCR load measurement and ii) bi-color in situ mtDNA genotyping by Padlock/rolling circle amplification (Padlock-RCA, (10;11)) in combination with image analysis for quantification purposes.

In preliminary experiments with Taqman and Molecular Beacon probes for closed-tube, real-time fluorescence read-out, it was found, however, that the mutant probes reported both mutant and wild type targets. Similar observations have been reported by Bai *et al.* (12). This poor discriminatory power is likely a consequence of the unfavorable thermodynamics associated with G-T mismatches. It complicates closed-tube assays anyhow, but is further exacerbated in this particular case, because the mutation locates in a GC-rich environment which, being in the

D-loop of the mitochondrial tRNA<sup>Leu</sup>(<sup>UUR</sup>), is additionally poised to form secondary structures.

With PCR-RFLP being a sturdy and time-honored approach for A3243G mutant detection, we thus resorted to non-gel based PCR-RFLP fragment analyses employing melting temperature characteristics (PCR-RFMT) of the fragments using SybrGreen as reporter. The only sacrifice to a closed-tube assay is the one-time addition of the restriction enzyme. Here we describe the development and performance of the PCR-RFMT method.

Recently, we described qualitative *in situ* genotyping of the 3243 locus by Padlock-RCA (10). Here we applied dedicated image analysis (13) to quantitatively correlate the *in situ* assay with the PCR-RFMT. Based on their specifications in terms of throughput and accuracy, we conclude that both methods are suitable for A3243G mtDNA segregation analyses.

## Materials and methods

### Cells, cell culture and cell sorting

The A3243G transmitochondrial 143B cybrid clones were grown on Dulbecco's Modified Eagle's medium containing 4.5 mg/ml glucose and 110 µg/ml pyruvate (DMEM) supplemented with 50 µg/ml uridine and 10% fetal bovine serum. Transmitochondrial cybrids used in this work were sampled from an ongoing mtDNA segregation study in which we cloned heteroplasmic cells, expanded them to 9-cm cultures, following continuously culture with a 10% split twice a week. Cybrid cells were produced by fusing skin fibroblasts from two maternally inherited diabetes and deafness, MIDD, patients (coded V and GB) with 143B  $\rho^0$  cells. For single cell sorting, cells at near-confluence were harvested in 2 ml trypsin/EDTA. 500 µl was resuspended in a 5 ml Falcon tube containing 1500 µl complete medium. Single cells were sorted in the wells of an optical 96-wells plate (Abgene, UK) with the FACS Advantage SE (BD, USA) cell sorter using forward and side scatter gating. Plates were sealed and stored with no further processing

at -20°C for at least one night up to several months.

For *in situ* genotyping cells of a given clone and passage number were harvested by trypsin treatment and seeded in a culture plate containing microscopic object slides. Cells were allowed to adhere overnight after which they were fixed for *in situ* genotyping with Padlock-RCA

#### Primers, probes and PCR

The primers for the PCR-RFMT were designed with PrimerExpress version 1.0 and were manufactured at Eurogentec, Belgium. The first forward primer 5'-CGCCTTCCCCGAAATGAT anneals from location 3162 to 3181 on the mtDNA. The second forward primer 5'-CCCACACCCACCCAAGAACA anneals from location 3204 to 3223 and the common reverse primer 5'-TGGCCATGGGTATGTTGTTA at 3300-3319. The first forward and the common reverse primers are referred to as primer pair A and the other pair as primer pair B. PCR was performed in an end-volume of 20 µl, containing 10 µl SYBRGreen Mastermix (Applied Biosystems, USA) and 250 nM of both primers. The PCR begins with 10 minutes hot-start at 95°C, followed by 42 cycles alternating between 15 seconds 95°C and 1 minute 63°C using an ABI 7700 or 7900 spectrofluorometric Thermal Cycler (Applied Biosystems, USA).

#### Restriction enzyme digestion and melt analysis

For restriction enzyme digestion of the amplicons, 5 µl ApaI restriction enzyme mix was added directly to the PCR product. The enzyme mix was composed of 0.5 µl BSA (10 mg/ml), 0.5 µl 10 x buffer A (Promega, the Netherlands), 50 nl ApaI enzyme (80 U/µl, Promega) and 4 µl of water. Digestion was performed overnight at 37°C and stored at 4°C until further processing up to a few weeks.

The melt curves were recorded with an ABI-Prism 7700 or 7500 spectrofluorimetric Thermal Cycler (Applied Biosystems, USA) by gradually increasing the temperature during

20 minutes from 65°C to 90°C. The ABI-Prism software package did not include software for baseline correction and peak area calculations. In order to perform automated analysis and data plotting, melt data were exported in Excel file format and a macro was developed in house, as described in the Results Section.

#### genotyping mtDNA at the 3243 locus *in situ* and image analysis

*In situ* mtDNA genotyping by Padlock-RCA was performed as described previously (Larsson *et al.* (10)) with slight modifications. In short, cells grown on microscopic object slides were fixed in 4% formaldehyde and 0.5% sucrose in PBS for 20 minutes at ambient temperature, washed with PBS and stored in 70% ethanol at 4°C. Following extensive rinses with PBS they were treated with 0.05% pepsin (Sigma, P7000) in 0.01 M HCl during 5 minutes to gain access to the mtDNA for enzymes and Padlock probes. Next, the cells were dehydrated with graded ethanol series followed by a pre-incubation of 15 minutes in the enzyme reaction buffer supplemented with 0.2 µg/µl BSA. Then, MscI (0.5 U/µl) and T7 exonuclease (10 U/µl) (New England Biolabs, USA) were added and incubated at 37°C at the specified times. After digestion and exonuclease treatment, the Padlock probes (100 nM) were hybridized and circularized simultaneously. The hybridization/ligation was performed for one hour at 55°C with Ampligase (Epicentre, USA) in the supplied buffer supplemented with 1 mM NAD<sup>+</sup>, 10% glycerol and 125 mM KCl. Subsequently, the cells were washed with TBS supplemented with 0.05% Tween-20. RCA was performed for 1 hour at 37 °C after addition of 1 U/µl of Φ29 DNA polymerase (Fermentas, Canada) and 0.2 mg/ml histone (Sigma, type 2A, Calf Thymus), to condense the RCA DNA product. For hybridization of the detection probes we used 250 nM Lin16-FITC for the wild type mtDNA and 250 nM Lin33-Cy5 for the A3243G mtDNA (Larsson *et al.* (10)). Incubation was for 30 minutes at 37°C in 2x SSC supplemented with 20% formamide. Following 3 washes with



Tris buffered saline, 0.01 % Tween-20, nuclear DNA was counterstained with 4',6-Diamidino-2-phenylindole (DAPI).

For digital microscopy a computer-controlled standard epi-fluorescence microscope (Leica DM) equipped with a 100 W mercury arc lamp, a 100 X 1.3 N.A. objective and a scientific grade 16-bit CCD camera are used. The computer controls image acquisition through a motorized 8-position filter-block rotor and shutters.

The image analysis algorithm has as the key feature that it segments cells in the absence of a cytoplasmic counter stain. Instead, cytoplasm delineation is based on a fixed radial distance from each cell nucleus, a strategy made possible due to the absence of Padlock-RCA signals outside the cytoplasm (Allalou

*et al.* (13)). The program runs as a plug-in for the VIS Image Analysis Software (Visiopharm, Denmark). The number of red (Cy5) over the number of red (Cy5) plus green (FITC) signals per cell is taken as the mutation load.

## Results

Development of the sybrgreen PCR-RFMT method

As measures of the mutant and wild type A3243G fractions in the single cell PCR products, we used the areas under the peaks of the first derivative of the SybrGreen fluorescence melting curve of the ApaI fragmented PCR product. Figure 1A presents relevant optimization experiments with two different primer pairs for amplification of the A3243G region and ~100 pg genomic DNA from cybrid clones that were 100% wild type and near 100% mutant. A heteroplasmic sample was also included in this experiment. Primer pair A generates a 158 bp long fragment with 43% GC and a T<sub>m</sub> of 79°C. Digestion with the restriction enzyme ApaI cleaves only the mutant amplicon into a piece of 83 bp (46% GC, T<sub>m</sub> = 76°C) and a piece of 75 bp (40% GC, T<sub>m</sub> = 74°C). Primer pair B generates a 116 bp long fragment with 45% GC and also a T<sub>m</sub> of 79°C. Digestion with the restriction enzyme ApaI cleaves the mutant amplicon into a piece of 41 bp and 54% GC and a piece of 75 bp and 40% GC, both with a T<sub>m</sub> of 74°C. These T<sub>m</sub>'s are measured in the PCR solution containing the restriction buffer and enzyme. In absence of the restriction enzyme mix, the (undigested) amplicon melts at a temperature of 77°C.

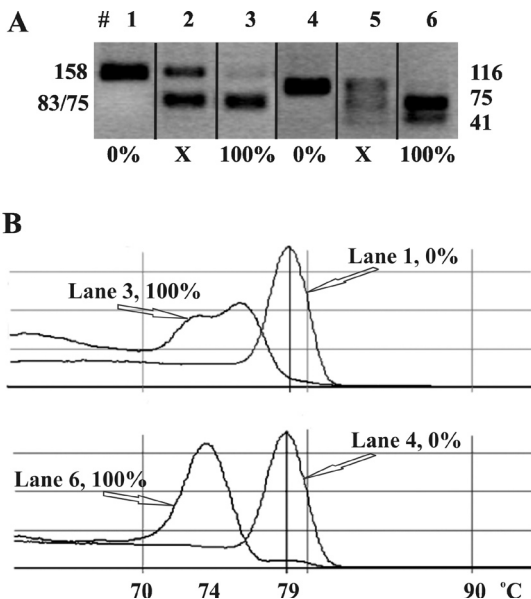


Figure 1 Electrophoretic and melt characteristics of the PCR-RFLP fragments.

(A) Gel electrophoresis of the restriction enzyme fragments obtained after ApaI digestion of PCR products obtained with primer sets A and B. The amount of input DNA was ~ 100 pg DNA, the equivalent of ~ 16 cells. Products in lane 1 and 4 are from homoplasmic wild type cybrid cells (0% mutant), lanes 3 and 6 from homoplasmic mutant cells (100% mutant) and lanes 2 and 5 from a heteroplasmic cybrid cell clone.

(B) Derivatives of the melting curves of homoplasmic A3243G mtDNA. The top graph in (B) corresponds to lane 1 and 3 of Fig 1A, the bottom graph to lanes 4 and 6. The curves represent the derivative of the SYBR Green signal intensity (y-axis) as a function of temperature (x-axis).

Note that the two mutant fragments generated with primer set A do not resolve electrophoretically (lane 3 in Fig 1A) while they do so in the melt analysis. The two mutant fragments generated with primer set B, in contrast, resolve electrophoretically (lane 6 in Fig 1A) but not in the melt analysis.

The T<sub>m</sub> of both mutant fragments is ~74°C.

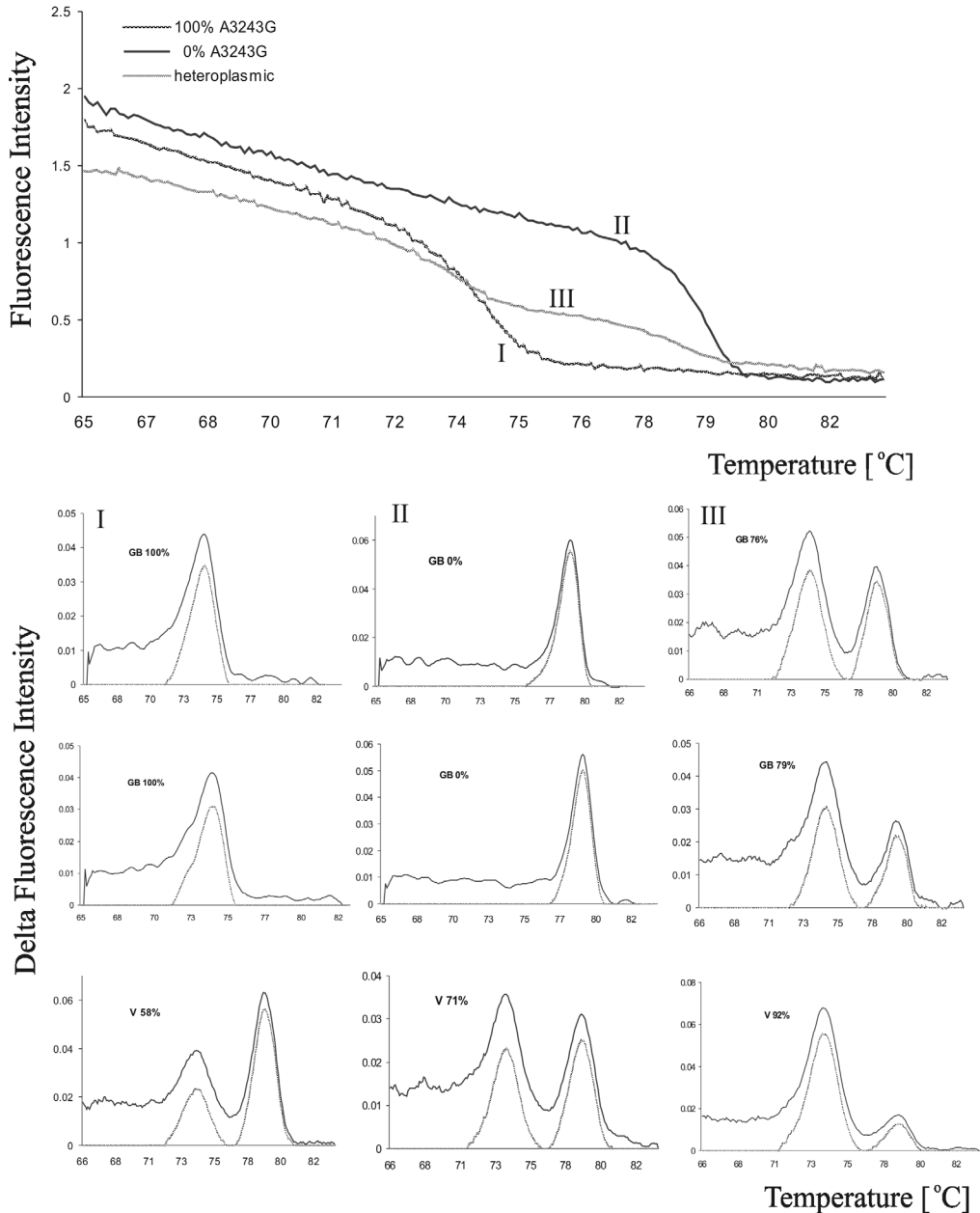


Figure 2 Single cell PCR-RFMT analysis.

Upper panel: Melt curves of PCR-amplified Apal digested DNA from two homoplasmic (I: wt; II: A3243G) and one heteroplasmic (III) A3243G mtDNA cybrid cell. Lower panel: Examples of derivative melt curves and their analysis. The experimental data (black line) are processed by an Excel macro to generate baseline corrected peaks (grey line) from which the mutant peak fraction is determined. Roman numbers refer to the melt curves in the upper panel. The remaining 6 plots represent the analysis of single cybrid cells derived from two patients, GB and V.

The electrophoretic behavior of the PCR-RFLP fragments generated from the genomic DNA of the three clones in a 3% agarose gel is shown in figure 1A while figure 1B shows the derivatives of the fluorescent melting curves of the homoplasmic DNAs. The mutant restriction fragments of the amplicon from primer pair A do not resolve electrophoretically, but do so in the melt analysis. Conversely, the mutant fragments of primer pair B do resolve electrophoretically but do not in the melt analysis. Note also that with primer pair B the wild-type fragment is much better separated from the mutant fragments in the melt analysis compared to primer pair A. The near-perfect co-incidence of the melt peaks of the mutant fragments of primer pair B, the bell-shapes of both peaks and their near complete separation provide an excellent starting point for baseline correction and estimation of the peak areas as measures for the mutant and wild type fractions. Primer pair B was therefore chosen for further development.

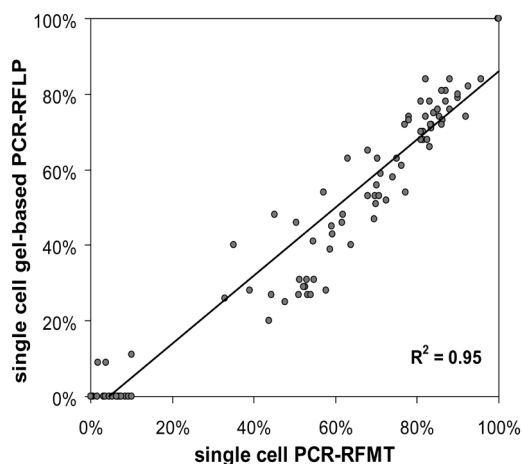


Figure 3 Correlation between A3243G mtDNA gel-based RFLP and PCR-RFMT analysis at the single cell level.

Individually sorted cells were subjected to PCR-RFMT analysis followed by gel electrophoresis and image analysis of the same samples.

To evaluate the performance of the PCR-RFMT at the single cell level we sorted single cells from various passages of heteroplasmic cybrid clones in 96-well optical plates and performed the PCR-RFMT procedure. In Figure 2 melt curves are shown for a heteroplasmic cell and two cells with different homoplasmic states (top panel), as well as 9 derivative curves (lower panel). To exclude incomplete ApaI digestion under PCR-RFMT conditions, we mixed 100 % wild-type and 100 % mutant cell, single cell sorted them and performed PCR-RMFT. Only wild type and mutant melt curves were obtained. The results led us to conclude that also at the single cell level the PCR-RFMT principle works. To automatically measure the areas under the peaks and process the data into suitable plots we next developed a macro in Excel. The macro searches for the two maxima and the minimum between the two peaks. It then employs the bell-shapes of the peaks for baseline correction. The right-hand flank of the mutant peak (from mutant peak position to the minimum between the peaks) is mirrored to the left and the line connecting the base of the bell is used as baseline. Similarly, the left-hand flank of the wild type peak is mirrored to the right and baseline corrected. Base-line corrected peaks for 6 A3243G cybrid cells are plotted in the graphs (Figure 2, lower panel). Finally, the macro calculates mutation load from the areas under the peaks. The data from a complete 96-wells plate are plotted both as a histogram as well as a scatter plot as a function of Ct (threshold Cycle) value for easy evaluation of the results.

We next compared the single cell PCR-RFMT approach with traditional gel-based imaging and quantification of fragments. For this we used single cell PCR-RFLP fragments that by RFMT analysis showed a wide range of heteroplasmy. The correlation proved to be good (Figure 3). The correlation between the analysis methods may be good, but both methods likely suffer from underestimation of the mutant fraction due to heteroduplex formation and the inability of ApaI to digest heteroduplexes. To

analyze the magnitude of this problem and to eventually mathematically compensate for this phenomenon, we cloned wild type and mutant fragments, prepared mixtures of purified wild-type and mutant plasmids, and submitted them to PCR-RFMT analysis at various dilutions down to the sub-attomol range. If  $p$  represents the wild type and  $q$  the mutant fraction in the sample then, at maximum heteroduplex formation, the relation between the wild type homoduplex-, heteroduplex- and mutant homoduplex fractions and the original input fractions are given by the equation:  $p^2 + 2pq + q^2 = 1$ . Thus, the mutation load  $q$  may be derived from the square root of the cleavable fraction  $q^2$ , since both  $p^2$  and  $pq$  are not recognized by *ApaI*. Figure 4 plots the expected mutant fraction against the square root of the mutant peak fraction. The good linear relationship between expected mutation load and the square root of the mutant peak fraction shows that full heteroduplex formation occurs,

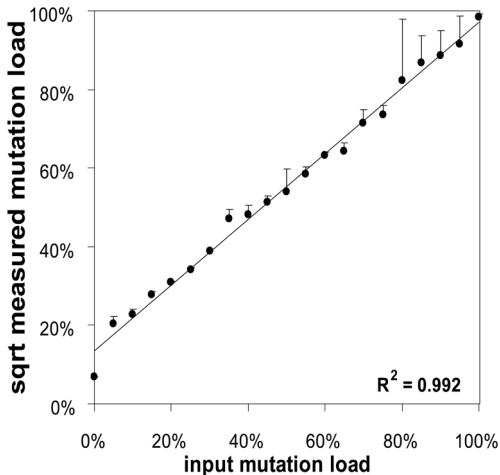


Figure 4 Heteroduplex formation during A3243G PCR-RFMT analysis. mtDNA from a heteroplasmic cybrid cell line was cloned into a plasmid vector. Plasmids containing either wild-type or mutant mtDNA sequences clones were identified, purified and mixed in predetermined ratios. Data are plotted as input mutation load (x-axis) versus the square root of the mutant peak fraction as measured by PCR-RFMT. Error-bars are the standard deviation of three measurements per data point.

Image analysis of in situ genotyped heteroplasmic A3243G cybrid cells and correlation with PCR-RFMT.

Previously, we developed an in situ A3243G mtDNA genotyping method. It is based on target primed, rolling circle amplification of in situ hybridized and ligated Padlock probes (10). The exquisite sensitivity of the ligase reaction to mismatches confers high specificity to A3243G sequence variant detection, not achievable by hybridization based methods such as Taqman, while the signal generation capacity of rolling circle amplification provides single molecule detection sensitivity with standard fluorescence microscopy and virtually no background signals. Results are primarily judged visually, but image analysis can confer quantitative information. We therefore recently developed dedicated image analysis software to quantify Padlock-RCA mtDNA signals in cells (13). Here we apply quantitative Padlock-RCA and correlate results with RFMT analysis. Figure 5A presents the mutation load histograms of cells from a given passage of clone GB\_20 measured with the PCR-RFMT and the quantitative Padlock-RCA technique. For PCR-RFMT 6 independently processed, single cell sorted 96-well plates were analyzed resulting in the mutation load histogram of 541 cells in Figure 5A. The peak average was 92.2% with a standard deviation of 3.4%. For Padlock-RCA with 458 cells analyzed from the same GB\_20 clone passage. The peak average was 92.5% with a standard deviation of 4.3%. Images of Padlock-RCA of a co-culture of homoplasmic wild-type and mutant cybrids, and GB\_20 clone are shown in Figure 5B and 5C, respectively.

## Discussion

In our segregation study we aim to measure mtDNA point mutation levels in individual members of cell populations with a priori unknown intercellular variability in mutation load reasons. We may thus expect relatively low accuracies in view of the high specificity and sensitivity demanded. Throughput is then obviously an important issue to get statistically

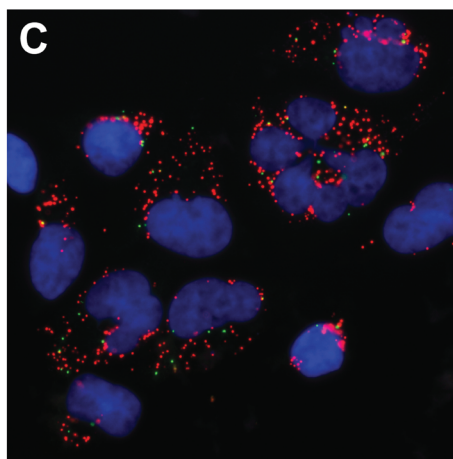
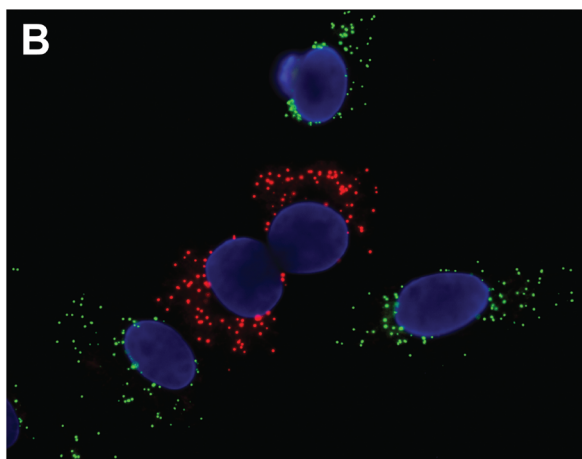
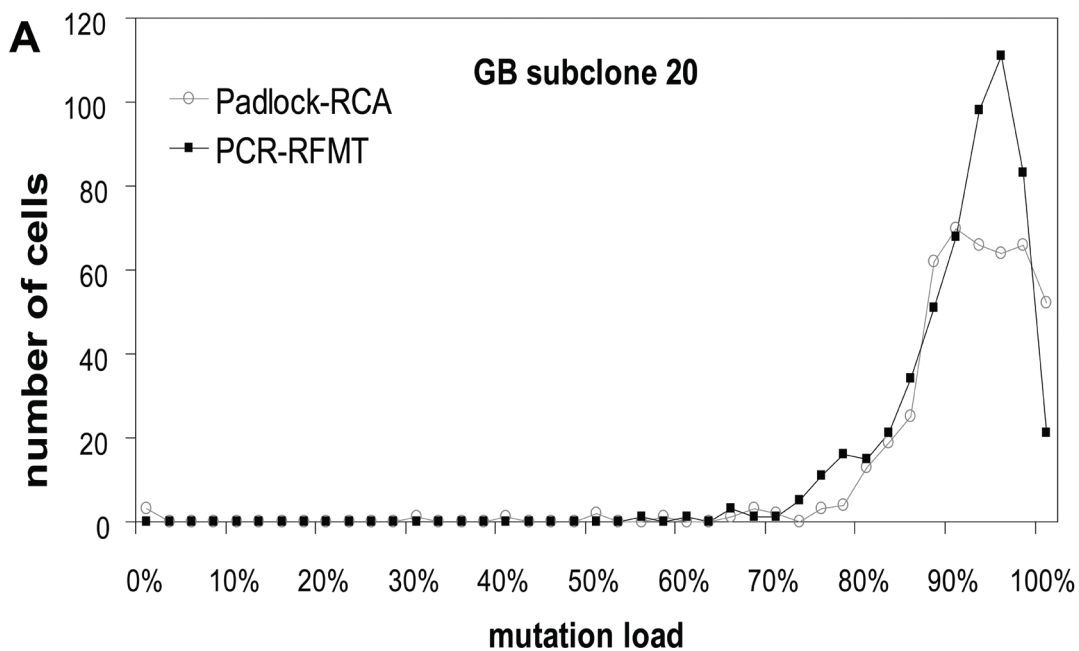


Figure 5 Correlating single cell A3243G mtDNA PCR-RFMT with Padlock-RCA. (A) Individual cells of a heteroplasmic A3243G clone (GB\_20) were analyzed by PCR-RFMT ( $n = 541$ ) and Padlock-RCA ( $n = 458$ ). According to computer simulations of random segregation, the very great majority of the cells in this late passage should have been genetically fixed, i.e. be homoplasmic mutant. (B)(C) Photomicrographs of cells from respectively a co-culture of wild-type and mutant cybrids, and the heteroplasmic GB\_20 clone genotyped in situ by Padlock-RCA (630x). Red dots correspond to mutant and green dots to wild-type mtDNA

sound data for biologically mechanistic interpretation.

We describe here development, performance and correlation of two single cell mutation load assays, based on different principles, for mtDNA segregation analysis.

In their current versions both methods perform about equally in terms of throughput: 100s of cells per person per day. Increase in throughput can be achieved by further automation by e.g. for RFMT-PCR robotized PCR and melt analysis. Use of 384-well plates would quadruple throughput of the PCR-RFMT but unfortunately single cell sorting is limited to 96-well plates. For padlock-RCA image acquisition has been identified as the rate-limiting factor, thus automation of microscopy and image acquisition will increase throughput. In terms of analytical accuracy differences exist. PCR-RFMT suffers of heteroduplex formation. Mathematical correction allows in principle the true mutation load to be determined, the square root relationship between found and true mutation level values leads to great inaccuracies in the 0 - 25 % range, indeed the reason why 'last hot' cycle methodology has been introduced. We note that the PCR-RFMT methodology has been developed for segregation analysis, not for clinical diagnosis of A3243G mtDNA mutation loads in, for example, blood samples. For the latter low level heteroplasmy detection is needed, likely because many cells in the sample will not carry mutant mtDNA. However, in pathophysiological studies with (microdissected) patient biopsy material of MELAS patients, the PCR-RFMT method likely will be a convenient alternative to conventional PCR-RFLP because it tends to be enriched in the A3243G mutation (20:21).

Padlock RCA is free of heteroduplex formation problems and in principle will have the same accuracy over the full heteroplasmy range. A point of concern may be that efficiencies of detection are likely low as they are in conventional FISH with extremely small targets. Cells that are low in mtDNA copy number and low in heteroplasmy levels may then be falsely classified as homoplasmic.

The results in figure 5A are interesting from an analytical and segregation mechanistic point of view. They originate from cell of a late passage. PCR RFMT results of earlier passages of this clone were near-identical (to be reported elsewhere). Computer simulations of random mtDNA segregation specified to this clone clearly indicated that at passage 15 segregation should have been obvious, by flattening of the peak and the appearance of homoplasmic mutant cells. It thus appears that this clone (and several others not shown here) displays the phenomenon of stable heteroplasmy first reported by Lehtinen. If truly so, then variance in mutation load due to biology of segregation is absent and the variance observed in heteroplasmy is due to assay variability.

In the high mutant load range tested, both our methods perform equally well analytically with standard deviations of 3% in RFMT and 4% in RCA at  $n = 400$ . At decreasing mutation levels the padlock-RCA method will likely maintain accuracy while the PCR-RFMT will lose accuracy particularly below 25%.

In conclusion, we have developed single cell A3243G mtDNA mutation loads assays that meet the needs of segregation studies.

## Acknowledgements

This work was supported by the LUMC Matching Fund, the Prinses Beatrix Fonds and the EC-Strep Project ENLIGHT.

The authors wish to thank Visiopharm, Denmark, for a free license and help with integration of new functionality in VIS.

## References

1. Enriquez, J.A. (2003) Segregation and dynamics of mitochondrial DNA in mammalian cells. In Holt, I.J. (ed.), *Genetics of Mitochondrial Diseases*. Oxford University Press, Oxford, pp. 279-294.
2. Jenuth, J.P., Peterson, A.C., Fu, K. and Shoubridge, E.A. (1996) Random genetic drift in the female germline explains the rapid segregation of mammalian mitochondrial DNA. *Nat.Genet.*, 14, 146-151.
3. Cao, L., Shitara, H., Horii, T., Nagao, Y., Imai, H., Abe, K., Hara, T., Hayashi, J.I. and Yonekawa, H. (2007) The mitochondrial bottleneck occurs without reduction of mtDNA content in female mouse germ cells. *Nat. Genet.*, 39, 386-390
4. Jenuth, J.P., Peterson, A.C. and Shoubridge, E.A. (1997) Tissue-specific selection for different mtDNA genotypes in heteroplasmic mice. *Nat.Genet.*, 16, 93-95.
5. Chinnery, P.F., Zwijnenburg, P.J., Walker, M., Howell, N., Taylor, R.W., Lightowlers, R.N., Bindoff, L. and Turnbull, D.M. (1999) Nonrandom tissue distribution of mutant mtDNA. *Am.J.Med.Genet.*, 85, 498-501.
6. Chinnery, P.F. (2002) Modulating heteroplasmy. *Trends Genet.*, 18, 173-176.
7. Torroni, A., Campos, Y., Rengo, C., Sellitto, D., Achilli, A., Magri, C., Semino, O., Garcia, A., Jara, P., Arenas, J. et al. (2003) Mitochondrial DNA haplogroups do not play a role in the variable phenotypic presentation of the A3243G mutation. *Am.J.Hum.Genet.*, 72, 1005-1012.
8. Lehtinen, S.K., Hance, N., El Meziane, A., Juhola, M.K., Juhola, K.M., Karhu, R., Spelbrink, J.N., Holt, I.J. and Jacobs, H.T. (2000) Genotypic stability, segregation and selection in heteroplasmic human cell lines containing np 3243 mutant mtDNA. *Genetics*, 154, 363-380.
9. Turner, C.J., Granycome, C., Hurst, R., Pohler, E., Juhola, M.K., Juhola, M.I., Jacobs, H.T., Sutherland, L. and Holt, I.J. (2005) Systematic segregation to mutant mitochondrial DNA and accompanying loss of mitochondrial DNA in human NT2 teratocarcinoma Cybrids. *Genetics*, 170, 1879-1885.
10. Larsson, C., Koch, J., Nygren, A., Janssen, G., Raap, A.K., Landegren, U. and Nilsson, M. (2004) In situ genotyping individual DNA molecules by target-primed rolling-circle amplification of padlock probes. *Nat.Methods*, 1, 227-232.
11. Nilsson, M. (2006) Lock and roll: single-molecule genotyping in situ using padlock probes and rolling-circle amplification. *Histochem.Cell Biol.*, 126, 159-164.
12. Bai, R.K. and Wong, L.J. (2004) Detection and quantification of heteroplasmic mutant mitochondrial DNA by real-time amplification refractory mutation system quantitative PCR analysis: a single-step approach. *Clin.Chem.*, 50, 996-1001.
13. Allalou, A., van de Rijke, F.M., Jahangir Tafrechi, R.S., Raap, A.K. and Wahlby, C. (2007) Image based measurements of single cell mtDNA mutation load. In: *Image Analysis; Lecture Notes in Computer Science Vol 4522* pp 631-640. Springer Berlin/Heidelberg







# 3

## Suppressed and quantal mtDNA segregation in heteroplasmic cell cultures

Roshan S. Jahangir Tafrechi\*, Frans M. van de Rijke\*, Karoly Szuhai\*, Rene F. M. de Coos<sup>§</sup>, Harsha Karur Rajasimha<sup>°</sup>, Mats Nilsson<sup>°</sup>, Patrick F. Chinnery<sup>‡</sup>, David C. Samuels<sup>°</sup>, George M.C. Janssen\* and Anton K. Raap\*

\*Department of Molecular Cell Biology, Leiden University Medical Center, P.O. Box 9503, 2300 RA Leiden, The Netherlands

<sup>§</sup>Department of Molecular Cell Biology and Genetics, Maastricht University, PO Box 1475, 6201 BL Maastricht, The Netherlands,

<sup>°</sup>Virginia Bioinformatics Institute, Virginia Polytechnic Institute and State University, Blacksburg, USA

<sup>‡</sup>Department of Neurology, University of Newcastle upon Tyne, UK

<sup>°</sup> Department of Genetics and Pathology, The Rudbeck Laboratory, Uppsala, Sweden



## Abstract

At cytokinesis mitochondrial DNA (mtDNA) molecules are assumed to be physically partitioned to daughter cells in a stochastic fashion. In the presence of two mtDNA sequence variants (a situation referred to as heteroplasmy) continuation of this chance distribution process leads to random genetic segregation of the alleles. Here we present results of *in vitro* experiments and computer simulations indicating absence of A3243G mtDNA mitotic segregation. Occasionally, however, discrete heteroplasmy shifts or quantal segregations are observed. To explain the observations a metastable, heteroplasmic mtDNA segregation unit is postulated. Inherently this unit is thus multi-copy in mtDNA and as a rule faithfully replicating its wild type/mutant ratio. The nucleoid, the mitochondrial matrix DNA-protein complex that carries 8 - 10 mtDNA molecules, likely is the physical equivalent of the segregation/segregation suppression unit. The discrete heteroplasmy shifts observed may result from rearrangements leading to nucleoids of variable heteroplasmy, which segregate to fixation at a rate one order of magnitude more rapid than single mtDNAs would do. Reorganization of nucleoids may thus underlie A3243G mtDNA segregation in heteroplasmic cybrid cultures

## Introduction

When two neutral mtDNA alleles are present in the founding cell of a clone, the process of random mitotic segregation leads to genetic drift and ultimately to genetic fixation of mtDNA alleles in descendant cells. Two homoplasmic cell populations will eventually emerge with the proportion of their sizes, reflecting the mutation load in the founding cell (1). The lower the mtDNA copy number, the more rapid cells will emerge that have homoplasmic mtDNA, as illustrated in figure 1. mtDNA genetic drift is not only driven by mitosis, but also by mtDNA turnover (2;3).

In case of heteroplasmy with a deleterious mutation, cells drifting towards homoplasmy for the mutant allele can therefore acquire merely on stochastic grounds high levels of the deleterious mtDNA. Up to a point at which the critical threshold heteroplasmy is reached (~80% for the A3243G cell used here), cells experience too little compensation from the neutral variants leading, under selective conditions, to their elimination from the population.

Mice carrying neutral mtDNA haplotypes in a heteroplasmic fashion have been instrumental in establishing the germ line mitochondrial genetic bottleneck/random segregation hypothesis (4). Recently this hypothesis has been challenged by the fact that the dramatic reduction of the mtDNA copy number needed

to create a genetic bottle neck that leads by random segregation to great variance in heteroplasmy (and even homoplasmy) in offspring, does not appear to occur in the mouse germ line (5). Studies with these neutral heteroplasmic mice have also shown that post-natally, tissue-specific non-random or directional segregation occurs (6), which appears to be under nuclear genetic control (7) and points to the existence of segregation controlling genes. Also a multitude of clinical studies with pathogenic mtDNA mutations indicate that directional segregation occurs in human post-embryonic life (8;9). It is not understood how diversity in mtDNA mutation load among different tissues, and hence how a wide spectrum of mtDNA disease phenotypes can occur with one specific mutation. Obviously, segregation is important in this respect, but mechanisms are elusive.

In absence of heteroplasmic mouse models for pathogenic mtDNA point mutations, transmitochondrial cybrids provide valuable sources for experimental mitotic segregation analysis. They are created by fusion of enucleated cells carrying two different mtDNA sequence variants with a nucleated cell that has no mtDNA ( $\rho^0$  cells). Mostly by analysis of bulk DNA of passages of cybrid clones carrying the A3243G pathogenic mutation, two patterns have been found:

stable heteroplasmy and heteroplasmy drift to either wild-type or mutant. The number of stable A3243G clones exceeded the number of drifting clones by a factor of ~3. We counted 42 stable clones against 15 drifting clones in three studies (10-12) (for review see Enriquez (13)). Of significance, stable heteroplasmy as measured on bulk DNA of cells in passages of cultured cybrid clone can be the result of random mitotic mtDNA segregation or from non-segregation. Only single cell analyses can reveal the cellular heteroplasmy distribution of a given cell population, but such studies are rare. In one such study, it was found that the distribution of single cell mutation loads after 30 weeks of culture of A3243G cybrid

clones was too narrow to fit the random segregation model (14). It led to the concept of a multi-copy mtDNA segregation unit, the nucleoid, that is heteroplasmic itself and that replicates its wild type/mutant content faithfully. To explain changes in heteroplasmy e.g. in drifting cybrid clones it was proposed that the faithfully replicating nucleoid may occasionally reorganize its wild type/mutant ratio, possibly under genetic control (14; 15). Experimental evidence for reorganizing heteroplasmic nucleoids lying at the base of segregation is, however, very limited. Here we report experiments that are in strong support of the 'metastable' nucleoid model.

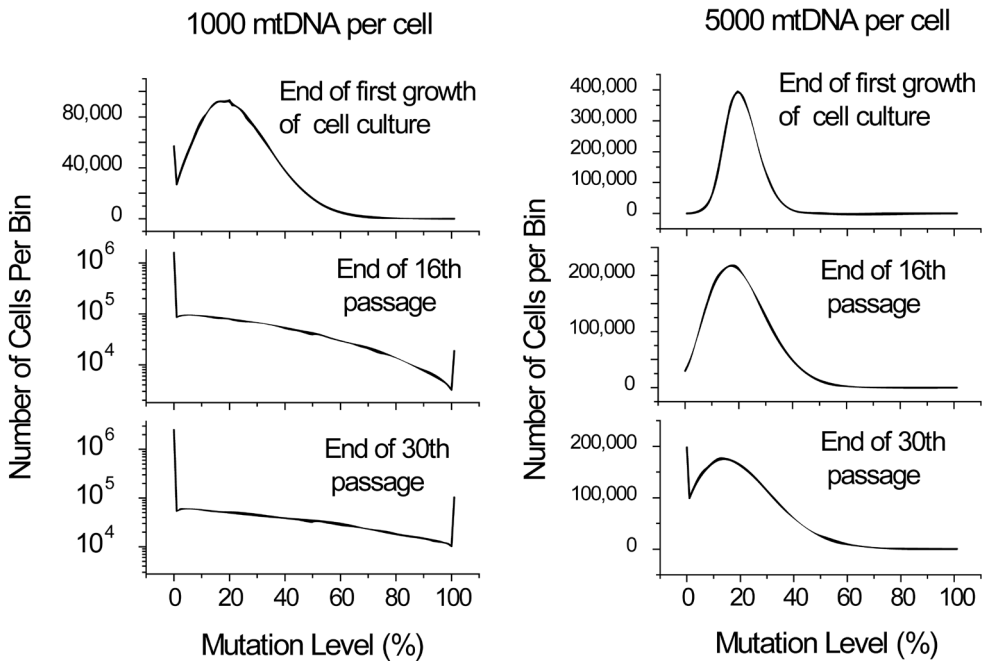


Figure 1: The rate of mitochondrial segregation as a function of the mtDNA copy number

The graphs represent computer-simulated mutation load distributions of the cells in the first outgrowth (passage 1), passage 16 and 30 of a founding cell with 20% mutation load with 1000 (left) and 5000 (right) mtDNA molecules. When reaching 0 and 100% mutation, the cells are genetically fixed on the wild-type and mutant mtDNA respectively. Such cells appear more rapid in the clone with the lower mtDNA copy number. The average mutation level as measured on bulkDNA cells remains steady at the initial value since in this simulation there is no advantage or disadvantage to the mutation. The contributions of mtDNA turnover to genetic drift in this situation is minor (mtDNA half life ~10 days (2)), because mtDNA replication is mostly driven by mitosis (~1 day).

## Material and methods

A3243G transmitochondrial 143B cybrid were produced by fusing skin fibroblasts from two maternally inherited diabetes and deafness, MIDD, patients (coded V and GB) and a mitochondrial myopathy encephalopathy lactic acidosis and stroke-like episodes, MELAS, patient (G) with 143 B  $\rho^0$  cells as described (16). Cybrid cloning was by limiting dilution or single cell flow sorting. Cybrid cells were grown on Dulbecco's Modified Eagle's medium containing 4.5 mg/ml glucose and 110  $\mu$ g/ml pyruvate (DMEM) supplemented with 50  $\mu$ g/ml uridine and 10% fetal bovine serum. After the first outgrowth to near-confluence ( $\sim$ a million cells) in 9 cm dishes, they were cultured with a 10% split of cells twice a week.

The A3243G mutation load of single cells was determined using a PCR/RFLP method (referred to as PCR/RFMT) as well as by *in situ* genotyping with Padlock/Rolling Circle Amplification (17) in combination with image analysis as described by Jahangir Tafrechi *et al.* (18). Average cellular mtDNA copy numbers were determined on bulk DNA with the aid of  $\Delta$ Ct method using the SybrGreen Master mix (Applied Biosystems, USA) for real-time PCR, assuming two  $\beta$ -globin genes per cell. Primers for  $\beta$ -globin and mtDNA as well as PCR conditions were as described (19).

Array-Comparative Genome Hybridization is described in Knijnenburg *et al.* (20).

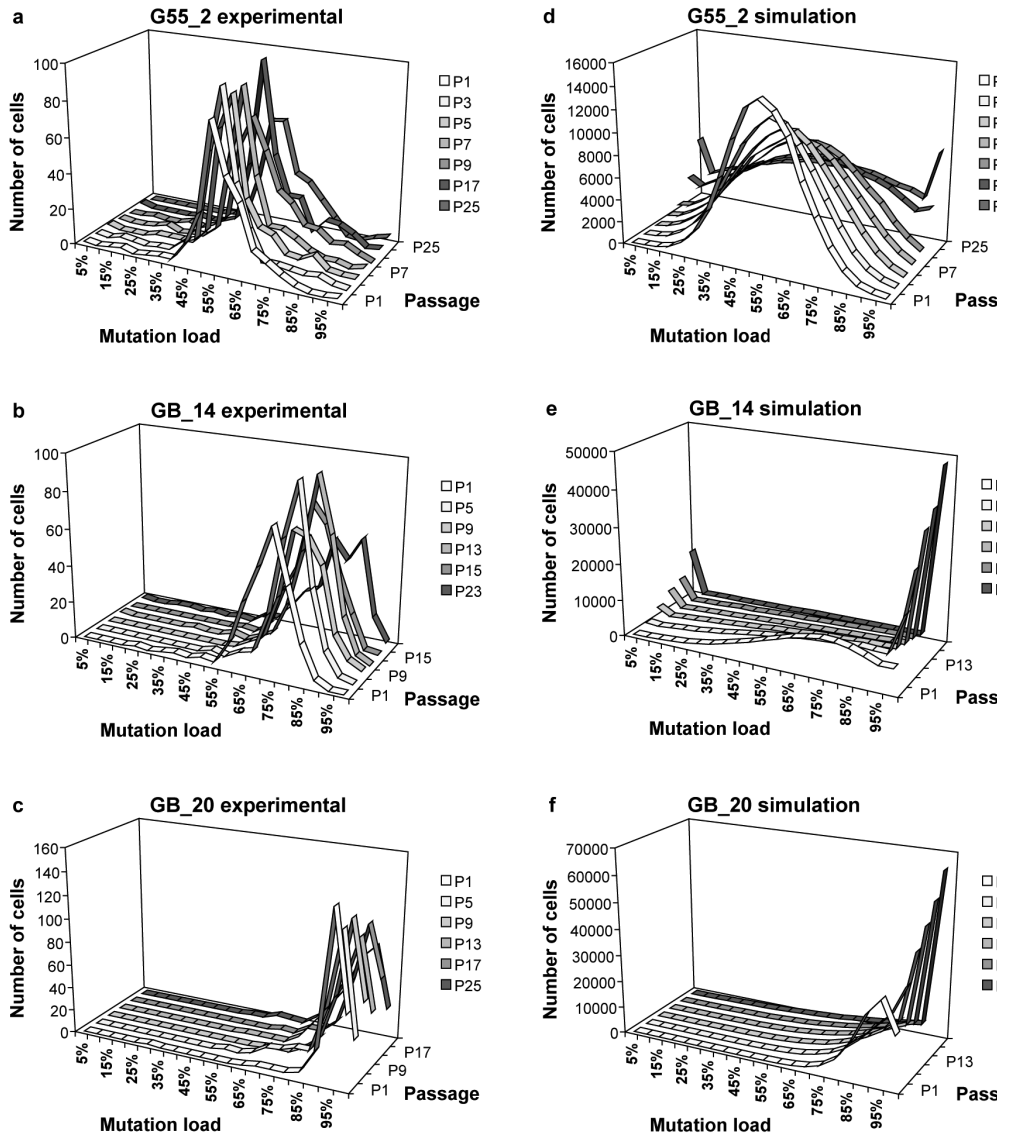
Computer simulations were started with a single cell containing M mutant mtDNA molecules and W wild-type mtDNA. The mtDNAs in the simulation were not organized into any structure. The simulated cells were divided at random intervals, with a mean division period of  $D = 1$  day. At cell division, the mtDNA molecules were individually randomly distributed to the two daughter cells. The mtDNA molecules were also randomly destroyed with a half-life of  $T_{1/2} = 10$  days (2). mtDNA replication was modeled by copying individual mtDNA molecules at a set rate  $R = \ln(2) Nt [ (1/T_{1/2}) + (1/D) ]$ , where  $Nt$  was the

copy number of mtDNA in the simulated cells. The mtDNA molecules to be copied were chosen at random, with no preference to either wild-type or mutant (3). After the simulated cell population has reached 1 million cells we began simulating cell culture passages by selecting 100,000 cells (1/10th of the population) at random from the total cell population, with this sampling taken every 3½ days.

## Results and discussion

In a first series of experiments we generated, by PCR-FMT (21), mutation load histograms of individual cells in multiple passages of 3 sub-cloned A3243G mtDNA 143B transmitochondrial cybrid founding cells cultured under non-selective conditions and performed computer simulations of random mitotic segregation specified to these cells in terms of heteroplasmy and mtDNA copy number. The experimental and computer simulation results are presented in Figure 2. Cells in the first outgrowth of the founding cell ( $\sim$ 20 generations; passage 1) of clone G55\_2 proved to possess mutation loads of  $\sim$ 50-55 % with a distribution that is substantially narrower than the simulated one. Cells in passage 1 of clones GB\_14 and GB\_20 had mutation loads of 70-75 % and 90-95 % respectively, also at a much more narrow distribution than predicted. All clones maintained a narrow distribution in subsequent passages, whereas according to the simulation, homoplasmic cells should have been very abundant at passages  $> 17$  for G55\_2 and passage  $\geq 5$  for GB\_14 and GB\_20. As cellular mtDNA copy number values for the computer simulations, 500 was used for G55\_2, which is actually above the experimentally determined copy number of 284 (SD=117, n=3). For G55\_2 and for GB\_14 and GB\_20 1500 was used, which is representative of the mtDNA copy number in 24 GB sub-clones analyzed: 1469 (SD=544, n=24). Under a random segregation regime, the clones theoretically would need to have very much higher mtDNA copy numbers to explain the experimental histograms.

Figure 2: Experimental and computer simulation single cell mutation load histograms of multiple passages of A3243G mtDNA heteroplasmic 143B transmittochondrial stable cybrid clones G55\_2 (a,d), GB\_14 (b,e), GB\_20 (c,f)



(a-c) Cybrids cells were cloned, expanded to a million cells (~20 generations, passage 1) and continuously cultured with a 10% split twice a week. At the indicated passages, single cells were sorted in 96-well optical plates and processed for single cell mutation load measurements by PCR-RFMT (~250 cells per histogram).

(d-f) For computer simulated histograms (10,000 cells per histogram) the algorithm for random segregation used as heteroplasmy value for the founding cell, the average mutation load found in passage 1: 56% for clone G55\_2, 70% for GB\_14 and 92% for GB\_20. As values for cellular mtDNA copy number, 500 was used for G55\_2 and for GB\_14 and GB\_20 1500 was used.

Yet we considered whether at moderate copy numbers, the stable heteroplasmies observed can still be explained by random segregation of mtDNAs. Theoretically negative selection for cells drifting towards mutant and wild-type mtDNA provides an explanation, but this is biologically highly improbable. Alternatively, it can be envisaged, that a delicate balance between negative selection of cells that drift to mutant and replicative advantage for mutant mtDNA creates a situation in which a population gets enriched for cells that have a heteroplasmy just under the threshold level. However, we observed stable heteroplasmy at 3 different levels, including one above the threshold level.

In view of the existence of the nucleoid with its multi-copy mtDNA nature, absence of segregation can best be explained with the nucleoid being a multi-copy segregation unit that is discretely heteroplasmic and faithfully replicating its wild type/mutant ratio as

proposed by Lehtinen (14) and illustrated in Figure 3a.

In our cybrid repository we identified a A3243G cybrid sub-clone (V\_50) that by gel-based PCR-RFLP mutation load measurement on bulk DNA showed to be drifting from ~ 98% mutant to wild type over a period of a year under non-selective culture conditions. (Figure 4, left panel). It provided a unique occasion to test the idea of a reorganizing nucleoid underlying segregation by analyzing its heteroplasmy evolution at the single cell level. Individual cells of the first passage analyzed were mostly 95-100% wild type. At passage 6 the great majority of the individual cells was shifted to 90-95% heteroplasmy, following which a second discrete shift to ~50-55% heteroplasmy occurred as evidenced by the significant subpopulations at 50-55% heteroplasmy in passages 42 48 and 62. Finally, a third shift to homoplasmy wild type occurred (Figure 4, right panel).

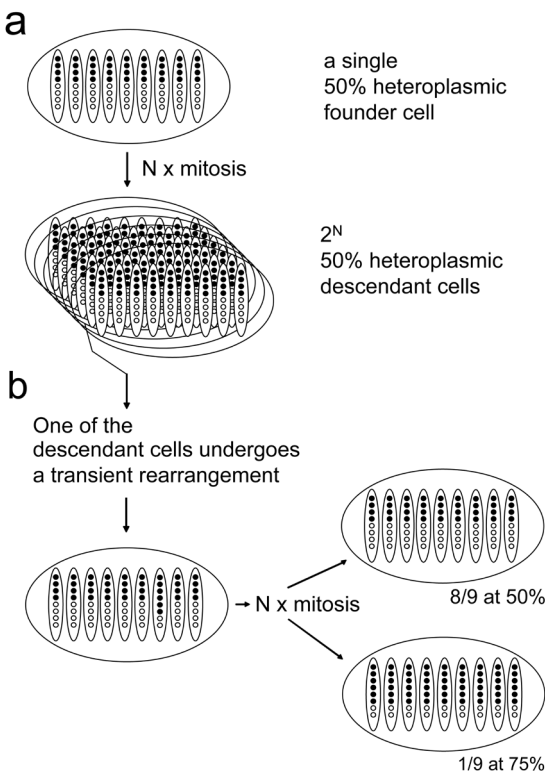


Figure 3: Model for the mitotic consequences of a genetically stable heteroplasmic segregation unit and of its rearrangement.

(a) Schematic representation of the mitotic consequences of random mtDNA segregation and a stable heteroplasmic mtDNA segregation unit. The hypothetical founding cell is 50% heteroplasmic with 72 mtDNA arranged in 9 segregation units each with 8 mtDNAs, 4 of which are variant. Upon their faithful replication and partitioning to daughter cells for  $N$  mitosis, all  $2^N$  descendant cells acquire the same 50% heteroplasmy level.

(b) Schematic representation of the mitotic consequences of a transient loss of faithful replication in one segregation unit of a cell from (a) which acquired 6 instead of 4 variant mtDNA molecules. Upon random mitotic segregation of the units, 1/9th of the cells will become fixed at 75% heteroplasmy and 8/9th at 50%. Reassembly of mtDNAs in nucleoids following a complete transient loss of nucleoid structure will result in descendant cells with heteroplasmies from 0% to 100% in discrete steps of 12.5% with binomially distributed frequencies.



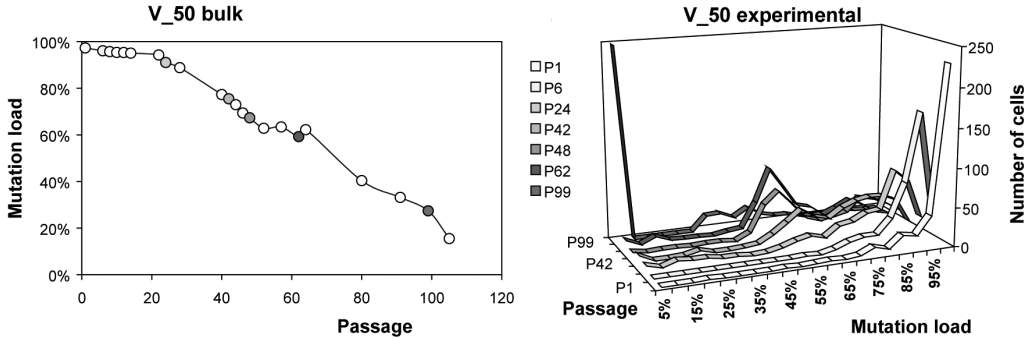


Figure 4: Bulk and single cell mutation loads of the shifting clone V\_50. Heteroplasmy evolution in V\_50 by bulk DNA mutation load analysis as a function of passage number showed apparent drift for this clone. Grey symbols correspond to the passages analyzed at the single cell level. Single cell analysis of selected passages of V\_50 (~350 cells per histogram) revealed discrete shifts in cellular mutation load.

Results described thus far were obtained with a PCR-RFLP mutation load assay based on melting curve analysis (PCR-RFMT). We confirmed qualitatively and quantitatively the G55\_2 results as well as the discretely shifted 50-55 % heteroplasmy peak in V\_50 with a different method based on direct *in situ* hybridization and ligation of A3243G padlock probes and target-primed rolling circle amplification (padlock/RCA) in combination with image analysis for quantitation purposes (17;22) as shown in Figure 5.

We explained the heteroplasmy shifts of V\_50 in terms of the metastable nucleoid, but not after having considered random segregation in combination with selection against the higher mutant cells either and/or replicative advantage for wild type. These combinations intuitively explain the overall shift from near 100% mutant to wild type. However, these combinations do predict gradual appearance of homoplasmic wild type cells only and no heteroplasmic peak such as the one seen at 50-55%, making it very unlikely that random mitotic segregation of mtDNAs is operational in these cells.

For the emergence in V\_50 of the 90-95% heteroplasmy subpopulation, we inferred that in the founding cell at least one faithfully

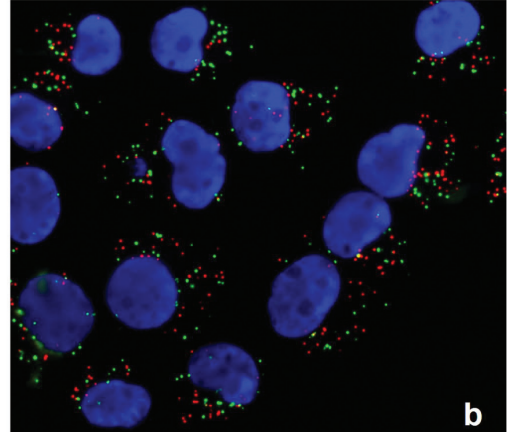
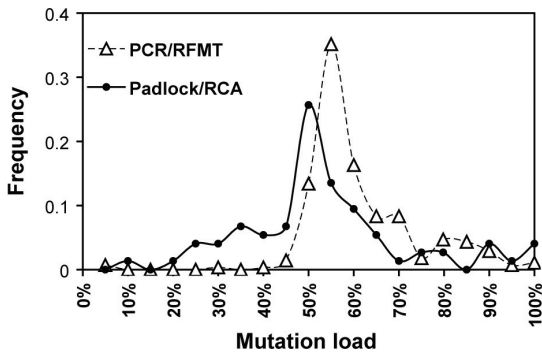
replicating 90-95% heteroplasmic segregation unit (nucleoid) was present amongst homoplasmic mutant nucleoids and that it segregated randomly so that in relative low frequency stable heteroplasmic cells emerged with uniform, 90-95% heteroplasmic, faithfully replicating nucleoids. Such a cell then clonally expanded due to growth advantage as witnessed by the significant sub-population in passage 6 at 90-95% heteroplasmy.

With chromosome instability and presence of multiple karyotypically different subclones being a hallmark of cancer cell lines, we reasoned that genetic instability of the 143B nucleus generated, by chance, nuclear determined growth advantage to one or more such 90-95% heteroplasmy cells. Chromosome analysis by Combined Binary Ratio FISH (23) showed the cybrids to possess aberrant karyotypes (not shown). Although this is indicative for genomic instability it is no formal proof. Array Comparative Genomic Hybridization (array-CGH), however, proved the nuclear genomic instability of the 143B nuclear genome (Fig. 6). Thus a scenario is plausible in which the nuclear genomic constitution of a cell, that hosted uniform 90-95% heteroplasmic mtDNA nucleoids, provided it with growth advantage, effectively leading to genetic hitchhiking of the heteroplasmic nucleoid.

We next reasoned that the heteroplasmy shifts in V\_50 from 90-95% to 50-55% and then on to 0-5% can be explained with the nucleoid if it occasionally makes errors in replication of its wild type/mutant ratio or undergoes genetic rearrangements, similar but not identical to imbalanced nuclear chromosome translocations (see Figure 3b). Such events will lead to altered wild type/mutant ratios of the nucleoids.

In the example of Figure 3b, such newly emerged 'homologous' nucleoids will segregate at a rate 8-fold faster than single mtDNAs would and thus rapidly seed cells in the population with uniform heteroplasmic nucleoids of altered genetic composition, which then may hitchhike with cells with nuclear determined growth advantage, as outlined above.

**a PCR- RFMT versus Padlock /RCA in G55\_2**



**c PCR- RFMT versus Padlock /RCA in V\_50**

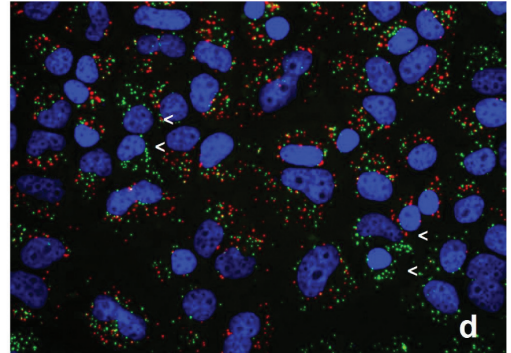
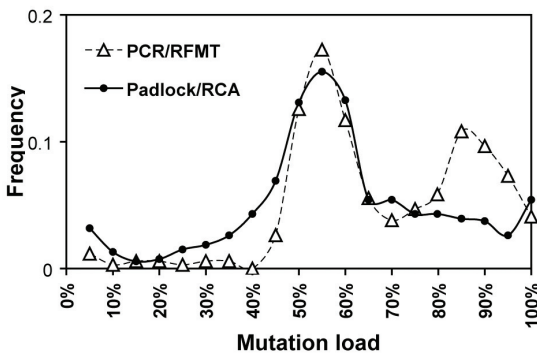


Figure 5:Quantitative and qualitative correlations between single cell A3243G mtDNA PCR-RFMT and Padlock/RCA results.

(a) Relative single cell mutation load histograms generated by PCR/RFMT for G55\_2 passage 17 (n=276) and by Padlock/RCA for passage 17 + 4 (n=74). For Padlock/RCA a liquid nitrogen aliquot was re-grown for an additional 4 passages.

(b) Photomicrographs of cells from clone G\_55 passage 17 + 4 (400x) genotyped *in situ* by Padlock/RCA. Red dots correspond to mutant and green dots to wild type mtDNA.

(c) Relative single cell mutation load histograms generated by PCR/RFMT for V\_50 passage 48 (n = 342) and by Padlock/RCA for passage 48 + 4 (n= 535). The reduction in frequency of the 85-95% range for the Padlock/RCA likely relates to the liquid nitrogen archiving and re-growth. See also Jahangir Tafrechi *et al.* for a similar correlation for GB\_20 Passage 17 (21).

(d) Photomicrographs of cells from V\_50 passage 62 + 4 (630x). Note the presence in this image of wild type daughter cells (arrow heads) amidst the heteroplasmic cells. Eventually these overtook the culture in passage 99.

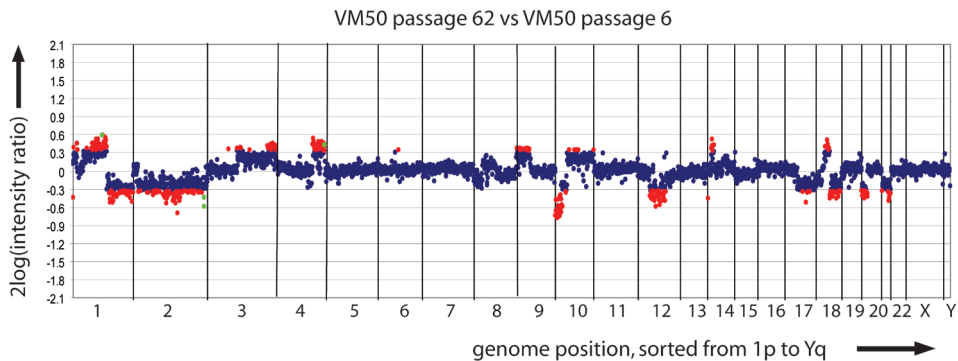


Figure 6: Chromosome instability of the 143B nuclear genome assessed by Array-Comparative Genome Hybridization with  $\sim 1$  Mbp resolution of genomic DNA from V\_50 passage 6 as test-DNA and V\_50 passage 62 as reference-DNA. Red, blue and green dots represent respectively, copy number change, no copy number change and natural copy number polymorphisms. Thresholds for gains and losses were set at a  $2\log$  change of  $\pm 0.33$  (y-axis) and all data were sorted according to chromosome number (x-axis). These results indicate the changes which did occur during 28 weeks of culturing.

This line of reasoning (reorganization and subsequent segregation of heteroplasmic nucleoids, followed by nuclear determined growth advantage of a cell with altered but uniform heteroplasmic nucleoids) may as such explain the discrete shifts from mutant to wild type seen in V\_50; it also predicts discrete shifts in cellular mutation loads from wild type to mutant. In an ongoing second similar long term segregation analysis initiated during this Thesis work with 10 subclones of passage 42 of V\_50 this was exactly what was observed. Clone, V3.18 by bulk DNA analysis gradually shifted to mutant and showed upon single cell padlock/RCA analysis a discrete cellular heteroplasmy shift from wild type to mutant (see Chapter 6 for Figure). Furthermore in support of the 'stable' element of the metastable nucleoid model, another subclone with  $\sim 1800$  mtDNAs proved to be stable at  $\sim 65\%$  heteroplasmy up to passage 81 (see Chapter 6, page 81 for Figure). Mitochondrial nucleoids are nucleo-protein complexes located in the matrix of the

mitochondrial compartment. They physically are associated with multiple mtDNAs. Molecular cytological studies indicated that the average number of mtDNA per nucleoid varies per cell type, but that it is in the range of 2-10, with  $\sim 8$  for the 143B host cell line used here (24;25). This approximate one order of magnitude difference between mtDNA and nucleoid copy number is compatible with our results. Thus the nucleoid, as a metastable segregation unit with multiple mtDNAs, likely mediates the segregation suppression and quantal segregation observed here. More similar, long term segregation studies will be needed, however, to arrive at the exact quantal number, to document cell type dependence and to answer the question whether or not the metastable nucleoid model holds for neutral and other pathogenic mtDNA mutations.

### Acknowledgements

This study was supported by grants from the Prinses Beatrix Fonds / Stichting Spieren voor Spieren and the EC-Strep Project ENLIGHT

## Reference List

1. Birky, C.W., Jr. (2001) The inheritance of genes in mitochondria and chloroplasts: laws, mechanisms, and models. *Annu.Rev.Genet.*, 35, 125-148.
2. Gross, N.J., Getz, G.S. and Rabinowitz, M. (1969) Apparent turnover of mitochondrial deoxyribonucleic acid and mitochondrial phospholipids in the tissues of the rat. *J.Biol.Chem.*, 244, 1552-1562.
3. Chinnery, P.F. and Samuels, D.C. (1999) Relaxed replication of mtDNA: A model with implications for the expression of disease. *Am.J.Hum.Genet.*, 64, 1158-1165.
4. Jenuth, J.P., Peterson, A.C., Fu, K. and Shoubridge, E.A. (1996) Random genetic drift in the female germline explains the rapid segregation of mammalian mitochondrial DNA. *Nat.Genet.*, 14, 146-151.
5. Cao, L., Shitara, H., Horii, T., Nagao, Y., Imai, H., Abe, K., Hara, T., Hayashi, J.I. and Yonekawa, H. (2007) The mitochondrial bottleneck occurs without reduction of mtDNA content in female mouse germ cells. *Nat. Genet.*, 39, 386-390
6. Jenuth, J.P., Peterson, A.C. and Shoubridge, E.A. (1997) Tissue-specific selection for different mtDNA genotypes in heteroplasmic mice. *Nat.Genet.*, 16, 93-95.
7. Battersby, B.J., Loredó-Ostí, J.C. and Shoubridge, E.A. (2003) Nuclear genetic control of mitochondrial DNA segregation. *Nat.Genet.*, 33, 183-186.
8. Chinnery, P.F., Zwijnenburg, P.J., Walker, M., Howell, N., Taylor, R.W., Lightowers, R.N., Bindoff, L. and Turnbull, D.M. (1999) Nonrandom tissue distribution of mutant mtDNA. *Am.J.Med.Genet.*, 85, 498-501.
9. Chinnery, P.F. (2002) Modulating heteroplasmy. *Trends Genet.*, 18, 173-176.
10. Yoneda, M., Chomyn, A., Martinuzzi, A., Hurko, O. and Attardi, G. (1992) Marked replicative advantage of human mtDNA carrying a point mutation that causes the MELAS encephalomyopathy. *Proc.Natl.Acad.Sci.U.S.A.*, 89, 11164-11168.
11. Dunbar, D.R., Moonie, P.A., Jacobs, H.T. and Holt, I.J. (1995) Different cellular backgrounds confer a marked advantage to either mutant or wild-type mitochondrial genomes. *Proc.Natl.Acad.Sci.U.S.A.*, 92, 6562-6566.
12. Bentlage, H.A. and Attardi, G. (1996) Relationship of genotype to phenotype in fibroblast-derived transmittochondrial cell lines carrying the 3243 mutation associated with the MELAS encephalomyopathy: shift towards mutant genotype and role of mtDNA copy number. *Hum.Mol.Genet.*, 5, 197-205.
13. Enriquez, J.A. (2003) Segregation and dynamics of mitochondrial DNA in mammalian cells. In Holt, I.J. (ed.), *Genetics of Mitochondrial Diseases*. Oxford University Press, Oxford, pp. 279-294.
14. Lehtinen, S.K., Hance, N., El Meziane, A., Juhola, M.K., Juhola, K.M., Karhu, R., Spelbrink, J.N., Holt, I.J. and Jacobs, H.T. (2000) Genotypic stability, segregation and selection in heteroplasmic human cell lines containing np 3243 mutant mtDNA. *Genetics*, 154, 363-380.
15. Jacobs, H.T., Lehtinen, S.K. and Spelbrink, J.N. (2000) No sex please, we're mitochondria: a hypothesis on the somatic unit of inheritance of mammalian mtDNA. *Bioessays*, 22, 564-572.
16. King, M.P. and Attardi, G. (1989) Human cells lacking mtDNA: repopulation with exogenous mitochondria by complementation. *Science*, 246, 500-503.
17. Larsson, C., Koch, J., Nygren, A., Janssen, G., Raap, A.K., Landegren, U. and Nilsson, M. (2004) In situ genotyping individual DNA molecules by target-primed rolling-circle amplification of padlock probes. *Nat.Methods*, 1, 227-232.
18. Jahangir Tafrechi, R.S., van de Rijke, F.M., Allallou, A., Larsson, C., Sloos, W.C., van de, S.M., Wahlby, C., Janssen, G.M. and Raap, A.K. (2007) Single-cell A3243G mitochondrial DNA mutation load assays for segregation analysis. *J.Histochem.Cytochem.*, 55, 1159-1166.
19. Suzhai, K., Ouweland, J., Dirks, R., Lemaitre, M., Truffert, J., Janssen, G., Tanke, H., Holme, E., Maassen, J. and Raap, A. (2001) Simultaneous A8344G heteroplasmy and mitochondrial DNA copy number quantification in myoclonus epilepsy and ragged-red fibers (MERRF) syndrome by a multiplex molecular beacon based real-time fluorescence PCR. *Nucleic Acids Res.*, 29, E13.

20. Knijnenburg,J., Szuhai,K., Giltay,J., Molenaar,L., Sloos,W., Poot,M., Tanke,H.J. and Rosenberg,C. (2005) Insights from genomic microarrays into structural chromosome rearrangements. *Am.J.Med. Genet.A*, 132, 36-40.
21. Jahangir Tafrechi,R.S., Rijke F.M.van de, Allalou,A., Larsson,C., Sloos,W.C.R., van de Sande,M., Wahlby,C., Janssen,G.M.C. and Raap,A.K. Single cell A3243G mitochondrial mtDNA mutation load assays for segregation analyses. *J Histochem.Cytochem.* 2007.
22. Allalou,A., van de Rijke,F.M., Jahangir Tafrechi,R.S., Raap,A.K. and Wahlby,C. (2007) Image based measurements of single cell mtDNA mutation load. In: *Image Analysis; Lecture Notes in Computer Science Vol 4522* pp 631-640. Springer Berlin/Heidelberg
23. Tanke,H.J., Wiegant,J., van Gijlswijk,R.P., Bezrookove,V., Pattenier,H., Heetebrij,R.J., Talman,E. G., Raap,A.K. and Vrolijk,J. (1999) New strategy for multi-colour fluorescence in situ hybridisation: COBRA: COmbined Binary RAtio labelling. *Eur.J Hum.Genet.*, 7, 2-11.
24. Legros,F., Malka,F., Frachon,P., Lombes,A. and Rojo,M. (2004) Organization and dynamics of human mitochondrial DNA. *J.Cell Sci.*, 117, 2653-2662.
25. Iborra,F.J., Kimura,H. and Cook,P.R. (2004) The functional organization of mitochondrial genomes in human cells. *BMC.Biol.*, 2, 9.





# 4

## Distinct nuclear gene expression profiles in cells with mtDNA depletion and homoplasmic A3243G mutation

Roshan S. Jahangir Tafrechi\*, J. Peter Svensson‡, George M. C. Janssen\*, Karoly Szuhai\*, J. Antonie Maassen\* and Anton K. Raap\*§

\* Department of Molecular Cell Biology, Leiden University Medical Center, P.O. Box 9503, 2300 RA Leiden, The Netherlands

‡ Department of Toxicogenetics, Leiden University Medical Center, P.O. Box 9503, 2300 RA Leiden, The Netherlands and  
Department of Oncology, Radiology and Clinical Immunology, University Hospital, 75185, Uppsala, Sweden.





## Abstract

The pathobiochemical pathways determining the wide variability in phenotypic expression of mitochondrial DNA (mtDNA) mutations are not well understood. Most pathogenic mtDNA mutations induce a general defect in mitochondrial respiration and thereby ATP synthesis. Yet phenotypic expression of the different mtDNA mutations shows large variations that are difficult to reconcile with ATP depletion as sole pathogenic factor, implying that additional mechanisms contribute to the phenotype. Here we use DNA micro-arrays to identify changes in nuclear gene expression resulting from the presence of the A3243G diabetogenic mutation and from a depletion of mtDNA ( $\rho^0$  cells). We find that cells respond mildly to these mitochondrial states with both general and specific changes in nuclear gene expression. This observation indicates that cells can sense the status of mtDNA. A number of genes show divergence in expression in  $\rho^0$  cells compared to cells with the A3243G mutation, such as genes involved in oxidative phosphorylation. As a common response in A3243G and  $\rho^0$  cells, mRNA levels for extracellular matrix genes are up-regulated, while the mRNA levels of genes involved in ubiquitin-mediated protein degradation and in ribosomal protein synthesis is down-regulated. This reduced expression is reflected at the level of cytosolic protein synthesis in both A3243G and  $\rho^0$  cells.

Our finding that mitochondrial dysfunction caused by different mutations affects nuclear gene expression in partially distinct ways, suggests that multiple pathways link mitochondrial function to nuclear gene expression and contribute to the development of the different phenotypes in mitochondrial disease.

Key words: mitochondria, mtDNA, expression, diabetes

## Introduction

Mitochondrial dysfunction caused by mutations in the mitochondrial genome is related to a variety of diseases such as type two diabetes mellitus (DM2), cancer and neuro-muscular diseases (1). Mitochondria are involved in multiple cellular processes of which ATP production by oxidative phosphorylation (OXPHOS) is the most prominent one. However, mitochondria also accommodate other processes such as the tricarboxylic acid cycle and fatty acid oxidation. In addition, mitochondrial function is linked to calcium, iron and ROS signalling and apoptotic pathways. The variation in clinical phenotype of mitochondrial diseases is difficult to explain by merely a reduced respiration rate (2). Rather the consequences of additional mitochondrial dysfunction on retrograde signalling pathways may determine the distinct nature of the clinical manifestation (3). A genome-wide differential gene transcription profile of normal cells and cells with dysfunctioning

mitochondria is expected to give insight in the pathobiochemical pathways affected in mitochondrial disease (4;5).

In order to investigate how mitochondrial mutations affect the nuclear gene expression profile we created 143B cybrid cells with mitochondrial DNA being the only variable (6). The first state of respiratory dysfunction is induced by an A to G conversion at location 3243 in the tRNA<sup>Leu</sup> gene of the mitochondrial DNA. This mutation causes Maternally Inherited Diabetes and Deafness (MIDD) (7) in most carriers and associates also with the neuromuscular MELAS syndrome (8). Another state of mitochondrial dysfunction is induced by a depletion of mtDNA ( $\rho^0$  cells). Using cybrid cells with 100% wild-type mitochondrial DNA, cybrid cells with 100% A3243G mutant mitochondrial DNA of the same haplotype and  $\rho^0$  cells, we found both common mitochondrial-defect and MIDD specific responses in nuclear gene expression.

## Materials and methods

Cell culture, cell characteristics and GeneChip hybridization

The cybrid cells used in this report have been previously described (2;9). In short, 143B osteosarcoma cells were treated with ethidium bromide to create  $\rho^0$  cells devoid of mitochondrial DNA. Next,  $\rho^0$  cells were fused with enucleated cells from a MIDD patient, generating clones with different but stable heteroplasmy levels for the 3243 mutation. Two apparently homoplasmic mutant (VM48 and VM50) and two apparently homoplasmic wild-type (VW6 and VW7) cybrid clones were selected and used as biological replicates in this study. The cells were grown on Dulbecco's Modified Eagle's medium containing 4.5 mg/ml glucose and 110 g/ml pyruvate (DMEM) supplemented with 50 g/ml uridine and 10% fetal bovine serum. Heteroplasmy levels were monitored by use of PCR-RFLP and ApaI, which cleaves the mutated PCR product.

The oxygen consumption of the cells was measured as described previously (6). Mitochondrial copy numbers were determined by comparing the amount of mitochondrial DNA with the amount of  $\alpha$ -globin DNA, in a SybrGreen Real Time PCR reaction with the primers described in Szuhai *et al.* (10) and using the ABI Prism 7700 spectrofluorometric thermal cycler (Applied Biosystems, USA). The same system was used for validation of the mRNA concentration data obtained by chip hybridisation analysis. Primer sets for ten different genes were used, including three that were found to be differentially and consistently expressed:

NADH dehydrogenase 18 (5'ACGAACCT-TACCCGGATGATG + 5'CATGGATCTCTCT-CATGCTGTGAG), ubiquitin-conjugating enzyme E2D3 (5'ATCACAGTGGTCGCCT-GCTT + 5'ATAGATCCGTGCAATCTCTGGC) and collagen VI2 (5'CATCGATGACATGGAG-GACGT + 5'CAGCTCTGTTTGGCAGGGAA). The primers were all manufactured by Eurogentec, Belgium.

Cytoplasmic protein synthesis rate was estimated from the incorporation of L-[4,5- $^3$ H]-leucine into trichloroacetic acid precipitable material essentially as described (2). In brief, series of cells at different densities in 6-well plates were washed with phosphate-buffered saline and incubated for 60 min. at 37° C in 0.75 ml of leucine-free complete medium containing 10  $\mu$ Ci of L-[4,5- $^3$ H]-leucine and 10  $\mu$ M unlabelled leucine. Cells were then again washed three times with phosphate-buffered saline and thoroughly dissolved in 1 ml 0.2 M NaOH. 100  $\mu$ l aliquots were precipitated by the addition of 100  $\mu$ l 20 % trichloroacetic acid, and assayed for total protein content by a bicinchoninic acid based protein assay (Pierce, USA) and for the incorporation of [ $^3$ H]-leucine into protein using a GF/C filter assay. The rate of protein synthesis is expressed as the amount of [ $^3$ H]-leucine incorporated into 1  $\mu$ g protein during the 1-hour incubation period (cpm. $\mu$ g $^{-1}$ .h $^{-1}$ ). Protein concentration was also used as an estimate for cell density.

Biotinylated cRNA samples were prepared according to the Affymetrix GeneChip protocol. In short, cells at 90% confluency were washed with phosphate buffered saline and directly lysed in RNA-Bee solution (Tel-Test, USA). RNA purification was performed with the RNeasy mini kit (Qiagen, Germany). With the intensity-ratio of the 28S/18S rRNA bands being over 1.8, the integrity of the RNA was confirmed. 20  $\mu$ g of total RNA was used to perform double-stranded cDNA synthesis with an oligo T<sub>7</sub>-dT<sub>24</sub> primer and SuperScript kit (Invitrogen Life Technologies, USA). The cDNA was purified with Phase Lock Gel-reaction tubes (Eppendorf, Germany) and the complete pellet was used for a simultaneous 6-hour *in vitro* transcription and labeling reaction using the MegaScript T7 kit (Ambion, USA) and biotin-11-CTP/biotin-16-UTP (PerkinElmer Life Sciences, USA). Finally, 20  $\mu$ g fragmented cRNA was used for hybridization on Affymetrix HG-U133 chips, according to the manufacturer's instruction. Affymetrix' Microarray Suite 5.0 Software (MAS) was used to determine the percentage

of transcripts Present and the 3'/5' intensity ratios for  $\beta$ -actin and GAPDH.

Probe Level Analysis (PLA) and Gene Set Enrichment Analysis (GSEA)

Most data analyses were performed in R ([www.r-project.org](http://www.r-project.org)) using the Bioconductor functions ([www.bioconductor.org](http://www.bioconductor.org)). Intensity data was corrected for background arising from optical noise as well as from non-specific hybridisation, according to the procedure developed by Wu *et al.* (11) and annotations were added using the annotation package `hgu133a`, version 1.3.1 (12). The arrays were normalized using the VSN-transformation (13).

To determine differential expression of the genes on the array, the pre-processed data were handled using the algorithms described in Liu *et al.* (14) which makes use of the feature that each transcript is represented by eleven 25-mer perfect-match probes. The scripts for data processing are available at [www.medgencentre.nl/pla](http://www.medgencentre.nl/pla). In short, the eleven probe-intensities of each transcript from a reference hybridisation (VW6 or VW7) were compared to the eleven probe-intensities of the corresponding transcript from a test-hybridisation (VM48, VM50,  $\rho^0_1$  or  $\rho^0_2$ ) using paired Wilcoxon statistics (15) to calculate a one-tailed p-value. The signals from the mismatch probes were not subtracted. A perturbation factor was set at 1.1 to exclude transcripts with very small changes in their intensity levels (14). The most conservative one-tailed p-value (the one closest to 0.5) was assigned as the change-value. If the p-values after perturbation are on opposite sides of 0.5, the transcript will be classified as 'not changed' and it will be assigned a change-value of 0.5.

For all transcripts in pair-wise comparisons the test will assign a change-value between 0 and 1. A change-value of 0 indicates that all probe-intensities of a test-transcript are higher than the corresponding probe-intensities of the reference-transcript. Conversely, a change-value of 1 corresponds to an overall decrease.

All change-values between these two extremes indicate a partial or complete overlap of the probe intensity-patterns. When there is a totally random pattern (at noise-level intensity) the change-value will be 0.5 and the corresponding transcript is considered as not changed in mRNA concentration.

Subtle changes are considered to be of biological relevance if the change is consistent within a gene set. Therefore, as a second approach, Gene Set Enrichment Analysis (GSEA) was performed on all 22,283 transcripts to pinpoint the most coherently changed gene sets per comparison (16). Gene sets were derived from the Kyoto Encyclopaedia of Genes and Genomes (KEGG) and from the Gene Ontology consortium (GO). Expression changes were calculated with Signal to Noise Ratio's.

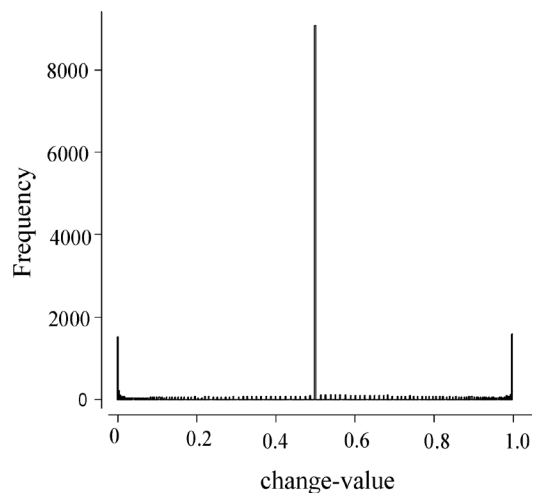


Fig. 1. Frequency histogram of the PLA change-values.

This histogram depicts the amount of transcripts with a change in expression level between 3243 mutant clone VM48 and wild type clone VW6. Values between 0 and 0.5 indicate an increase, values between 0.5 and 1 a decrease.

A perturbation factor of 1.1 has been used.

## Results

### Cell characteristics and quality controls

The cybrid cell lines selected for gene expression profiling were comparable to each other with respect to cell morphology, doubling time (range 13h - 18h) and cell viability (~ 4% trypan blue stained cells). The average oxygen consumption of the wild-type cybrids was  $1.3 \pm 0.3$  fmol/min/cell ( $n = 10$ ), while this value for the 100% 3243 mutant cybrids was  $0.1 \pm 0.1$  fmol/min/cell ( $n = 5$ ).  $\rho^0$  cells did not respire at all. Mitochondrial copy numbers of the wild type and the 3243 mutant cybrids were comparable (Real Time PCR data not shown). For mRNA expression profiling the cells were grown under standardized conditions to ~90% confluence. Quality control was performed at each step of RNA isolation and cRNA synthesis and no variations were detected in yields and length distribution of the products. Before starting PLA and GSEA analysis we demanded that the fraction of detectable or 'present' genes and the 3'/5' hybridisation ratio fell within Affymetrix' boundaries (< 10% variation and < 3 respectively). For the 6 hybridisations, the mean percentage 'present' transcripts was  $47.5 \pm 0.9\%$  and the 3'/5' ratios were  $1.2 \pm 0.09$  for actin and  $0.9 \pm 0.04$  for GAPDH. Quantitative RT-PCR data for 10 different mRNAs correlated very well qualitatively and to large extent quantitatively with chip hybridisation and PLA data (not shown), which is in accord with recent literature comparing different gene expression platforms (17;18).

### Probe Level Analysis

An intensity frequency histogram was generated using all the transcripts from all 6 hybridisations after correction for optical noise and non-specific hybridisation. Based on this histogram the threshold for minimal intensity was set to 25. 30% of the 22,283 transcript represented on the HG-U133A micro-array was expressed above threshold in at least one cell type. The average expression of these 6691 transcripts was 516.

The frequency histogram of the PLA change-values in the comparison VM48 versus VW6 is shown in figure 1 as an example. It illustrates that the majority of transcript are not changed in expression and that most of the remaining transcripts have a change-value of 0 or 1. For a given transcript to be included in the list of differentially expressed transcripts, we demanded that all four change-values associated with it are either all > 0.5 (decreased) or all < 0.5 (increased). With this criterion, 553 of the 6691 transcripts (8%) were considered differentially expressed when comparing the 3243 mutant to wild type cells. The number of differentially expressed transcripts in the comparison between  $\rho^0$  cells and wild type cells was more than 3-fold higher (28%). Notably, in the comparison of  $\rho^0$  and 3243 mutant 1581 transcripts (24%) were found to be changed (Table 1). The 553 transcripts found in the 3243 mutant versus wild type comparison do not constitute a full subset of the 1869 transcripts of the  $\rho^0$  versus wild type comparison. The single-nucleotide A3243G substitution and the absence of mt-DNA apparently reschedule the nuclear gene expression in different ways.

Table 1. Number of transcripts changed in two-way comparisons

Two-way comparison	# Changed Transcripts	Relative amount	# Down-regulated	# Up-regulated
3243_Wt	553	8,3 %	295	258
$\rho^0$ _Wt	1869	27,9 %	719	1150
$\rho^0$ _3243	1581	23,6 %	1031	550

The transcripts changed in the 3243 versus wild type comparison is not a complete subset of any other comparison

A three-way cell type comparison technique was used to identify the transcripts that behave similarly in the two types of dysfunctioning cells (A3243G and  $\rho^0$ ) as well as the transcripts that behave distinctively. Note that in this comparison with duplicate hybridisation experiments, eight change-values are to be considered: 2 A3243G cell clones versus 2 wild type cell clones and 2 times  $\rho^0$  versus the 2 wild type cell clones. As a result the stringency for inclusion of transcripts in the lists of differentially expressed transcripts is further increased, because for generation of the 'common change' list it was demanded that all eight (2 x 4) change-values indicate a change in the same direction. Similar, to generate the 'specific' lists, it was demanded that none of the four corresponding change-values of the other mutant versus wild type comparison indicate a change in the same direction. All transcripts that did not exactly meet one of these two criteria were rejected. The results are presented as a Venn diagram in figure 2, which shows that 229 transcripts have a similar change of expression in both mitochondrial mutant cell lines. Interestingly, 155 transcripts are changed specifically in  $\rho^0$  cells whereas 73 additional transcripts are specifically altered in 3243 mutant cells.

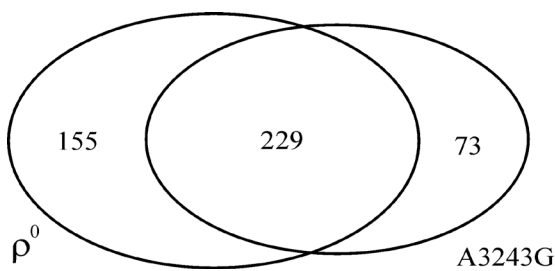


Fig. 2. Three-way comparison  
This Venn diagram shows the number of transcripts that are changed in common and specifically when compared to wild type cybrids cells. The three groups shown in this figure correspond to the 6 supplemented lists, where the up- and down-regulated transcripts are presented separately.

The relative changes in gene expression due to mtDNA mutations appear to be rather mild with maximal differences of  $\sim 5$ -fold and no on/off situations. The transcripts with a 2-fold change in any of the three cell-type comparisons are listed in Table 2. The quantitative RT-PCR data of three differentially expressed genes are included. Tables 4 through 9 in the supplementary material contain the PLA data of all 457 differentially expressed transcripts.

#### Gene Set Enrichment Analysis

In contrast to PLA, which analyses differences in expression of individual transcripts, Gene Set Enrichment Analysis (GSEA) pinpoints sets of genes that are coherently changed in their expression. When using the Kyoto Encyclopaedia of Genes and Genomes (KEGG) and the Gene Ontology consortium (GO) data bases as predefined input gene sets, GSEA calculates for each cell type comparison an enrichment score for all gene sets (16), ranging from 0 to well over 300. Both KEGG and the GO consortium provide a controlled vocabulary to describe gene products, which are grouped together according to process, pathway or localization. In the case of KEGG, the transcripts on the HG-U133A chip are divided into 107 pathway-specific gene sets. The GO consortium on the other hand, makes use of three different classifications according to Biological Process (GO-BP), Cellular Component (GO-CC) and Molecular Function (GO-MF). GO-CC divides the transcripts into 356, GO-BP into 1317 and GO-MF into 1461 gene sets. For all of these predefined gene sets, enrichment scores were calculated for all three comparisons (supplementary material table 10). Gene sets with an ES above a threshold of 300 may be considered as biologically significant since they represent 2.5% of all 3241 gene sets. Representative gene sets of these 82 gene sets are depicted in Table 3. Three types of effect may be distinguished: mutant-specific effects, effects common to both  $\rho^0$  and A3243G and opposite effects.

Table 2. Transcripts changed more than two fold.

Affy-code	R/W	M/W	R/M	Description
Opposite effect				
39729_at	2,16	0,44	4,86	peroxiredoxin 2
200734_s_at	2,89	0,93	3,12	ADP-ribosylation factor 3
218275_at	2,04	0,90	2,27	solute carrier family 25 (mit, carrier; dicarboxylate transporter), member 10
213421_x_at	2,00	0,99	2,01	protease, serine, 3 (mesotrypsin)*
201227_s_at	1,93 (1.99)	0,92 (0.98)	2,10 (2.23)	NADH dehydrogenase (ubiquinone) 1 beta subcomplex, 8, 19kDa
207076_s_at	1,53	5,27	0,29	argininosuccinate synthetase
213506_at	0,73	2,07	0,35	chaperonin containing TCP1, subunit 3 (gamma)*
201012_at	0,48	1,49	0,32	annexin A1
208944_at	0,49	1,46	0,34	transforming growth factor, beta receptor II (70/80kDa)†
44783_s_at	0,33	1,39	0,24	hairy/enhancer-of-split related with YRPW motif 1
202006_at	0,44	1,13	0,38	protein tyrosine phosphatase, non-receptor type 12
Common effect				
209156_s_at	4,50 (1.50)	4,08 (1.47)	1,09 (1.02)	collagen, type VI, alpha 2†
201438_at	3,01	3,68	0,81	collagen, type VI, alpha 3†
213905_x_at	2,91	2,48	1,17	biglycan†
201673_s_at	2,77	2,39	1,16	glycogen synthase 1 (muscle)
220642_x_at	2,53	2,27	1,12	putative G-protein coupled receptor
211964_at	3,10	2,20	1,41	collagen, type IV, alpha 2†
200815_s_at	2,38	2,03	1,17	platelet-activating factor acetylhydrolase, isoform Ib, alpha subunit 45kDa
212048_s_at	2,27	1,87	1,21	tyrosyl-tRNA synthetase
200623_s_at	2,31	1,71	1,36	calmodulin 3 (phosphorylase kinase, delta)
203137_at	0,50	0,45	1,10	Wilms tumor 1 associated protein
203008_x_at	0,44	0,53	0,84	ATP binding protein associated with cell differentiation
209137_s_at	0,50	0,69	0,72	ubiquitin specific protease 10*
200667_at	0,40 (0.58)	0,60 (0.62)	0,66 (0.94)	ubiquitin-conjugating enzyme E2D 3 (UBC4/5 homolog, yeast)*
203432_at	0,50	0,77	0,66	thymopoietin
201901_s_at	0,46	0,79	0,58	YY1 transcription factor

W = 100% wild type cybrid cells, M = 100% A3243G mutant and R = depletion of mtDNA.

Data in brackets is calculated from real time pcr data.

\*Transcripts associated with ubiquitinylation.

†Transcripts associated with extracellular matrix formation.



Table 3. Enrichments scores for biological clustering groups.

GSEA	3243_wt (ES)*	$\rho^0$ _wt	$\rho^0$ _3243
Common effect			
MF: ubiquitin-protein ligase activity†	316 ↓	321 ↓	217 ↓
MF: RNA binding activity	533 ↓	583 ↓	196 ↓
KEGG: ribosome†	360 ↓	306 ↓	↑ 260
CC: collagen	↑ 231	↑ 353	↑ 121
A3243G specific			
MF: actin binding activity	↑ 428	↑ 173	255 ↓
MF: Ca2+ binding activity	↑ 333	↑ 138	157 ↓
CC: basement membrane	↑ 327	↑ 135	192 ↓
KEGG: alanine and aspartate metabolism	↑ 326	↑ 199	138 ↓
$\rho^0$ specific			
BP: amino acid transport	↑ 195	↑ 326	↑ 302
CC: nuclear pore	227 ↓	535 ↓	500 ↓
BP: mitosis	202 ↓	367 ↓	321 ↓
Opposite effect			
CC: mitochondrion†	271 ↓	↑ 341	↑ 584
KEGG: ubiquinon biosynthesis	215 ↓	↑ 237	↑ 310
BP: TGF- $\beta$ receptor signaling pathway	↑ 142	191 ↓	322 ↓

\*The threshold for the enrichment score (ES) is set at 300. The arrows indicate either a global decrease or increase of the transcripts in the cluster.

†The three criteria 'ubiquitin-protein ligase activity', 'ribosome' and 'mitochondrion' have similar results for comparable criteria in all of the other groups.

### Correlation of GSEA and PLA

Both the PLA and GSEA techniques indicate moderate but significant effects of mtDNA mutations on the nuclear expression profile of osteosarcoma cells. Because it is reasonable to assume that relatively mild effects of mtDNA mutations on nuclear gene expression are of biological interest, we have chosen to focus on coherently changed gene sets using the GSEA method and to use PLA as confirmation.

The KEGG gene set 'ribosome' was found down-regulated in both the 3243 mutant (ES = 360) and in  $\rho^0$  cells (ES = 306). The three corresponding GO groups gave similar results. The average effect on ribosomal protein gene expression was small (< 10%) but consistent ( $p < 0,01$ ), and always found more strongly down-regulated in 3243 mutant cells than in  $\rho^0$  cells.

The mRNA expression of both the mitochondrial and the cytoplasmic ribosomal proteins was affected, but the expression of cytoplasmic protein genes for the small ribosomal subunit 40S (GO:0005843) seems to be affected most (Figure 3A). To analyse whether this small reduction in expression of cytosolic ribosomal protein genes has any biological consequence we measured the rate of cytosolic protein synthesis as reflected by [ $^3$ H]-leucine incorporation in these cell lines. Both the A3243G and  $\rho^0$  cells do indeed show an unambiguous reduction in protein synthesis rate compared to the wild type cell lines as shown in figure 3B.

The proteins involved in ubiquitin-mediated proteolysis were also found coherently down-regulated in both mutant cells. Within the KEGG data base one can find the 'ubiquitin



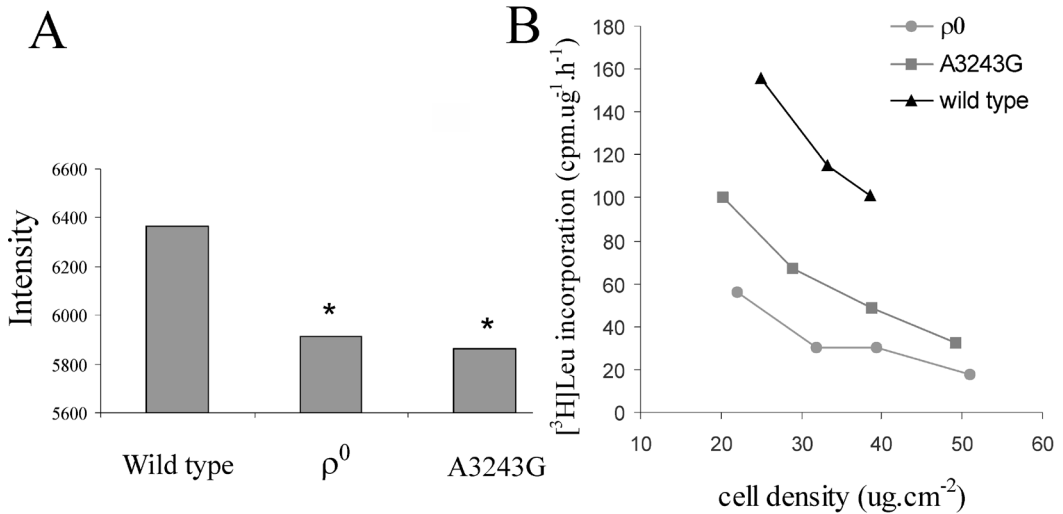


Fig. 3. A: Comparison of the average mRNA levels of all 47 proteins of the cytoplasmic small ribosomal subunit

\*The change is highly significant for both  $\rho^0$  and 3243 mutant according to a standard paired t-test ( $p=3 \times 10^{-3}$  and  $3 \times 10^{-8}$  respectively).

B: Cytoplasmic protein synthesis is lower in both mutant cell lines

Because protein synthesis slows down when cells reach confluence (2), its rate is shown as a function of cell density, which is expressed as the amount of protein per cm<sup>2</sup> substratum.

For gene expression profiling, cells were harvested at a density of ~40 g protein/cm<sup>2</sup>.

mediated proteolysis' gene set. However in the GO data base, these genes are found rather scattered throughout the gene sets: Within GO-MF four different gene sets with ubiquitin-related proteins can be recognized: 'ubiquitin-protein ligase activity', 'ubiquitin C-terminal hydrolase activity', 'ubiquitin-specific protease activity' and 'ubiquitin conjugating enzyme activity'. Within GO-BP there are two gene sets present: 'ubiquitin cycle' and 'ubiquitin-dependent protein catabolism'. All these gene sets have an ES > 300 for down-regulation in  $\rho^0$  and an ES ~300 for down-regulation in 3243 cells. In line with this, two transcripts involved in ubiquitin mediated proteolysis were found > 2-fold down-regulated according to PLA (Table 2).

The extracellular matrix proteins were found to be up-regulated in both mutant cell lines. In the GO-CC data base the group 'collagen' clearly emerged for the  $\rho^0$  cells and to a lesser extent also for the 3243 mutant cell. This result was confirmed by PLA, where three different collagens as well as the pericellular

matrix protein biglycan can be found strongly up-regulated, this time with the 3243 mutant showing a much larger effect compared to the  $\rho^0$  cells (Table 2).

The KEGG defined gene set 'oxidative phosphorylation' was found specifically up-regulated in  $\rho^0$  cells (ES = 384). The enrichment score for the oxidative phosphorylation genes is even larger (ES = 424) in the  $\rho^0$  versus 3243 comparison. Comparable enrichment scores were found for GO-MF 'NADH dehydrogenase activity', GO-CC 'mitochondrion' and GO-BP 'oxidative phosphorylation, NADH to ubiquinone'.

## Discussion

With the aim to elucidate pathways involved in mitochondrial-nuclear genome cross-talk, we have undertaken a genome-wide analysis of the alterations in nuclear gene expression in response to two different types of mtDNA mutations that both provoke mitochondrial dysfunction such as loss of mtDNA encoded

proteins and respiration (8;19). The transmitochondrial fusion technique developed by Attardi and co-workers (6) permitted the generation of cybrid cell lines with the mtDNA genome being the only variable, thus excluding variations due to mtDNA haplotype and nuclear background (20). Depletion of mtDNA or introduction of MIDD-derived A3243G mtDNA in 143B osteosarcoma cells led to failure of the cells to respire. As a control we used cells containing wild type mtDNA derived from the same MIDD patient.

Relative mRNA abundances were measured using Affymetrix GeneChip technology on two independently grown clones of each cell type. With a novel Probe Level Analysis technique we distinguished changes in the expression of individual genes that are common to the two types of mutation as well as mutation-specific ones (Table 2). Overall, the magnitude of changes in expression was moderate; only a handful genes reached  $\sim 4$ -fold changes. The genes and associated pathways identified by Probe Level Analysis overlapped considerably with those found independently by Gene Set Enrichment Analysis, which is well suited for identifying consistent changes in gene sets involved in given pathways (16). Our main conclusion therefore is that the mutational mtDNA status is sensed by the nuclear genome and reacted upon in a common and a mutation specific way.

The common responses likely originate from a failure of oxidative phosphorylation. They include down-regulation of ribosomal protein genes and up-regulation of extracellular matrix genes, the latter also observed in respiration-deficient cybrids containing dimer mtDNA (4). The presence of the A3243G mutation and the absence of mtDNA also seem to induce mutation-specific signals towards the nuclear genome. A similar view has emerged from studies in yeast (21) where different respiratory chain inhibitors and the absence of mtDNA also induced different transcriptional responses. Taken together, it is conceivable that nuclear transcription is reprogrammed by the mitochondrial DNA status through different

sensing mechanisms, similar to retrograde signalling in yeast (3). On its turn, mtDNA replication and transcription is stimulated by the nuclear co-activator PGC-1, the nuclear respiratory factors, the general transcription factor Sp1 and mitochondrial transcription factor TFAM (22;23), emphasizing the mutual dependence and interplay between both genomes.

We were intrigued by the small but consistent change in expression of the ribosomal proteins. Therefore we conducted an experiment to confirm these data on protein synthesis activity. Indeed the protein synthesis rate, in both the A3243G mutant and the  $\rho^0$  cells, is significantly lower compared to wild type cells. The view emerges that cells with defective energy supply down regulates energy demanding processes like protein synthesis (24). In accordance, genes involved in protein breakdown are also down-regulated, possibly in an attempt to compensate for the danger of an unbalance in protein metabolism. A study in yeast recently revealed that the abundance of ribosome biogenesis factors, which are more often co-ordinately down-regulated, is controlled at the level of mRNA stability (25). Since insulin production is highly depending on ribosome activity, it is tempting to speculate that a decreased rate of protein synthesis in the pancreatic  $\beta$ -cell might contribute to the pathogenesis of the diabetic phenotype. Notwithstanding the limitations of a model system like cultured osteosarcoma cells for the diabetic phenotype, it is remarkable that mitochondrial dysfunction often associates with diabetes and at least in the case of the A3243G mutation this is due to a reduction in insulin secretion capacity of the pancreatic beta cell (26). Mitochondrial dysfunction is strongly linked with development of diabetes type 2 (27;28). Expression studies with muscle tissue from diabetic humans (16;29) and mice (30;31) show mild down-regulation of nuclear OXPHOS genes, likely a consequence of hyperglycemia. In contrast, expression studies with muscle tissue and fibroblast cells from mitochondrial disease patients show

an increased expression of nuclear OXPPOS genes (32;33). As such, up-regulation may be considered a compensatory effect for the mitochondrial dysfunction. Accordingly, we found an up-regulation in OXPPOS genes in the mtDNA depleted  $\rho^0$  cell line, but no significant effect of OXPPOS gene expression was seen in the cells with the diabetogenic A3243G mutation. Taken together these observations, indicate the existence of at least two different mechanisms for OXPPOS gene regulation.

In conclusion, our data clearly demonstrate the presence of both general and specific communication routes between the mtDNA and the nuclear genomes and may contribute to the identification of pathways determining the specificity of mitochondrial diseases.

## Reference List

1. Leonard, J.V. and Schapira, A.H. (2000) Mitochondrial respiratory chain disorders I: mitochondrial DNA defects. *Lancet*, 355, 299-304.
2. Janssen, G.M., Maassen, J.A. and van Den Ouweland, J.M. (1999) The diabetes-associated 3243 mutation in the mitochondrial tRNA(Leu)(UUR) gene causes severe mitochondrial dysfunction without a strong decrease in protein synthesis rate. *J.Biol.Chem.*, 274, 29744-29748.
3. Butow, R.A. and Avadhani, N.G. (2004) Mitochondrial signaling: the retrograde response. *Mol.Cell*, 14, 1-15.
4. Clark, K.M., Brown, T.A., Davidson, M.M., Papadopoulou, L.C. and Clayton, D.A. (2002) Differences in nuclear gene expression between cells containing monomer and dimer mitochondrial genomes. *Gene*, 286, 91-104.
5. Delsite, R., Kachhap, S., Anbazhagan, R., Gabrielson, E. and Singh, K.K. (2002) Nuclear genes involved in mitochondria-to-nucleus communication in breast cancer cells. *Mol.Cancer*, 1, 6.
6. King, M.P. and Attardi, G. (1989) Human cells lacking mtDNA: repopulation with exogenous mitochondria by complementation. *Science*, 246, 500-503.
7. van Den Ouweland, J.M., Lemkes, H.H., Ruitenbeek, W., Sandkuijl, L.A., de Vijlder, M.F., Struyvenberg, P.A., van de Kamp, J.J. and Maassen, J.A. (1992) Mutation in mitochondrial tRNA(Leu)(UUR) gene in a large pedigree with maternally transmitted type II diabetes mellitus and deafness. *Nat.Genet.*, 1, 368-371.
8. Jacobs, H.T. (2003) Disorders of mitochondrial protein synthesis. *Hum.Mol.Genet.*, 12 Suppl 2, R293-R301.
9. van Den Ouweland, J.M., Maechler, P., Wollheim, C.B., Attardi, G. and Maassen, J.A. (1999) Functional and morphological abnormalities of mitochondria harbouring the tRNA(Leu)(UUR) mutation in mitochondrial DNA derived from patients with maternally inherited diabetes and deafness (MIDD) and progressive kidney disease. *Diabetologia*, 42, 485-492.
10. Szuhai, K., Ouweland, J., Dirks, R., Lemaitre, M., Truffert, J., Janssen, G., Tanke, H., Holme, E., Maassen, J. and Raap, A. (2001) Simultaneous A8344G heteroplasmy and mitochondrial DNA copy number quantification in myoclonus epilepsy and ragged-red fibers (MERRF) syndrome by a multiplex molecular beacon based real-time fluorescence PCR. *Nucleic Acids Res.*, 29, E13.
11. Wu, Z. and Irizarry, R.A. (2004) Preprocessing of oligonucleotide array data. *Nat.Biotechnol.*, 22, 656-658.
12. Liu, G., Loraine, A.E., Shigeta, R., Cline, M., Cheng, J., Valmeekam, V., Sun, S., Kulp, D. and Siani-Rose, M.A. (2003) NetAffx: Affymetrix probesets and annotations. *Nucleic Acids Res.*, 31, 82-86.

## Acknowledgements

We thank Marchien van de Sande for her excellent overall technical assistance.

The micro-array hybridizations were performed by E. Mank at the Leiden Genome Technology Center

## Supplementary material

Tables 4 through 10 are available via DOI:10.1016/j.mrfmmm.2005.02.002 (<http://dx.doi.org>).

13. Huber,W., von Heydebreck,A., Sultmann,H., Poustka,A. and Vingron,M. (2002) Variance stabilization applied to microarray data calibration and to the quantification of differential expression. *Bioinformatics.*, 18 Suppl 1, S96-104.
14. Liu,W.M., Mei,R., Di,X., Ryder,T.B., Hubbell,E., Dee,S., Webster,T.A., Harrington,C.A., Ho,M.H., Baid,J. et al. (2002) Analysis of high density expression microarrays with signed-rank call algorithms. *Bioinformatics.*, 18, 1593-1599.
15. Wilcoxon.F (1945) Individual comparisons by ranking methods. *Biometrics bulletin*, 1, 80-83.
16. Mootha,V.K., Lindgren,C.M., Eriksson,K.F., Subramanian,A., Sihag,S., Lehar,J., Puigserver,P., Carlsson,E., Ridderstrale,M., Laurila,E. et al. (2003) PGC-1 $\alpha$ -responsive genes involved in oxidative phosphorylation are coordinately downregulated in human diabetes. *Nat.Genet.*, 34, 267-273.
17. Wu,Y., de Kievit,P., Vahlkamp,L., Pijnenburg,D., Smit,M., Dankers,M., Melchers,D., Stax,M., Boender,P. J., Ingham,C. et al. (2004) Quantitative assessment of a novel flow-through porous microarray for the rapid analysis of gene expression profiles. *Nucleic Acids Res.*, 32, e123.
18. Chuaiqui,R.F., Bonner,R.F., Best,C.J., Gillespie,J.W., Flaig,M.J., Hewitt,S.M., Phillips,J.L., Krizman,D. B., Tangrea,M.A., Ahram,M. et al. (2002) Post-analysis follow-up and validation of microarray experiments. *Nat.Genet.*, 32 Suppl, 509-514.
19. Jansen,J.J., Maassen,J.A., van der Woude,F.J., Lemmink,H.A., van Den Ouweland,J.M., t' Hart,L. M., Smeets,H.J., Bruijn,J.A. and Lemkes,H.H. (1997) Mutation in mitochondrial tRNA(Leu(UUR)) gene associated with progressive kidney disease. *J.Am.Soc.Nephrol.*, 8, 1118-1124.
20. Dunbar,D.R., Moonie,P.A., Jacobs,H.T. and Holt,I.J. (1995) Different cellular backgrounds confer a marked advantage to either mutant or wild-type mitochondrial genomes. *Proc.Natl.Acad.Sci.U.S.A.*, 92, 6562-6566.
21. Epstein,C.B., Waddle,J.A., Hale,W., Dave,V., Thornton,J., Macatee,T.L., Garner,H.R. and Butow,R.A. (2001) Genome-wide responses to mitochondrial dysfunction. *Mol.Biol.Cell*, 12, 297-308.
22. Wu,Z., Puigserver,P., Andersson,U., Zhang,C., Adelman,G., Mootha,V., Troy,A., Cinti,S., Lowell,B., Scarpulla,R.C. et al. (1999) Mechanisms controlling mitochondrial biogenesis and respiration through the thermogenic coactivator PGC-1. *Cell*, 98, 115-124.
23. Scarpulla,R.C. (2002) Transcriptional activators and coactivators in the nuclear control of mitochondrial function in mammalian cells. *Gene*, 286, 81-89.
24. Rolfe,D.F. and Brown,G.C. (1997) Cellular energy utilization and molecular origin of standard metabolic rate in mammals. *Physiol Rev.*, 77, 731-758.
25. Grigull,J., Mnaimneh,S., Pootoolal,J., Robinson,M.D. and Hughes,T.R. (2004) Genome-wide analysis of mRNA stability using transcription inhibitors and microarrays reveals posttranscriptional control of ribosome biogenesis factors. *Mol.Cell Biol.*, 24, 5534-5547.
26. Maassen,J.A., t' Hart,L.M., Van Essen,E., Heine,R.J., Nijpels,G., Jahangir Tafrechi,R.S., Raap,A.K., Janssen,G.M. and Lemkes,H.H. (2004) Mitochondrial diabetes: molecular mechanisms and clinical presentation. *Diabetes*, 53 Suppl 1, S103-S109.
27. Maechler,P. and Wollheim,C.B. (2001) Mitochondrial function in normal and diabetic beta-cells. *Nature*, 414, 807-812.
28. Lowell,B.B. and Shulman,G.I. (2005) Mitochondrial Dysfunction and Type 2 Diabetes. *Science*, 307, 384-387.
29. Patti,M.E., Butte,A.J., Crunkhorn,S., Cusi,K., Berria,R., Kashyap,S., Miyazaki,Y., Kohane,I., Costello,M., Saccone,R. et al. (2003) Coordinated reduction of genes of oxidative metabolism in humans with insulin resistance and diabetes: Potential role of PGC1 and NRF1. *Proc.Natl.Acad.Sci.U.S.A.*, 100, 8466-8471.
30. Yechoor,V.K., Patti,M.E., Saccone,R. and Kahn,C.R. (2002) Coordinated patterns of gene expression for substrate and energy metabolism in skeletal muscle of diabetic mice. *Proc.Natl.Acad.Sci.U.S.A.*, 99, 10587-10592.
31. Yechoor,V.K., Patti,M.E., Ueki,K., Laustsen,P.G., Saccone,R., Rauniyar,R. and Kahn,C.R. (2004) Distinct pathways of insulin-regulated versus diabetes-regulated gene expression: an in vivo analysis in MIRKO mice. *Proc.Natl.Acad.Sci.U.S.A.*, 101, 16525-16530.
32. Van Der Westhuizen,F.H., Van Den Heuvel,L.P., Smeets,R., Veltman,J.A., Pfundt,R., Van Kessel,A. G., Ursing,B.M. and Smeitink,J.A. (2003) Human mitochondrial complex I deficiency: investigating transcriptional responses by microarray. *Neuropediatrics*, 34, 14-22.
33. Heddi,A., Stepien,G., Benke,P.J. and Wallace,D.C. (1999) Coordinate induction of energy gene expression in tissues of mitochondrial disease patients. *J.Biol.Chem.*, 274, 22968-22976.



# 5

## Effects of mtDNA variants on the nuclear transcription profile and the cytosolic protein synthesis machinery

Roshan S. Jahangir Tafrechi\*, J. Peter Svensson‡, George M. C. Janssen\*, Rene F. de Coo°, Peter de Knijff#, J. Antonie Maassen\* and Anton K. Raap\*

\* Department of Molecular Cell Biology, Leiden University Medical Center, P.O. Box 9600, 2300 RC Leiden, The Netherlands

‡ Department of Toxicogenetics, Leiden University Medical Center, P.O. Box 9600, 2300 RC Leiden, The Netherlands and

Department of Oncology, Radiology and Clinical Immunology, University Hospital, 75185, Uppsala, Sweden

° Department of Child Neurology, Erasmus University Medical Center, Molewaterplein 60, 3015GJ, Rotterdam, The Netherlands and supported by EU-FP6 STREP MITOCIRCLE

# Department of Human Genetics, Leiden University Medical Center, P.O. Box 9600, 2300 RC Leiden, The Netherlands



## Summary

To explain the variation in clinical phenotype of mitochondrial diseases caused by point mutations in mtDNA such as the A3243G tRNA<sup>Leu</sup>(<sup>UUR</sup>) mutation, it has been proposed that signaling pathways from mitochondria to the nucleus (the retrograde response) leads to tissue and cell type specific responses. To identify such responses we extensively compared nuclear expression profiles of cell clones proficient and deficient in mitochondrial respiration because of A3243G mtDNA mutation. The cell clones had in principle identical nuclear background and, next to variation in mutation load, two different haplogroups well represented. Thus the system is well suited to see effects of mtDNA sequence variants on nuclear expression profiles. The results led us to conclude that the number of genes changed  $\geq 1.5$ -fold in expression is minimal when comparing respiration pro- and deficient cells and no relevant genes, let alone pathways, were identified. Many differentially expressed genes were, however, found when the two haplogroups were compared. The fact that differences in expression exist between two haplogroups may indicate that the mtDNA haplotype can modulate phenotypic expression, but it will be difficult to unravel its contribution in view of the general nature of the gene sets differentially affected by the haplotypes. As in the previous Chapter, we found that 100% mutant cells reduce global cytosolic translation rates 2-4 times. Preliminary experiments and ongoing research indicate the involvement of the elongation factor EF-2 and its upstream regulator AMP Kinase, while mTOR down regulation seems not involved in this translation repression. This highlights the importance of translational control in response to loss of mitochondrial respiratory function.

## Introduction

Mitochondrial DNA (mtDNA) is a small, multi-copy, circular extra-nuclear genome of 16.569 base pairs, which in mammals is maternally inherited and thought to segregate randomly. Compared to the nuclear genome, it is more vulnerable to mutations. The lack of an efficient mtDNA repair mechanism and the location near the oxygen radical producing respiratory chain are considered to be the main reason for the high mutation rate of mtDNA. A cell may contain hundreds to thousands copies of mtDNA and a mutated form can co-exist with the original sequence. The occurrence of both wild type and mutated mtDNA is called heteroplasmy as opposed to homoplasmy. Homoplasmy is the preferred state in oocytes, but heteroplasmy does occur in the germ line, with wide variation in mutation load, as testified by patients with mtDNA disease. From studies with (neutral) heteroplasmic mouse models, it has been inferred that during early oogenesis a reduction of the number of mtDNA molecules (the mitochondrial genetic bottleneck) and their random segregation,

creates great variation in mutation load of the primary oocytes and hence offspring (1). As a consequence of the small number of segregating mtDNA molecules in the maternal germ line, return to homoplasmy in offspring is established by random segregation in relatively few and even one generation. This rapid genetic drift to fixation is considered key to purging the population from deleterious variants by negative selection, while positive selection during many generations may lead to the best adapted homoplasmic sequence variant for a given (climatic) environment. Characteristic demographic distribution of neutral mtDNA sequence variants is also thought to result from this rapid drift. The human population indeed harbors a high level of population-specific mtDNA sequence variants, which are especially abundant in the only non-coding part of the mtDNA, the ~1000 basepair D-loop. By means of D-loop sequencing and RLFP analysis a single mtDNA tree can be drawn originating in Africa approximately 150.000 years ago (2). The West Eurasian



population can be divided in 11 haplogroups, at least 20 subgroups and numerous haplotypes (3). These haplotype mutations are present in all mtDNA molecules of an individual, in contrast to the heteroplasmic occurrence of most pathogenic mtDNA mutations. Pathogenic point mutations in mtDNA are remarkable in that a single specific mutation can cause variable disease phenotypes, whereas a much more common expression of disease is expected considering that in the end they all cause failure of oxidative phosphorylation. A relevant example of a variably expressing, pathogenic mtDNA mutation is the A to G transition at location 3243 in the tRNA<sup>Leu</sup>(UUR) gene, which causes Maternally Inherited Diabetes and Deafness (MIDD) in most carriers (4), but also associates with the neuromuscular syndrome characterized as mitochondrial encephalomyopathy, lactic acidosis and stroke-like episodes (MELAS) (5), in which it was originally discovered. Also disease expressions like Alport-like kidney failure and Chronic Progressive External Ophthalmoplegia are found to be associated with the A3243G mutation. Several hypotheses have been brought forward to explain the variation in clinical phenotype of mitochondrial DNA diseases. One is based on tissue-variation in heteroplasmy levels, resulting from enigmatic segregation patterns. Another is based on tissue and cell type specific effects of mitochondrial dysfunction, affecting signalling pathways from mitochondria to the nucleus (the retrograde response) (6). It has also been suggested that mtDNA haplotype modulates disease expression. In the previous chapter we demonstrated, in a particular mtDNA haplotype, effects of the homoplasmic A3243G mutation on the nuclear gene expression profile. Here we considered whether the effects were specific to the A3243G-induced respiratory dysfunction or influenced by the mtDNA haplotype. For this purpose we created additional A3243G cybrids, both respiratory proficient and respiratory deficient, with a different mtDNA haplogroup (7).

## Materials and Methods

### Patients

The clinical manifestations and family history for patients V and A have been described previously. Patient V was a 56 year old male with MIDD, with an age-of-onset of 36 and a heteroplasmy level of 4% A3243G in blood and 41% in fibroblasts (4). Patient A was a 56 year old female with Alport-like renal failure, who developed diabetes after kidney transplantation at the age of 38, and had a heteroplasmy level of 12% A3243G in her blood (8). Patient GB was a 34 year old female diagnosed with non-obese diabetes at the age of 16 and a severe hearing disorder. As a complication she started to develop nephropathy. The A3243G mutation load was measured in fibroblast cells and reached 20%. Patient Wo is a nephew of patient V from the same maternal bloodline. He was born in 1965 and his A3243G mutation load reached 40% in blood platelets. His glucose-tolerance was normal. Patient G55 was a 35 year old female when diagnosed with MELAS. She developed hearing loss and exercise intolerance from the age of 25 and her mitochondrial mutation load reached up to 32% A3243G in her blood, 55% in fibroblast and 61% in muscle. Relatives from the female bloodline also suffered from MELAS symptoms like strokes and seizures. Additional both an aunt and brother developed diabetes.

### Trans-mitochondrial cybrids

In short, 143B-p<sup>0</sup> osteosarcoma cells were fused with enucleated fibroblasts from the patients, thus generating clones with homoplasmic as well as different but stable heteroplasmy levels for the A3243G mutation. The cybrid cells were grown on Dulbecco's Modified Eagle's medium containing 4.5 mg/ml glucose and 110 µg/ml pyruvate (DMEM) supplemented with 50 µg/ml uridine and 10% fetal bovine serum. Heteroplasmy levels were monitored by use of PCR and RFLP using ApaI digestion. The oxygen consumption of the cells was measured as described previously (7).

### GeneChip hybridization

Biotinylated cRNA samples were prepared according to the Affymetrix GeneChip protocol as described previously (9). Several quality-controls were included. With the intensity-ratio of the 28S/18S rRNA bands being over 1.8, the integrity of the RNA was confirmed. The optical density at 260 nm compared to 280 nm was used to verify the purity of the sample. Affymetrix' Microarray Suite 5.0 Software (MAS) was used to determine the percentage of transcripts Present and the 3'/5' intensity ratios for  $\beta$ -actin and GAPDH as final quality control on the input material.

### Data analysis

Most data analyses were performed in R ([www.r-project.org](http://www.r-project.org)) using the Bioconductor functions ([www.bioconductor.org](http://www.bioconductor.org)). Intensity data was corrected for background arising from optical noise as well as from non-specific hybridization, according to the procedure developed by Wu *et al.* (10) and annotations were added using the annotation package hgu133a, version 1.3.1 (11). The linear model:  $\text{signal} \sim \beta_1 \text{ probe} + \beta_2 \text{ status} + \beta_3 \text{ patient} + \varepsilon$  was fitted to the 2log-transformed signals of each transcript. The calculated  $\beta$ 's are a measure for the fold change in average signal intensity of a transcript between the groups compared and are used to obtain p-values for the reliability of the difference. The proportion of unchanged genes,  $\pi_0$ , was calculated according to Storey and Tibshirani (12).

### Mitochondrial haplogroup analysis

The mitochondrial haplogroups were analyzed using cybrid DNA samples according to the method described by Quintáns *et al.* (3). 17 SNPs and the sequence of both hyper variable regions of the D-loop were used to determine the haplogroups. Protein synthesis and Western blotting  
Protein synthesis was measured as described in Chapter 4. Western blots were made following a standard protocol from a 10% SDS-poly-acrylamide gel. 10  $\mu\text{g}$  of protein of the cell lysates was used to detect eukaryotic Elongation Factor 2 (eEF2, 100 kDa). The anti-bodies were

used in a 1:1000 dilution and manufactured by Cell Signalling Technology, #2332 for eEF2 and #2331 for the antibody directed against the phosphorylated form of threonine 56 of eEF2.

## Results

### Cell characteristics

The cell characteristics including the mitochondrial haplogroups of the patients are depicted in table 1. As can be seen, the mtDNAs of the clones belong to different West-Eurasian haplogroups. Haplogroups N\* and H6 of patients V and GB are the most dissimilar, haplogroup R\* of patient G55 is the most central. The difference between haplogroups J and T is the order in which the mutations at locations 4216 and 10398 have occurred and they are not distinguishable with the method used here. All cells have, in principle, the same nuclear background and the trans-mitochondrial

Table 1: Cell characteristics

Cell line	haplogroup	A3243G	O <sub>2</sub> consumption
VW1	N*	0 %	1.3
VW2	N*	0 %	1.7
VM1	N*	100 %	0.1
VM2	N*	100 %	0.1
GBW	H6	0 %	1.8
GBH1	H6	24 %	2.2
GBH2	H6	25 %	2.0
GBH3	H6	29 %	1.9
GBH4	H6	46 %	2.8
GBH5	H6	54 %	2.3
GBH6	H6	76 %	2.4
GBH7	H6	84 %	0.4
GBH8	H6	87 %	1.4
GBM1	H6	100 %	0.1
GBM2	H6	100 %	0.1
WoW	N*	0 %	n.d.
WoM	N*	100 %	n.d.
G55M	R*	100 %	n.d.
AM	J/T	100 %	n.d.

Mitochondrial haplogroups according to Quintáns *et al.* (3)

Subject Wo is related to patient V

O<sub>2</sub> consumption in fmol/min/cell;

n.d. = not determined

All data are averages of at least 3 measurements, except for the oxygen consumption of cell line GBH4, which is a single measurement (see also figure 1).

cybrid system is therefore focused on revealing the effects of mtDNA variants on nuclear gene expression. Previously we have analyzed the expression profiles of the 4 cybrid clones (two homoplasmic mutant and two homoplasmic wild type) from patient V and found some coherent changes in genes grouped according to their function. In order to dissect the influences of the A3243G mtDNA mutation and haplotype on nuclear gene expression with more samples including different heteroplasmic mutation loads, we have now added 11 cybrid samples from cybrids from another A3243G patient (GB). In total we thus have used the mRNA of 15 different cell lines in two separate comparisons, the first is based on respiration status due to the A3243G mutation load and the second based on the patients-mtDNA haplotype.

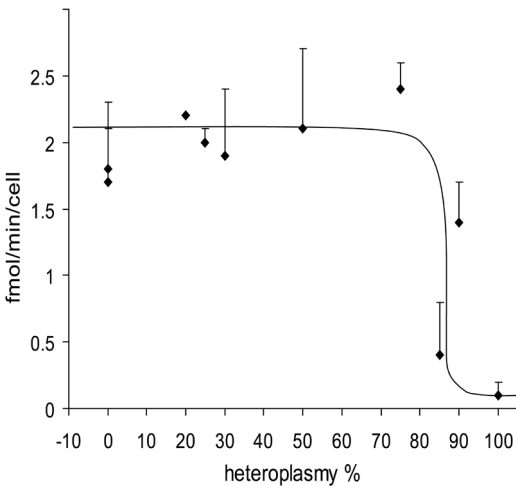


Figure 1: oxygen consumption of GB cybrids  
The different heteroplasmic cell lines derived from mtDNA of patient GB show a threshold effect in oxygen consumption and therefore in functionality of the respiratory chain. Above 75% A3243G the amount of oxygen consumed per cell per minute drops from an average 2 to 0,1 fmol. The standard deviation is calculated from minimal 3 independent samples. The variation in average mutation load of a particular cell line is less than 5%.

### Respiratory status comparison

The mutation load and respiratory status of the 11 GB clones is given in table 1 and depicted in figure 1. The V clones were all homoplasmic with a >10-fold difference in oxygen consumption between the wild type and A3243G-mutant clones as described in Jahangir Tafrechi *et al.* (9). On the basis of these results the respiration status was defined as being deficient when clones have a mutation load exceeding 75% and as proficient with lower heteroplasmy percentages. By comparing 9 RNA samples from respiration-proficient cells to 6 RNA samples from respiration-deficient cells, the effect of the A3243G mutation was analyzed (respiratory status comparison). In figure 2A, the p-values of all 22.283 transcripts in the respiratory status comparison are represented in a frequency histogram. The dashed line represents the distribution if truly none of the transcripts would have been differentially expressed. In other words it represents the histogram when the null hypothesis of no differential expression between respiration proficient and deficient cells is true. According to Storey and Tibshirani (12) it corresponds to a  $\pi_0$  value of 1, with  $\pi_0 = m_0 / m$ , where  $m$  = the total number of transcripts and  $m_0$  the number of transcripts that are not truly changed. The  $\pi_0$  value is based on the false discovery rate and represents the proportion of unaffected genes. The  $\pi_0$  value in the respiratory status comparison is 0.85. Thus it appears that of all the transcripts 85% is actually not changed at all in the respiratory status comparison. For the genes in the  $p \leq 0.02$  bin this implies a false discovery rate of approximately 1/6th. In a search for potentially relevant differentially expressed genes we used three criteria: t-statistics, fold-change and a minimum expression level. For the respiratory status comparison 840 transcripts were found to be changed when applying a cut-off value of  $p = 0.001$  in the t-statistics, 4% of the 22283 transcripts on the HG-U133A chip (data available on request). Only 16 transcripts (2% of the 840) in the respiratory status comparison

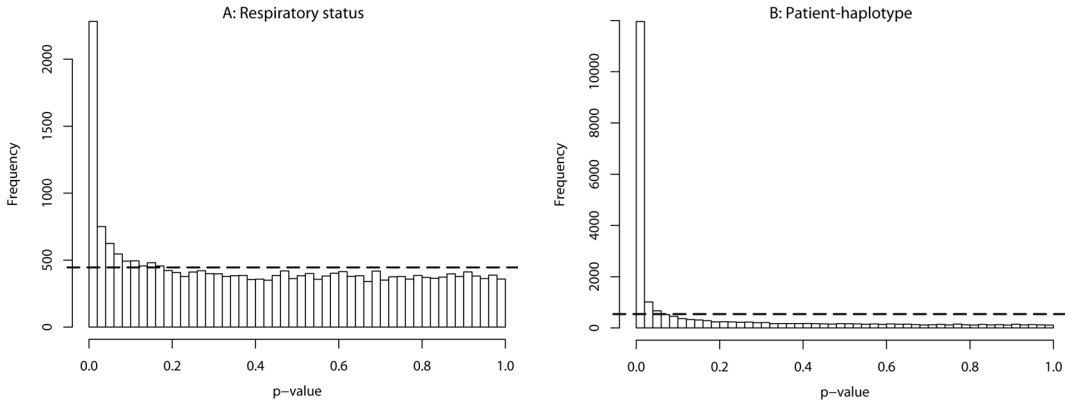


Figure 2:  $\pi_0$  graphs for false discovery percentage calculation

The p-values (x-axis) of all 22,283 transcripts are represented in frequency histograms. The dashed line represents the distribution if none of the transcripts would have been differentially expressed and corresponds to a  $\pi_0$  value of 1 (y-axis of the corresponding density histogram). The larger the part of the histogram under this line the better the correlation of the gene expression profiles. The  $\pi_0$  value for the A3243G-respiratory status comparison (A) is 0.85 and for the patient-haplotype comparison (B) it is 0.27. Note that the y-axes have a different scale.

were changed 1.5 fold or more in a signal-to-noise ratio analysis (Figure 3). These 16 transcripts were checked individually for relative expression levels. Most of them express below the threshold (defined in the previous chapter as  $<25$ ) except for, eukaryotic translation initiation factor 5A, a receptor-like protein tyrosine phosphatase and adrenomedullin. We tried to find functionally related groups of genes over-represented among the 840 differentially expressed genes. As in the previous chapter we used Gene Set Enrichment Analysis (13) to see whether one of the gene sets found earlier would give the same small but consistent change. The gene sets emerging as most enriched in the respiratory status comparison include “nucleotide binding”, “ribosome” and “MAPK signaling” with “ribosome” being the only reoccurring one.

#### Patients-mtDNA haplotype comparison

By regrouping the samples into the 4 independent clones from patient V on one side and the 11 clones from patient GB on the other, the possible influence of the haplotype by itself was analyzed (patient-haplotype comparison). The correlation of the 15 GB

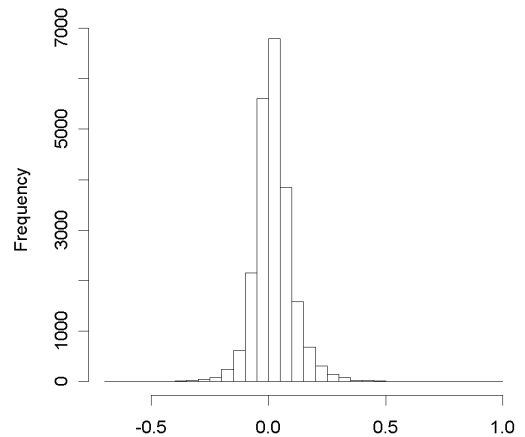


Figure 3: Fold Change of all 22,283 transcripts in the respiratory status comparison  
The change in gene expression of non-respiring A3243G cells compared to respiring cells is shown on a logarithmic scale. Note the absence of genes with a  $> 2$  fold change

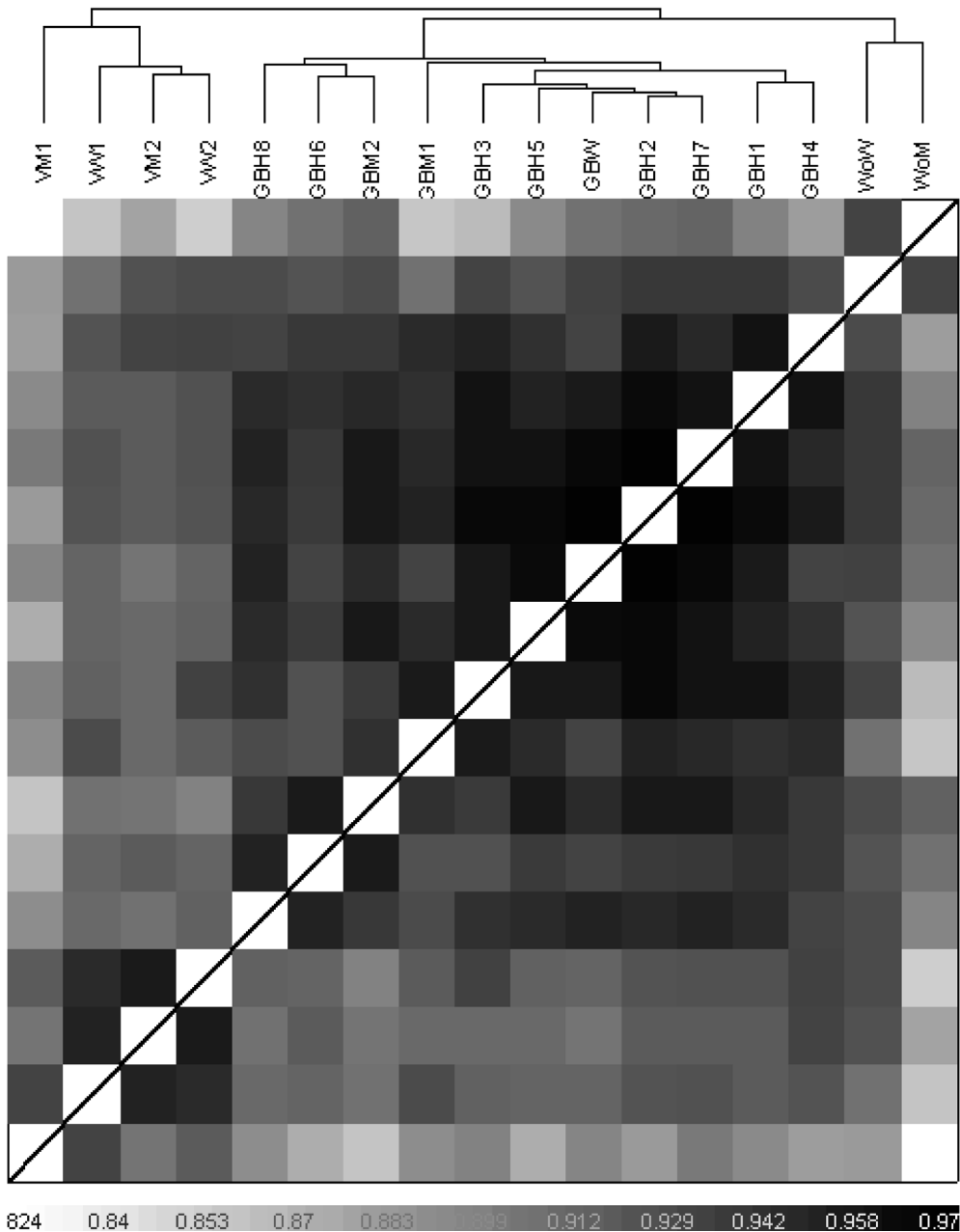


Figure 4: Diagram illustrating haplotype correlations of cybrid cell expression profiles

The distances in the tree are calculated according to a Pearson's correlation test. The shading of the boxes correspond to the correlation coefficient as shown in the bar under the figure (the darker the color the better the correlation).

and V samples in the patient-haplotype comparison and of 4 additional samples is visualized in the Pearson's diagram of figure 4. The correlation found in the Pearson's diagram between the samples with the same patient-mtDNA haplotype is very strong, leading to a clear separation of the samples of patient GB with haplogroup H6 and patient V with haplogroup N\*.

The results obtained with four additional RNA samples for which expression data were available (patients A (one 100% mutant clone), G55 (also one 100% mutant clone) and Wo (two homoplasmic clones, one wild type and one mutant)) corroborate the notion that the mtDNA haplotype can influence nuclear gene expression. The samples of patients A (M) and G55 (M) are both respiratory deficient, but

differ in haplotype. They are clearly separated in the correlation diagram (data not shown). The two samples of patient Wo (W and M) are similar in haplotype but differ in respiratory status. Yet, they show strong similarity in expression pattern. It should be noted that contrary to expectation, RNA samples obtained from cybrids with mtDNAs of patient Wo and V (nephews from the same maternal bloodline, both haplogroup N\*) do not appear in the same branch. Speculatively, this may be due to additional mutations not visible with the method used here to define the haplogroups. Consistent with the results of the respiratory status comparison of the previous paragraph, it is clear that no separation between the samples on basis of A3243G-respiratory status can be made, since both respiration proficient and respiration deficient cells of a given patient can be found in the same branch of the correlation-tree.

In the patient V (haplogroup N\*) versus patient GB (haplogroup H6) comparison 9136 or 41% of the 22.283 transcripts are changed according to t-statistics with the same cut-off p-value of  $p=0.001$  used in the respiratory status comparison. Of these a total of 297 transcripts (3% of the previous selected 9136) are changed over two-fold. A batch-wise analysis seemed appropriate to get an indication of biologically relevant gene sets in this pile of differentially expressed genes. The Gene Ontology gene sets most enriched in the haplogroup comparison proved to be very general like “intracellular” and “cytoplasm”.

#### Global translational repression

As in the previous Chapter we measured cytosolic translation rates. The cells used here have a different haplogroup (patient GB, haplogroup H6) compared to the cells used in the previous chapter (patient V, haplogroup N\*), but results are similar: protein synthesis rates are 2-4 times lower in cells with a high A3243G mutation load (Figure 5). As can be seen in figure 5, the protein synthesis rate is density-dependent,

but the mutation-dependent decrease is found at every measured density of the cells. Protein synthesis is highly demanding on cellular ATP (~4 ATPs per peptide bond) and to exclude the trivial explanation of dramatic ATP depletion cellular ATP content was measured and found to be reduced only 20-25% in 100% A3243G cybrids (results not shown). It seemed likely therefore, that respiratory dysfunction is signaled to the cytosolic translation apparatus and therefore we choose to investigate the activity of proteins involved in controlling translation rates, notably initiation and elongation factors and their upstream regulators, since other cellular stresses are known to signal to these proteins (14). Figure 6 depicts the signaling framework that guided us in setting up the experiments. The initial results reported here identify elongationfactor2 to be a major target (Figure 7).

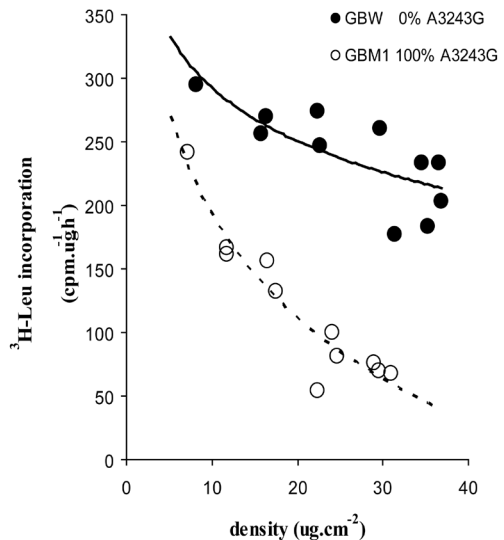


Figure 5: Cytoplasmic protein synthesis rates of wild type and 100% A3243G cells derived from patient GB

The protein synthesis rates and the difference between the wild type and mutant rates are comparable to those of cells derived from patient V, which are shown in Chapter 4 (9). Protein synthesis is reflected by  $^3\text{H}$ -leucine incorporation. For gene expression profiling, cells were harvested at a density of ~ 40 mg protein/cm<sup>2</sup>.

Phosphorylation of EF-2 by eEF2 kinase and hence translational repression proved to correlate with AMPK phosphorylation (not shown). The degree of phosphorylation of EF-2 in  $\rho^0$  (mtDNA depleted) cells is even higher than in A3243G 100% mutant cells and correlates to both lower oxygen consumption and protein synthesis rate. Importantly S6 phosphorylation, as a convenient read-out of mTOR activity, and phosphorylation of mTOR itself were not reduced in A3243G nor  $\rho^0$  cells (data not shown)

## Discussion

Nuclear gene expression profiles are characteristic for the functioning of a cell. With oxidative phosphorylation taking a central position in energy metabolism and

thus cell functioning, an effect of OXPHOS dysfunction on expression profiles lies within reason. Particularly with the A3243G pathogenic mtDNA at a heteroplasmy level above the critical threshold (when cells have lost the ability to respire) we expected the nuclear gene expression to be changed significantly and by large scale mRNA expression analysis we expected to find clues of the 'retrograde signaling' (that is mitochondria to nucleus signaling resulting from mtDNA mutation) to further insight in the pathobiochemistry of mitochondrial diseases. However, using a 1.5-fold difference as a criterion, essentially no mRNA expression differences were found when comparing A3243G cells on basis of respiratory status (Figure 2A and 3).

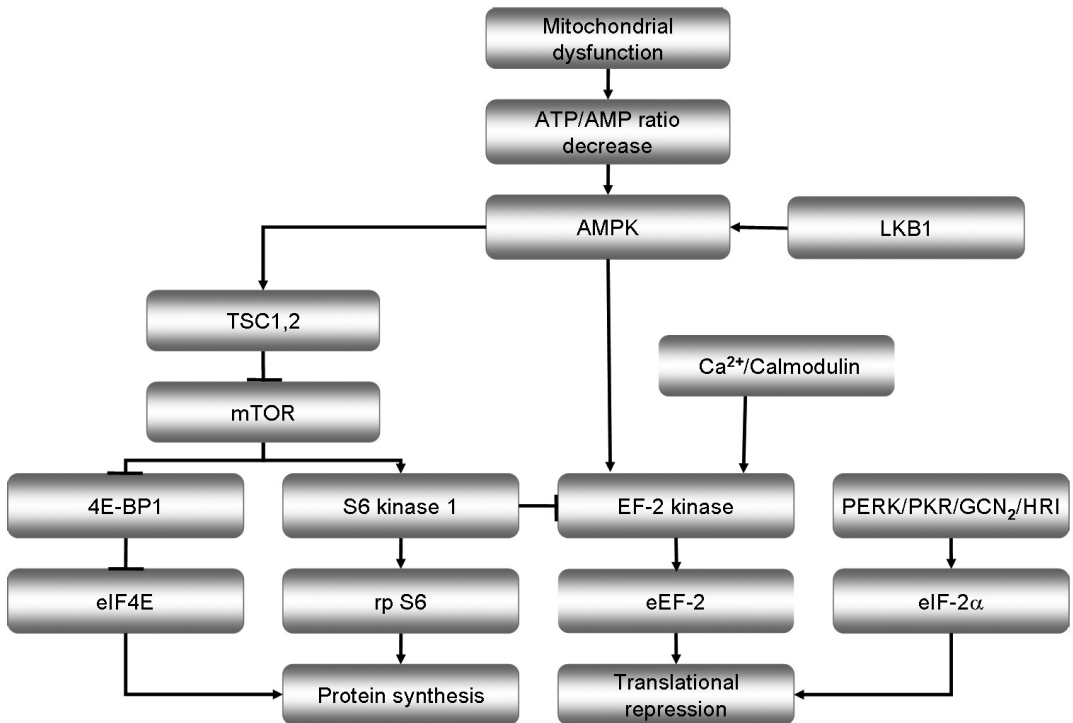


Figure 6: Schematic outline of the translation factors and their upstream pathways. The scheme is adapted from Ruvinsky *et al.* (34)



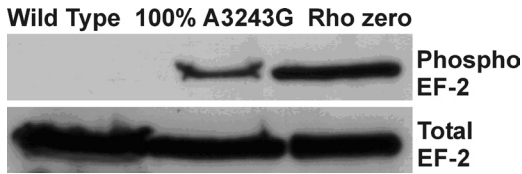


Figure 7: The effect of mitochondrial dysfunction on the phosphorylation status of Elongation Factor 2

The amount of phosphorylated eEF-2 compared to the total amount of eEF-2 is lower in wild type cells compared to 100% homoplasmic A3243G mutant cells and much lower compared to cells depleted of mitochondrial DNA ( $\rho^0$ ). Phosphorylation inactivates EF-2 and consequently protein translation is inhibited. The total amount of EF-2 is used as loading control.

Of the three differentially expressed genes eIF5A was potentially interesting in view of the translation repression observed (Chapter 4 and Figure 5). However its role in translation initiation is obscure (15) and by far not so well defined as the translation factors studied by us such as eIF2 $\alpha$ , 4E-BP1 and eEF2 (Fig 6). In view of their broad pathway involvement, the receptor like protein tyrosine phosphatase and adrenomedullin were not studied further. Thus, at the nuclear transcriptional level no strong leads were found that may help explain variation in clinical phenotype of A3243G mtDNA diseases. It seems likely therefore, that under the conditions used nuclear transcriptional responses to high levels of A3243G mutation leading to loss of respiration are subtle.

In Chapter 4, the analysis of translation rates showed a >2-fold down-regulation in the protein synthesis rate in 100 % A3243G cybrid cells derived from patients V (haplogroup N\*). For the A3243G-samples derived from patient GB with mitochondrial haplogroup H6 used here similar results were obtained. In these cells ATP is not limiting, thus it appears that cells cope with the energy crisis (loss of mitochondrial ATP synthesis) by down regulating translation by phosphorylation of eEF-2, thus saving (glycolytic) ATP for other

cellular processes. This signalling is mediated by AMP-Kinase which recently has been found to directly phosphorylate, and inactivate, the eEF2 kinase (16). Noteworthy AMPK is implied in mitochondrial biogenesis by activating PGC-1 $\alpha$  (17), providing a compensatory pathway for loss of mitochondrial function. In muscle, AMPK phosphorylation also activates fatty acid  $\beta$ -oxidation via Acetyl Co-enzyme A Carboxylase (ACC) phosphorylation and stimulates glucose uptake by increased translocation to the plasma-membrane of the GLUT4 transporter. These facts may illustrate the central role played by AMPK in maintaining energy homeostasis: when cells consume large amounts of ATP or face problems with mitochondrial ATP production (e.g. by mtDNA mutation accumulation), AMPK as the energy sensor down regulates energy demanding anabolic processes and upregulates energy releasing catabolic processes. Note in this respect that Red-Ragged Fibers as found in muscle fibers of mtDNA patients and also aged muscles are considered a token of mitochondrial biogenesis. It seems reasonable to assume that they result from chronic (but alas futile) AMPK activation by irreversible damage of mitochondria that accumulated pathogenic mutations. Down regulating the mTOR pathway would be another pathway that leads to translational repression. The ongoing research confirmed the preliminary S6 results and shows that this pathway is not operational in the cells used (Janssen *et al.*, in preparation).

Like control of gene transcription, regulation of translation (be it globally or mRNA specific) is an essential element of gene expression. While basics of cytosolic translational control are well established, cell- and tissue specific aspects are largely unknown. Remarkably in this respect, inherited diseases with pathogenic mutation in nuclear genes coding for cytosolic translation factors or key components of the translation machinery are expected to express in all cell types and to lead to similar phenotypes. It has become clear, however that such nuclear gene mutations affect a range of tissues and



organs thus presenting with variable disease expression. (For recent authoritative review see (18)). In this context, our results indicate the importance of translational control in response to loss of mitochondrial respiratory function. In contrast to the pathogenic A3243G mutation, the multiple, presumably neutral mutations that define a particular haplogroup lead to a large number of transcripts that show a change in expression level (figure 2B), indicating that mtDNA haplotype as such can modify the nuclear expression profile which may or may not predispose to disease. We realize that the 143B nucleus is genomically unstable and this may contribute to the observed mRNA expression profile changes. However, since in the respiratory status comparison hardly any changes in gene expression profiles were found we conclude that such contributions will be minor.

Several studies, ranging from mouse behavioral studies to human mtDNA association studies, have been carried out to search for an effect of mtDNA haplotype on phenotype. The mouse model study by Roubertoux *et al.* (19), makes a strong point in this respect. Cross transfer of a different mtDNA haplogroup modified brain anatomy, sensory development and learning abilities in nuclear congenic mice, indicating that mitochondrial polymorphisms may not be as neutral as is generally believed. Indeed, very recently it was reported that a naturally occurring variation in the mitochondrial genome, independent of nuclear genome variation, is a risk factor for type 2 diabetes in rats (20). On the other hand, an association study in Spain (20) reports that mitochondrial DNA haplogroup does not play a significant role in the variable phenotypic presentation of the A3243G mutation, based on data of 35 independent patients. Several studies have attempted to associate common mitochondria haplotypes with common diseases such as diabetes (22;23), cancer (24;25), cardiovascular diseases (26), Parkinson's (27) and Alzheimers Disease (28;29) as well as with longevity (30) often with inconsistent results. Likely this

is related to issues known to affect results of genetic association studies such as sample size, matching of cases, controls regarding geographical origin and ethnicity and phenotyping and data analysis quality (31;32). Based on the observation that the analyzed mtDNA haplogroups differ quite dramatically in gene expression profile, we tentatively conclude that mtDNA haplogroup can modify nuclear gene expression. This would support the notion that mtDNA haplogroup may predispose to common diseases. The changes we found between the haplogroups were randomly distributed over Gene Ontology pathways and numerous, implying that should a significant association between a haplogroup and a common disease be unambiguously proven, it will be difficult to molecularly disentangle the contribution of haplotype to the predisposition (33).

In conclusion, subtle differences in mRNA expression profiles between respiratory deficient and proficient A3243G cells likely prevented us from identifying genes that are implied in signaling from a defective mitochondrial compartment to the nucleus. Thus at the nuclear transcriptional level no leads were found to tissue and cell type specific responses that may help explain variation in clinical phenotype of A3243G mtDNA diseases. Large differences were, however, found when mtDNA haplogroups were compared for nuclear gene expression, indicating that mtDNA sequence variants per se can affect nuclear expression programs. At the translational level, a clear effect was observed: global cytosolic translational repression mediated by AMPK and elongation factor eEF2 was identified, indicating the importance of translational control in response to loss of mitochondrial respiratory function

## Acknowledgements

We thank Dr G. Schoonderwoerd for OXPHOS analysis and Dr. H.J.M. Smeets for DNA analysis of the MELAS patient.

## Reference List

1. Jenuth, J.P., Peterson, A.C., Fu, K. and Shoubridge, E.A. (1996) Random genetic drift in the female germline explains the rapid segregation of mammalian mitochondrial DNA. *Nat.Genet.*, 14, 146-151.
2. Wallace, D.C., Brown, M.D. and Lott, M.T. (1999) Mitochondrial DNA variation in human evolution and disease. *Gene*, 238, 211-230.
3. Quintans, B., Alvarez-Iglesias, V., Salas, A., Phillips, C., Lareu, M.V. and Carracedo, A. (2004) Typing of mitochondrial DNA coding region SNPs of forensic and anthropological interest using SNaPshot minisequencing. *Forensic Sci.Int.*, 140, 251-257.
4. van Den Ouweland, J.M., Lemkes, H.H., Ruitenbeek, W., Sandkuijl, L.A., de Vijlder, M.F., Struyvenberg, P.A., van de Kamp, J.J. and Maassen, J.A. (1992) Mutation in mitochondrial tRNA(Leu)(UUR) gene in a large pedigree with maternally transmitted type II diabetes mellitus and deafness. *Nat.Genet.*, 1, 368-371.
5. Jacobs, H.T. (2003) Disorders of mitochondrial protein synthesis. *Hum.Mol.Genet.*, 12 Suppl 2, R293-R301.
6. Butow, R.A. and Avadhani, N.G. (2004) Mitochondrial signaling: the retrograde response. *Mol.Cell*, 14, 1-15.
7. King, M.P. and Attardi, G. (1989) Human cells lacking mtDNA: repopulation with exogenous mitochondria by complementation. *Science*, 246, 500-503.
8. Jansen, J.J., Maassen, J.A., van der Woude, F.J., Lemmink, H.A., van Den Ouweland, J.M., t' Hart, L.M., Smeets, H.J., Bruijn, J.A. and Lemkes, H.H. (1997) Mutation in mitochondrial tRNA(Leu)(UUR) gene associated with progressive kidney disease. *J.Am.Soc.Nephrol.*, 8, 1118-1124.
9. Jahangir Tafrechi, R.S., Svensson, P.J., Janssen, G.M., Szuhai, K., Maassen, J.A. and Raap, A.K. (2005) Distinct nuclear gene expression profiles in cells with mtDNA depletion and homoplasmic A3243G mutation. *Mutat.Res.*, 578, 43-52.
10. Wu, Z. and Irizarry, R.A. (2004) Preprocessing of oligonucleotide array data. *Nat.Biotechnol.*, 22, 656-658.
11. Liu, G., Loraine, A.E., Shigeta, R., Cline, M., Cheng, J., Valmeekam, V., Sun, S., Kulp, D. and Siani-Rose, M.A. (2003) NetAffx: Affymetrix probesets and annotations. *Nucleic Acids Res.*, 31, 82-86.
12. Storey, J.D. and Tibshirani, R. (2003) Statistical significance for genomewide studies. *Proc.Natl.Acad.Sci.U.S.A.*, 100, 9440-9445.
13. Mootha, V.K., Lindgren, C.M., Eriksson, K.F., Subramanian, A., Sihag, S., Lehar, J., Puigserver, P., Carlsson, E., Ridderstrale, M., Laurila, E. et al. (2003) PGC-1alpha-responsive genes involved in oxidative phosphorylation are coordinately downregulated in human diabetes. *Nat.Genet.*, 34, 267-273.
14. Patel, J., McLeod, L.E., Vries, R.G., Flynn, A., Wang, X. and Proud, C.G. (2002) Cellular stresses profoundly inhibit protein synthesis and modulate the states of phosphorylation of multiple translation factors. *Eur.J.Biochem.*, 269, 3076-3085.
15. Zanelli, C.F. and Valentini, S.R. (2007) Is there a role for eIF5A in translation? *Amino.Acids*, 33, 351-358.
16. Browne, G.J., Finn, S.G. and Proud, C.G. (2004) Stimulation of the AMP-activated protein kinase leads to activation of eukaryotic elongation factor 2 kinase and to its phosphorylation at a novel site, serine 398. *J Biol.Chem.*, 279, 12220-12231.
17. Jager, S., Handschin, C., St Pierre, J. and Spiegelman, B.M. (2007) AMP-activated protein kinase (AMPK) action in skeletal muscle via direct phosphorylation of PGC-1alpha. *Proc.Natl.Acad.Sci.U.S.A.*, 104, 12017-12022.
18. Schepers, G.C., van der Naaap, M.S. and Proud, C.G. (2007) Translation matters: protein synthesis defects in inherited disease. *Nat.Rev.Genet.*, 8, 711-723.
19. Roubertoux, P.L., Sluyter, F., Carlier, M., Marcet, B., Maarouf-Veray, F., Cherif, C., Marican, C., Arrechi, P., Godin, F., Jamon, M. et al. (2003) Mitochondrial DNA modifies cognition in interaction with the nuclear genome and age in mice. *Nat.Genet.*, 35, 65-69.
20. Pravenec, M., Hyakukoku, M., Houstek, J., Zidek, V., Landa, V., Mlejnek, P., Miksik, I., Dudova-Mothejzkova, K., Pecina, P., Vrbacky, M. et al. (2007) Direct linkage of mitochondrial genome variation to risk factors for type 2 diabetes in conplastic strains. *Genome Res.*, 17, 1319-1326.
21. Torroni, A., Campos, Y., Rengo, C., Sellitto, D., Achilli, A., Magri, C., Semino, O., Garcia, A., Jara, P., Arenas, J. et al. (2003) Mitochondrial DNA haplogroups do not play a role in the variable phenotypic presentation of the A3243G mutation. *Am.J.Hum.Genet.*, 72, 1005-1012.

22. Mohlke, K.L., Jackson, A.U., Scott, L.J., Peck, E.C., Suh, Y.D., Chines, P.S., Watanabe, R.M., Buchanan, T.A., Conneely, K.N., Erdos, M.R. et al. (2005) Mitochondrial polymorphisms and susceptibility to type 2 diabetes-related traits in Finns. *Hum.Genet.*, 118, 245-254.
23. Fuku, N., Park, K.S., Yamada, Y., Nishigaki, Y., Cho, Y.M., Matsuo, H., Segawa, T., Watanabe, S., Kato, K., Yokoi, K. et al. (2007) Mitochondrial haplogroup N9a confers resistance against type 2 diabetes in Asians. *Am.J Hum.Genet.*, 80, 407-415.
24. Booker, L.M., Habermacher, G.M., Jessie, B.C., Sun, Q.C., Baumann, A.K., Amin, M., Lim, S.D., Fernandez-Golarz, C., Lyles, R.H., Brown, M.D. et al. (2006) North American white mitochondrial haplogroups in prostate and renal cancer. *J Urol.*, 175, 468-472.
25. Wang, L., Bamlet, W.R., de Andrade, M., Boardman, L.A., Cunningham, J.M., Thibodeau, S.N. and Petersen, G.M. (2007) Mitochondrial genetic polymorphisms and pancreatic cancer risk. *Cancer Epidemiol.Biomarkers Prev.*, 16, 1455-1459.
26. Nishigaki, Y., Yamada, Y., Fuku, N., Matsuo, H., Segawa, T., Watanabe, S., Kato, K., Yokoi, K., Yamaguchi, S., Nozawa, Y. et al. (2007) Mitochondrial haplogroup N9b is protective against myocardial infarction in Japanese males. *Hum.Genet.*, 120, 827-836.
27. Ghezzi, D., Marelli, C., Achilli, A., Goldwurm, S., Pezzoli, G., Barone, P., Pellecchia, M.T., Stanzione, P., Brusa, L., Bentivoglio, A.R. et al. (2005) Mitochondrial DNA haplogroup K is associated with a lower risk of Parkinson's disease in Italians. *Eur.J.Hum.Genet.*, 13, 748-752.
28. Mancuso, M., Nardini, M., Micheli, D., Rocchi, A., Nesti, C., Giglioli, N.J., Petrozzi, L., Rossi, C., Ceravolo, R., Bacci, A. et al. (2007) Lack of association between mtDNA haplogroups and Alzheimer's disease in Tuscany. *Neurol.Sci.*, 28, 142-147.
29. Fesahat, F., Houshmand, M., Panahi, M.S., Gharagozli, K. and Mirzajani, F. (2007) Do haplogroups H and U act to increase the penetrance of Alzheimer's disease? *Cell Mol.Neurobiol.*, 27, 329-334.
30. Niemi, A.K., Moilanen, J.S., Tanaka, M., Hervonen, A., Hurme, M., Lehtimäki, T., Arai, Y., Hirose, N. and Majamaa, K. (2005) A combination of three common inherited mitochondrial DNA polymorphisms promotes longevity in Finnish and Japanese subjects. *Eur.J Hum.Genet.*, 13, 166-170.
31. Raule, N., Sevini, F., Santoro, A., Altilli, S. and Franceschi, C. (2007) Association studies on human mitochondrial DNA: methodological aspects and results in the most common age-related diseases. *Mitochondrion.*, 7, 29-38.
32. Samuels, D.C., Carothers, A.D., Horton, R. and Chinnery, P.F. (2006) The power to detect disease associations with mitochondrial DNA haplogroups. *Am.J Hum.Genet.*, 78, 713-720.
33. Kirches, E., Michael, M., Warich-Kirches, M., Schneider, T., Weis, S., Krause, G., Mawrin, C. and Dietzmann, K. (2001) Heterogeneous tissue distribution of a mitochondrial DNA polymorphism in heteroplasmic subjects without mitochondrial disorders. *J.Med.Genet.*, 38, 312-317.
34. Ruvinsky, I. and Meyuhas, O. (2006) Ribosomal protein S6 phosphorylation: from protein synthesis to cell size. *Trends Biochem.Sci.*, 31, 342-348.





# 6

General discussion



## Introduction

The multicopy 16.569 bp circular DNA of the mitochondrial compartment codes for 13 of the ~90 protein subunits of the oxidative phosphorylation system and 24 RNAs involved in mitochondrial protein synthesis of these 13 protein subunits. mtDNA mutates at a rate 5–10 fold higher than nuclear DNA. Deleterious mutations in mtDNA, be it in tRNA, rRNA or protein coding regions, will affect oxidative phosphorylation. However, this will only become overt at the cellular level if the mutation is present in the majority of the cell's mtDNA molecules. A remarkable feature of inherited mtDNA diseases is that a specific mtDNA point mutation can express in highly variable clinical phenotypes. This is remarkable because mtDNA mutations are assumed to segregate randomly from the fertilized heteroplasmic oocyte onwards, predicting much more common disease phenotypes. It has been proposed that non-random, but as yet enigmatic segregation mechanisms are responsible for variable disease expression. In recent years it has become apparent that mtDNAs are organized in so-called nucleoids with multiple mtDNAs per nucleoid (1-3), but only little is known how this organization impacts on segregation of mtDNA mutations (2). While it is indeed evident that mtDNA mutation accumulation needs to occur, it has also been suggested that variability in disease expression may result from aberrant mtDNA gene products, interacting in complex ways with the mitochondrial-nuclear cross-talk and thus affecting tissues and cells in different ways with –to complicate things further– influences from the nuclear genetic background and mtDNA haplotype. A highly relevant mtDNA mutation in this ‘one mutation-many phenotypes’ respect is the A3243G mutation in the *MTTL-1* encoding mt-tRNA-Leu<sup>(UR)</sup> (4).

The goal of this Thesis has been to shed more light on the complex pathways from the pathogenic A3243G mtDNA mutation to the phenotypical consequences by conducting,

with well defined *in vitro* cell culture models of the A3243G mtDNA mutation, segregation research and whole genome expression analysis for characterization of mitochondria-to-nucleus signaling. Ideally one would of course conduct such research with *in vivo* systems such as a mouse model, but manipulation of mtDNA *in vivo* is impossible. This explains the lack of animal models for the A3243G and other deleterious mtDNA mutations, although prospects are good for mouse models that are heteroplasmic for pathogenic point mutation (see below).

## Methods for analysis of mitotic A3243G mtDNA segregation

mtDNA segregation research requires single cell mutation analysis so as to be able to follow cellular mtDNA inheritance patterns. To get sufficient data, many individual cells need to be analyzed, e.g. in serial passages. Thus a high throughput assay needed to be developed. The relatively large number of mtDNA molecules in a cell readily allows single PCR amplification of the mtDNA region of interest, but the characteristics of the A3243G mutation (an A to G transition, a GC-rich environment and location in a region prone to hairpin formation), however, prohibited closed-tube fluorescent PCR assays on basis of Molecular Beacons or Taqman probes.

Polymerase Chain Reaction - Restriction Fragment Length Polymorphisms (PCR-RFLP) is a time honored mutation detection technology and has often been applied for A3243G mutation detection and quantization on bulk DNA. The procedure involves in the final manual steps, restriction enzyme digestions, gel electrophoresis, optionally Southern hybridization and image analysis. The workload inherent to such techniques, however, severely limits throughput. We therefore developed two alternative strategies. One is based on PCR-RFLP, but by-passes electrophoresis. It uses melting temperature characteristics of the PCR fragments to detect and quantify the mutation level after single cell PCR; hence it is referred to as PCR-RFMT.



The only compromise of PCR-RFMT to a closed tube-assay is the one time addition of the restriction enzyme. The other method is an *in situ* approach. It uses the high sensitivity of DNA ligases to mismatches in a padlock hybridization strategy. Additionally it uses  $\phi$ 29 DNA polymerase mediated rolling circle amplification of the circularized padlock for detection of wild-type and mutant mtDNA molecules *in situ* and automated image analysis for quantitation purposes. Both methods have the requisite throughput and are of sufficient accuracy (Standard Deviations of ~5%) for single cell-based segregation analysis. In the 0 – 25% mutation load range, however, PCR-RFMT is less accurate than padlock/RCA due to the square root relation between the measured and actual mutant load.

### **Suppressed and quantal mitotic A3243G segregation *in vitro***

With these newly developed methods it was shown with heteroplasmic cybrid cultures that the mutation load of descendants of three founder cells heteroplasmic for the A3243G mutation did not change mutation load, while computer simulations of random mitotic segregation showed that considerable changes should have occurred in consecutive passages of the three clones (see page 40, H3). This supports the faithful replicating or stable nucleoid model described by Jacobs *et al.* (5). With a fourth A3243G clone (V\_50), discrete or ‘quantal’ shifts in mutation load occurred. Such a pattern is also incompatible with random segregation. To explain the stable heteroplasmy and the discrete shifts, we postulated the mitochondrial nucleoid to be a genetically meta-stable segregation unit. This implies that most of the time the nucleoid is in a stable phase, replicating its mutation load faithfully and thereby effectively suppressing segregation. When occasionally in an unstable phase, genetic rearrangements or unfaithful replication gives rise to nucleoids of altered heteroplasmy which rapidly segregate randomly to daughter

cells to yield descendant cells of variable, but discrete heteroplasmy levels. We provided arguments that nuclear determined growth advantage enables us to see the significant subpopulation with altered heteroplasmy. As indicated in Chapter 3, a second series of long term segregation experiments has been initiated. To this end cells of passage 42 of V\_50 were sub-cloned and analyzed up to passage ~100, expecting some of them to be stable and some to shift to either wild type or mutant. Figure 1 shows preliminary results of two subclones. Subclone V\_3.2 (mtDNA copy number is ~1800) hardly showed change in cellular mutation loads from passage 1 up to 81 while according to random segregation model it should. V\_3.18 proved unstable. It shifted, in contrast to V\_50, toward mutant. Cells in passage 1 peaked at 35-45% heteroplasmy; cells in passage 63 at 65-75%. These observations substantially strengthen the notion that the nucleoid is metastable and that it is a nuclear, not mitochondrial determined growth advantage that enables us to see significant subpopulations of cells with a given altered heteroplasmy as it is very unlikely that increasing mtDNA mutation loads provide growth advantage. From the pattern seen with V\_3.18 it is inferred that early in the outgrowth of the founding V\_3.18 cell, nucleoids with a higher heteroplasmy emerged that following their segregation ‘hitchhiked’ with cells having slight nuclear determined growth advantages. Literature indicates that physically 8-10 mtDNA molecules are present per nucleoid in the 143B cells used here. The heteroplasmy levels found in this thesis are compatible with this estimate, but more work is needed to arrive at the exact ‘quantal’ number, to document cell type dependence and to answer the question whether or not the meta-stable nucleoid model holds for neutral and other pathogenic mtDNA mutations.

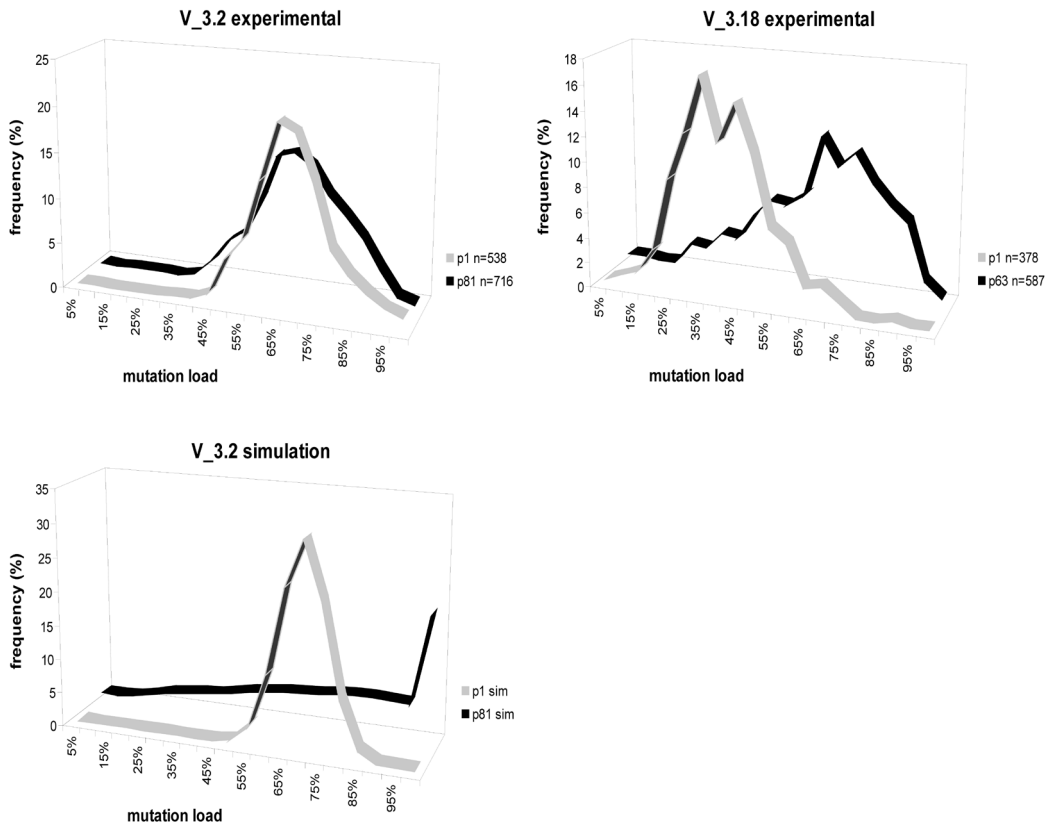


Figure 1: Single cell mutation load histograms of A3243G heteroplasmic mtDNA of two 143B transmitochondrial cybrid subclones derived from clone V\_50 passage 42. For the experimentally generated graphs the mutation loads (x-axis) of individual cells were measured by Padlock/RCA as described in Chapter 2 relative amount of cells are shown (z-axis) for two, far separated, passages (y-axis).

V\_3.2 (~1800 mtDNAs per cell) is a stable clone with a mutation load peak in the 65-70% bin at both passage 1 and passage 81, corresponding to 40 weeks of culturing. As comparison a simulation was run for the random segregation model, starting from a single cell with a mutation load corresponding to the average mutation load of V\_3.2 in passage 1 and 2000 mtDNAs. Note the considerable percentage of homoplasmic mutant cells in the simulation of passage 81.

V\_3.18 is an unstable clone which shows cellular heteroplasmy shifts towards mutant, in contrast to clone V\_50 which showed drift towards wild type. The peak for V\_3.18 at passage 1 is in the 35-45 % and at passage 63 in the 65-75 % range.

## **A role for nucleoids *in vivo*?**

The *in vitro* observations described in this Thesis strongly indicate that non-segregation (segregation suppression) rather than random segregation is the rule for mtDNA. An *in vivo* consequence of segregation suppression mediated by nucleoids would be that it provides for an alternative mechanism of maintaining mtDNA genotypical integrity in the face of high mutation rates for mtDNA (5). A faithfully replicating nucleoid can indeed accommodate many different mutations without giving descendants of high heteroplasmy. The classical view is that the relative high copy number of mtDNA protects descendant cells against mtDNA mutation accumulation by random genetic drift of naked mtDNA molecules, but this protection is more limited. It will require pathogenic heteroplasmic mouse model studies to objectively make distinction between the two views of protection against mtDNA mutation accumulation. The mtDNA mutator mouse which accumulates mtDNA mutations (and suffers from a wide range of age-associated conditions) provides a means to construct pathogenic heteroplasmic mouse models, because it allowed for the first time introduction of random mutations in the mtDNA (6-8). To generate heteroplasmic mouse models, female mutator mice can be crossed to male wild-type mice to obtain mouse strains carrying specific mtDNA mutations because of the (elusive) mitochondrial bottleneck in early embryogenesis (Larsson NG, personal communication).

In view of the large size of the germline mtDNA bottle neck recently reported in mice (9), it is tempting to speculate that genetic reorganization of nucleoids in early embryogenesis lies at the heart of the 'bottle neck'. Heteroplasmic mouse models with GFP marked germ line cells in combination with quantitative *in situ* genotyping methods such as padlock/RCA may provide the means to test the idea of a developmentally controlled reorganization of nucleoids.

Similarly, such mice and methodology will allow the study of the role of nucleoid (re) organization in pathogenic mtDNA segregation in somatic cells and tissues.

## **Mitochondrial-nuclear crosstalk in A3243G cybrid cells**

Next to mutation accumulation by still elusive segregation mechanisms, it has been suggested that mtDNA disease expression is modulated by aberrant mtDNA gene products, interacting in complex ways with the mitochondrial-nuclear cross-talk and thus affecting tissues and cells in different ways. To obtain insight in effects of A3243G mutations on the nuclear expression profile we conducted genome-wide expression studies of A3243G cell clones that are respiration deficient and proficient. Results with our well defined *in vitro* cell modelled us to conclude that the number of genes changed  $\geq 1.5$ -fold in expression is minimal, indicating that adaptation of the nuclear transcription program to loss of mitochondrial respiration because of A3243G mutation accumulation are more subtle. Much more differential gene expression was found when two haplogroups were compared, a fact that may indicate that mtDNA sequence variants can modulate phenotypic expression.

## **Global translational repression**

The fact that, given the sensitivity of the expression analysis, no nuclear response to loss of respiration was observed, prompted us to investigate post-transcriptional responses of the A3243G mtDNA mutation. A strong effect on global protein synthesis rates was consistently observed. In terms of disease development where mitochondrial dysfunction is implicated, such as diabetes, this finding is of great significance. Pancreatic  $\beta$ -cells are the most active protein synthesizing cells, demanding vast amounts of energy. Obviously translation of preproinsulin mRNA is a major

task of the  $\beta$ -cell's protein synthesis machinery and the process uses 25 to 30% of all ATPs produced. Thus a mitochondrial dysfunction in a pancreatic  $\beta$ -cell, be it by accumulation of inherited or acquired mtDNA mutation or by environmental or dietary factors, will negatively affect insulin production. In fact it acts as a double edged sword: it also derails glucose-stimulated insulin secretion because of its strong dependence on increased mitochondrial ATP production in response to elevated blood glucose levels. With ATP levels marginally affected in A3243G cells, it was obvious that signalling from the defective mitochondria to the cytosolic protein synthesis machinery must occur. Screening a number of translation factor candidates for phosphorylation, identified elongation factor 2 (eEF-2) and initiation factor 2 $\alpha$  (eIF-2 $\alpha$ ) as effector targets of the signaling pathway (Janssen *et al.*, in preparation). Phosphorylation of eIF-2 $\alpha$  leads to translation inhibition by preventing initiation. Of its four known kinases, PERK which is activated upon ER-stress (10), is the most likely candidate, because extensive mitochondrial-endoplasmatic interactions are known to exist and their perturbation lead to ER-stress (11;12). eEF2 is the translation factor that controls the most energy demanding step of translation: elongation (4 ATP equivalents per peptide bond). Phosphorylation of eEF2 by its only known kinase (eEF2kinase) leads to inhibition of protein synthesis. eEF-2 kinase is regulated directly (13) as well as indirectly (via mTOR) by the cellular energy sensor AMP-kinase, which indeed was found activated (Janssen *et al.*, in preparation). In all, these results show the importance of translational control in response to loss of mitochondrial respiratory function

### Concluding remarks

By development and application of newly developed methods for single cell A3243G mtDNA heteroplasmy measurements, it was found that segregation of mtDNA as a rule

is absent in *in vitro* cultured A3243G cybrid cells. The nucleoid, a mitochondrial matrix nucleoprotein complex carrying 8-10 mtDNA molecules, likely mediates this segregation suppression by faithfully replicating its mutant/wild type ratio. Occasionally discrete shifts in heteroplasmy were observed, suggesting that a transient genetic rearrangement of the nucleoid may underlie segregation. Subtle differences in nuclear mRNA expression profiles between respiratory deficient and proficient A3243G cells likely prevented us from identifying genes that are implied in signaling from defective mitochondria to the nucleus. Thus at the nuclear transcriptional level no leads were found to tissue and cell type specific responses that may help explain variation in phenotype of A3243G mtDNA diseases. However, global repression of cytosolic translation, mediated by at least two translation factors, was identified as a major adaptation to loss of respiration. This may indicate an important role for translational control mechanisms in response to loss of mitochondrial respiratory function.

## Reference List

1. Legros,F., Malka,F., Frachon,P., Lombes,A. and Rojo,M. (2004) Organization and dynamics of human mitochondrial DNA. *J.Cell Sci.*, 117, 2653-2662.
2. Iborra,F.J., Kimura,H. and Cook,P.R. (2004) The functional organization of mitochondrial genomes in human cells. *BMC.Biol.*, 2, 9.
3. Garrido,N., Griparic,L., Jokitalo,E., Wartiovaara,J., van der Blik,A.M. and Spelbrink,J.N. (2003) Composition and dynamics of human mitochondrial nucleoids. *Mol.Biol.Cell*, 14, 1583-1596.
4. Finsterer,J. (2007) Genetic, pathogenetic, and phenotypic implications of the mitochondrial A3243G tRNA<sup>Leu</sup>(UUR) mutation. *Acta Neurol.Scand.*, 116, 1-14.
5. Jacobs,H.T., Lehtinen,S.K. and Spelbrink,J.N. (2000) No sex please, we're mitochondria: a hypothesis on the somatic unit of inheritance of mammalian mtDNA. *Bioessays*, 22, 564-572.
6. Kujoth,G.C., Hiona,A., Pugh,T.D., Someya,S., Panzer,K., Wohlgemuth,S.E., Hofer,T., Seo,A.Y., Sullivan,R., Jobling,W.A. et al. (2005) Mitochondrial DNA mutations, oxidative stress, and apoptosis in mammalian aging. *Science*, 309, 481-484.
7. Larsson,N.G., Wang,J., Wilhelmsson,H., Oldfors,A., Rustin,P., Lewandoski,M., Barsh,G.S. and Clayton,D.A. (1998) Mitochondrial transcription factor A is necessary for mtDNA maintenance and embryogenesis in mice. *Nat.Genet.*, 18, 231-236.
8. Trifunovic,A., Wredenberg,A., Falkenberg,M., Spelbrink,J.N., Rovio,A.T., Bruder,C.E., Bohlooly,Y., Gidlof,S., Oldfors,A., Wibom,R. et al. (2004) Premature ageing in mice expressing defective mitochondrial DNA polymerase. *Nature*, 429, 417-423.
9. Cao,L., Shitara,H., Horii,T., Nagao,Y., Imai,H., Abe,K., Hara,T., Hayashi,J.I. and Yonekawa,H. (2007) The mitochondrial bottleneck occurs without reduction of mtDNA content in female mouse germ cells. *Nat. Genet.*, 39, 386-390
10. Gebauer,F. and Hentze,M.W. (2004) Molecular mechanisms of translational control. *Nat.Rev.Mol. Cell Biol.*, 5, 827-835.
11. Simmen,T., Aslan,J.E., Blagoveshchenskaya,A.D., Thomas,L., Wan,L., Xiang,Y., Feliciangeli,S. F., Hung,C.H., Crump,C.M. and Thomas,G. (2005) PACS-2 controls endoplasmic reticulum-mitochondria communication and Bid-mediated apoptosis. *EMBO J*, 24, 717-729.
12. Pizzo,P. and Pozzan,T. (2007) Mitochondria-endoplasmic reticulum choreography: structure and signaling dynamics. *Trends Cell Biol.*, 17, 511-517.
13. Browne,G.J., Finn,S.G. and Proud,C.G. (2004) Stimulation of the AMP-activated protein kinase leads to activation of eukaryotic elongation factor 2 kinase and to its phosphorylation at a novel site, serine 398. *J Biol.Chem.*, 279, 12220-12231.



Appendices



## Summary

Mitochondria are involved in a number of cellular processes of which energy metabolism, notably oxidative phosphorylation, is an important one. Oxidative phosphorylation accounts for ~80% of cellular ATP production and occurs in the mitochondrial inner membrane. The ~90 protein subunits of the 5 Complexes involved in this process are mostly nuclear encoded, but 13 of them are encoded on mitochondrial DNA (mtDNA). Next to these protein genes, the mitochondrial DNA codes for 22 mitochondrial tRNAs and 2 rRNAs, which are essential for translation of the 13 mtDNA encoded mRNAs. Mutations in these 37 mtDNA genes can cause disease. Remarkably, one specific mtDNA mutation can cause different syndromes. A relevant example is the A3243G mutation. This mutation is in the *MMTL-1* gene, coding for tRNA-leu<sup>(UUR)</sup>, and associates with Maternally Inherited Diabetes and Deafness (MIDD), but it is also causes Mitochondrial Myopathy Encephalopathy Lactic Acidosis and Stroke-like episodes (MELAS) as well as Chronic Progressive External Ophthalmoplegia (CPEO).

A cell may contain 100s to 1000s of maternally inherited mtDNA molecules and a mutation can occur in all or in a fraction of the mtDNAs. Above a given threshold of mutation load (heteroplasmy) cells will stop producing mitochondrial ATP. Accumulation of the A3243G mutation can therefore lead to energy stress and consequently be a cause of cell and organ dysfunction. To explain clinical heterogeneity, it has been proposed that in interaction with the nuclear genome, tissue and cell specific effects cause diversity in accumulation of the A3243G mtDNA mutation. It has also been suggested that signalling from defective mitochondria to the nuclear expression program (the retrograde response) underlies diversity of the clinical phenotypes, but mechanisms and relative contributions of these not mutually exclusive processes are elusive. This thesis attempted to contribute to a better understanding of these processes by studying segregation mechanisms underlying mutation accumulation as well as by studying which nuclear genes and cellular processes alter expression under A3243G mtDNA mutation. To this end transmitochondrial cybrids clones have been used: cells in which the original mtDNA is replaced by mtDNA from A3243G carriers in a homoplasmic or heteroplasmic fashion.

With respect to mtDNA mutation accumulation, it has become clear in recent years, that mtDNAs do not occur in the cell as single mtDNA molecules but that they are organized in so-called nucleoids, with multiple mtDNAs being present in a nucleoid. How heteroplasmy is accommodated by this nucleoid organization and how it mediates mtDNA segregation is poorly understood.

A few studies reported, by bulk DNA analysis, stable heteroplasmy in long term, non-selective cultures of A3243G cybrid clones, but also heteroplasmy shifts to either wild type or mutant were seen. By single cell mutation analysis at a time point where random segregation should have been obvious by appearance of homoplasmic cells (genetic fixation), it was found in one study that the individual cells of stable clones still had the original heteroplasmy; they had not segregated their mtDNAs. It led to the concept of a multi-copy mtDNA segregation unit, the nucleoid, that is heteroplasmic itself and that replicates its wild type/mutant content faithfully. To explain changes in heteroplasmy, as occurs in shifting cybrid clones, it was speculated that the faithfully replicating nucleoid may occasionally reorganize its wild type/mutant ratio, possibly under genetic control. Likely due to lack of semi-high throughput single cell mutation load measurements, experimental evidence for this meta-stability of nucleoids lying at the base of segregation in shifting A3243G clones is however absent.

Chapter 2 describes development of two methods to determine the A3243G mutation load of single cells in relatively high-throughput.



The hybridization-based methods are concerned with a difficult AG transition. The AT bond of the wild type/wild type hybrid is energetically comparable to the GT mismatch and the mutation is located in a GC-rich environment that additionally is prone to hairpin formation. Because of these limitations, single cell PCR based Taqman or Molecular Beacon assays were not feasible. Two alternatives were, however, successfully developed in Chapter 2. One is based on PCR-RFLP of single sorted cells. Instead of gel-based analysis it uses the melt characteristics of the restriction fragments to quantify mutation loads. The other is a bi-colour *in situ* genotyping approach that uses so-called padlock probing in combination with rolling circle amplification for detection of the genotypes as red and green dots and image analysis for their quantitation. Both methods perform equally well in terms of throughput and accuracy.

In Chapter 3 (and 6) the methods were applied to shifting and stable A3243G cybrid clones, cultured under non-selective conditions. When analyzed at the single cell level the shifting clones (one to wild type, one to mutant) proved to show discrete shifts in cellular heteroplasmy. This can not be easily reconciled with a random segregation mechanism, not even in combination with replicative mtDNA advantages and cellular selection. As illustrated in Figure 3 of Chapter 3 appearance of cells with an altered heteroplasmy can be explained with the meta-stable nucleoid model. The meta-stable nucleoid model predicts that clones can dwell in a state of non-segregation for extended periods of time. Support for this stable element of the model came from 4 additional clones analyzed: experimentally generated histograms of mutation loads were compared with computer simulated histograms generated on basis of a random mtDNA segregation model. The individual cells in these clones maintained heteroplasmy much longer than expected on basis of random segregation, pinpointing to considerable genetic stability of the heteroplasmic segregation unit. These experimental results indicated for the first time how nucleoids can mediate mtDNA segregation.

The nuclear gene expression pattern is influenced by many factors and the cell's demand for energy is amongst them. If and how the A3243G mtDNA mutation, at heteroplasmy levels that compromise energy metabolism, is redirecting the nuclear genome's expression profile has been examined in the cybrid system with mtDNA sequence variation being in principle the only variable. By the use of a DNA chip permitting analysis of 22.283 gene transcripts simultaneously, the gene expression profiles of cybrids heteroplasmic and homoplasmic for the A3243G mutation in two different mtDNA haplogroup backgrounds were compared in Chapters 4 and 5. Thus comparisons on basis of respiration status and haplogroup could be made independently. Where it stood to reason that substantial RNA gene expression differences are present between respiring and non-respiring cell hardly any > 1.5 fold changes were found when their profiles were compared. In sharp contrast hundreds of differences were found when comparing cells with the different mitochondrial DNA haplogroups. This indicates that the haplotype can as such affect nuclear gene expression. The fact that in the respiratory status comparison hardly any changes were found indicated that, in the cybrid system, adaptations of the nuclear expression profile to the loss of mitochondrial ATP production were either too small to be identified by our analytical approach or that these cells have adapted by post-transcriptional mechanisms. Indeed global translational repression appeared to be a major adaptive (energy saving) pathway. This repression is mediated by phosphorylation of Elongation factor 2 (eEF-2) and initiation factor 2 $\alpha$  (eIF-2 $\alpha$ ). Upstream of eEF-2 is eEF-2 kinase which is activated by the cell's energy sensor AMP-activated kinase (AMPK). Importantly, the eIF-2 $\alpha$  phosphorylation indicates involvement of the endoplasmic reticulum resident kinase PERK and identifies ER-mitochondrion interactions in energy stress sensing, independent of the AMPK route.

In conclusion, likely due to low level changes in gene expression, no genes or gene sets could be identified with gene wide expression analysis that would hint to the molecular pathways that are altered upon loss of mitochondrial ATP production as a consequence of A3243G mtDNA mutation. Extensive post-transcriptional adaptation in the form of global translation repression, was however apparent. A comparison between two mtDNA haplotypes indicated, that these presumably neutral sequence variants can affect the nuclear expression program, which tentatively indicates that mtDNA haplotype can affect phenotype.

Finally, using newly developed single cell A3243G mutation load assays a novel mechanism of mtDNA segregation was identified in which the multi-copy mtDNA nucleoid takes a central position.



## Samenvatting

Mitochondriën zijn betrokken bij verschillende cellulaire processen waarvan energie metabolisme, met name oxidatieve fosforylering, een belangrijke is. Oxidatieve fosforylering neemt zo'n 80% van de cellulaire energieproductie in de vorm van ATP voor z'n rekening en vindt plaats in het mitochondriële binnenmembraan. De genetisch code van de meerderheid van de ~90 eiwit subeenheden van de 5 complexen betrokken bij dit proces is in het kern DNA vastgelegd, maar 13 subeenheden zijn op het mitochondriël DNA (mtDNA) gecodeerd. Naast deze eiwitgenen bevat het mtDNA de codes voor 22 mitochondriële tRNAs en 2 rRNAs, die essentieel zijn voor de translatie van de 13 mitochondriële mRNAs. Mutaties in deze 37 mtDNA genen kunnen ziekten veroorzaken. Opmerkelijk daarbij is dat één specifieke mutatie verschillende ziektebeelden kan veroorzaken (klinische heterogeniteit). Een relevant voorbeeld is de A naar G transitie op locatie 3243. Deze mutatie bevindt zich in het *MTTL-1* gen, dat codeert voor het tRNA-Leu<sup>(UUR)</sup> en associeert met een bepaalde vorm van diabetes (MIDD: Maternally Inherited Diabetes and Deafness), maar ook met aandoeningen aan het neuro-musculaire systeem (MELAS: Mitochondrial Myopathy Encephalopathy Lactic Acidosis and Stroke-like episodes) en de oogzenuw (CPEO: Chronic Progressive External Ophthalmoplegia).

Een cel kan honderden tot duizenden van de moeder geërfd mtDNA moleculen bevatten en een mutatie kan in alle of in een gedeelte van de mtDNAs voorkomen. Boven een bepaalde grenswaarde van de mutatiegraad (heteroplasmie) zullen de cellen stoppen met het produceren van mitochondriël ATP. Ophoping van de A3243G mutatie kan dus leiden tot energie stress en daarmee tot disfunctie van cellen en organen. Om de klinische heterogeniteit te verklaren is er voorgesteld dat weefsel- en cel specifieke effecten, in combinatie met de werking van het kern genoom, verscheidenheid in ophoping van de A3243G mtDNA mutatie kunnen veroorzaken. Daarnaast wordt er gedacht dat signalen van niet goed functionerende mitochondriën naar de kern (de retrograde respons) aan de verscheidenheid van klinische fenotypen ten grondslag liggen. De mechanismen en relatieve bijdragen van deze elkaar niet uitsluitende processen zijn onduidelijk. Dit proefschrift probeert bij te dragen aan een beter begrip van deze processen door het bestuderen van enerzijds segregatie-mechanismen die mutatieophoping veroorzaken en anderzijds de expressie veranderingen van kerngenen en cellulaire processen die optreden ten gevolge van A3243G mtDNA mutatie. Hiervoor is er gebruik gemaakt van cybride cellen: cellen waarin het originele mtDNA is vervangen door homoplastisch dan wel heteroplastisch mtDNA van dragers van de A3243G mtDNA mutatie.

Het is de laatste jaren duidelijk geworden dat mtDNAs niet als losse moleculen in de cel voorkomen, maar dat ze georganiseerd zijn als groepjes in eiwit-DNA structuren die nucleoiden genoemd worden. Of en hoe deze nucleoiden zelf heteroplastisch zijn en hoe ze bijdragen aan mtDNA segregatie is echter onduidelijk. Enkele studies rapporteren, door analyses van het gemiddelde mutatieniveau, stabiele heteroplasmie tijdens het langdurig en niet-selectief kweken van A3243G cybride klonen, maar onder deze omstandigheden zijn er ook veranderingen in heteroplasmie niveau richting zowel wild type als mutant gevonden. Door middel van analyse van de mutatiegraad in individuele cellen op een tijdstip dat er volgens een segregatie mechanisme op basis van willekeur homoplastische cellen aanwezig zouden moeten zijn (het principe van genetische fixatie), is er in slechts één studie gevonden dat de cellen hun mtDNA niet segregeren, maar de originele mutatiegraad behouden. Dit heeft geleid tot het concept van een segregatie-eenheid met meerdere mtDNAs, het nucleoid, dat zelf heteroplastisch is en de wildtype/mutant sequentie tijdens replicatie exact behoudt. Om veranderingen in heteroplasmie te verklaren is er gespeculeerd dat het betrouwbaar replicerende nucleoid bij tijd en wijle de wild type/mutant ratio kan veranderen, mogelijk onder invloed van een genetisch programma.

Waarschijnlijk ten gevolge van gebrek aan individuele cel mutatiegraad metingen op grote schaal, is de experimentele bewijsvoering voor meta-stabiele nucleoiden als basis voor segregatie in veranderende A3243G klonen echter nog niet geleverd.

Hoofdstuk 2 beschrijft de ontwikkeling van twee methoden om de A3243G mutatiegraad te bepalen in individuele cellen op een relatief grote schaal. Op hybridisatie gebaseerde methoden moeten in dit geval werken met een lastige A naar G transitie. De AT binding van het wildtype/wildtype hybride is namelijk energetisch vergelijkbaar met de GT binding van het mutant/wildtype hybride, en daarnaast is de mutatie gelokaliseerd in een GC-rijke omgeving die ook nog eens makkelijk een secundaire structuur vormt. Vanwege deze beperkingen zijn op Taqman of Molecular Beacons gebaseerde PCR benaderingen niet haalbaar gebleken. Twee alternatieven zijn echter met succes ontwikkeld in hoofdstuk 2. Een methode is gebaseerd op PCR-RFLP van het mtDNA van individueel gesorteerde cellen. Hierbij wordt voor de kwantificering in plaats van de gebruikelijke gel-analyse gebruik gemaakt van de smelt-eigenschappen van de restrictie fragmenten. De andere methode is een twee-kleurige *in situ* genotypering, waarbij zogenaamde padlock probes in combinatie met rolling circle amplification worden gebruikt voor detectie van de genotypen. De genotypen worden als rode en groene stippen zichtbaar en door middel van beeldanalyse gekwantificeerd. Beide methoden voldoen goed in termen van snelheid en nauwkeurigheid.

In hoofdstuk 3 (en 6) zijn de methoden, toegepast bij A3243G cybride klonen die onder neutrale condities in continue kweek zijn gebracht. Metingen op individueel celniveau van klonen, die in gemiddelde mutatiegraad veranderden (een richting wild type en een richting mutant) laten discrete veranderingen zien in cellulaire heteroplasmie. Dit feit kan niet eenvoudig worden verklaard met een random segregatie mechanisme, zelfs niet in combinatie met mtDNA replicatie voordeel en cellulaire selectie. Zoals getoond in figuur 3 van hoofdstuk 3, kan het voorkomen van cellen met een veranderende mutatiegraad verklaard worden met het genoemde meta-stabiele nucleoid model.

Dit model voorspelt dat heteroplastische klonen gedurende langere tijd segregatie kunnen vermijden. Onderbouwing van dit stabiele element van het model is verkregen met de analyse van vier extra klonen, waarbij de experimenteel gegenereerde histogrammen voor mutatiegraad vergeleken zijn met computer gesimuleerde histogrammen uitgaande van een random segregatie model. De individuele cellen in deze vier klonen behielden de originele mutatiegraad veel langer dan verwacht op basis van random segregatie, wat duidt op significante genetische stabiliteit van het nucleoid als heteroplastische segregatie-eenheid. Deze experimentele resultaten geven voor het eerst aan hoe nucleoiden heteroplasmie accommoderen en segregatie kunnen beïnvloeden.

Het nucleaire expressie patroon is een resultaat van vele factoren, waarvan de energie-behoefte van de cel er een is. Of en hoe de A3243G mutatie, bij zo'n hoge heteroplasmie dat het energie metabolisme is aangedaan, het nucleair expressie patroon veranderd, is onderzocht in het cybride systeem waarbij de mtDNA sequentie in principe de enige variabele is. Gebruik makend van een DNA chip waarmee 22.283 gen transcripten tegelijkertijd geanalyseerd kunnen worden, is in hoofdstukken 4 en 5 het genexpressie profiel van heteroplastische en homoplastische A3243G cybriden in combinatie met twee verschillende mtDNA haplotypes vergeleken. Dus onafhankelijk van elkaar konden vergelijkingen gemaakt worden op basis van ademhalingscapaciteit (een maat voor oxidatieve fosforylering) en haplogroep. Tegen de verwachting in zijn er nauwelijks verschillen in RNA expressie gevonden van 1,5 keer of meer tussen wel en niet ademhalende cellen. Dit staat in tegenstelling tot de honderden verschillen die gevonden zijn in de vergelijking van de twee mitochondriële haplogroepen, wat een indicatie geeft dat het haplotype op zich het nucleaire gen expressie patroon zou kunnen beïnvloeden.

Het feit dat in het ademhalingsvergelijk nauwelijks verschillen zijn gevonden geeft aan dat, in het cybride systeem, aanpassingen aan het nucleaire expressie profiel ten gevolge van het verlies aan mitochondriëel ATP productie te klein waren om door onze analyse te worden geïdentificeerd of dat deze cellen zich post-transcriptioneel hebben aangepast. Algemene translatie remming blijkt inderdaad een belangrijke energie-besparende pathway. Deze remming wordt beïnvloed door fosforylering van Elongation factor 2 (eEF-2) en initiation factor 2 $\alpha$  (eIF-2 $\alpha$ ). Upstream van eEF2 bevindt zich eEF2-kinase welke geactiveerd wordt door het AMPK-geactiveerd kinase (AMPK), de energie-sensor van de cel. Fosforylering van eIF-2 $\alpha$  duidt op betrokkenheid van het endoplasmatisch reticulum kinase PERK en identificeert interactie tussen het ER en mitochondriën onafhankelijk van AMPK als energie stress sensor.

Concluderend, waarschijnlijk door kleine veranderingen in gen expressie niveau's zijn er geen moleculaire processen gevonden die betrokken zijn bij de reactie op verlies van mitochondriële ATP productie door de A3243G mtDNA mutatie. Wel is een duidelijke post-transcriptionele aanpassing in de vorm van algemene translatie remming vastgesteld. Vergelijking van twee mtDNA haplogroepen wijst er verder op dat neutraal veronderstelde mtDNA sequentie varianten een effect op het nucleaire expressie profiel hebben, wat gevolg zou kunnen hebben op expressie van fenotype. Tenslotte, gebruik makend van zelf ontwikkelde individuele mutatiegraad bepalingen is er een nieuw mechanisme voor mtDNA segregatie gepostuleerd, waarbij het meerdere mtDNAs bevattende nucleoid een centrale rol inneemt.



## Samenvatting voor de leek

Dat elke menselijke cel een kern heeft met daarin erfelijke informatie van de vader en de moeder opgeslagen in het DNA, weet tegenwoordig bijna iedereen. Dat er daarnaast nog een aantal andere organellen of onderdelen in de cel aanwezig zijn, waaronder de mitochondriën, is ook iets wat op de middelbare school geleerd wordt. Mitochondriën zijn de energiecentrales van de cel. Dat deze hun eigen DNA hebben is minder bekend en hoe dat DNA georganiseerd is en aan dochtercellen wordt overgedragen, is iets waar wetenschappers nog onderzoek naar doen.

Elke cel bevat meerdere kopieën mitochondriëel DNA (mtDNA) wat alleen geërfd wordt van moederskant. Omdat er meerdere kopieën in de cellen aanwezig zijn kan het gebeuren dat sommige mtDNA moleculen een mutatie bevatten en andere niet. Dit is een situatie die wordt aangeduid als heteroplasmie, in tegenstelling tot de uniforme homoplastische situatie. Mutaties op mtDNA kunnen tot een breed scala aan ziekten leiden en het meest opmerkelijke is wel dat bijvoorbeeld de mutatie op locatie 3243 voornamelijk tot diabetes leidt maar ook tot ziekten van de zenuwen en de spieren, van de nieren en van het oog. Er zijn meerdere hypothesen over hoe een enkele mutatie tot verschillende ziektebeelden kan leiden en twee worden toegelicht in dit proefschrift. De ene variant gaat ervan uit dat door verschillen die ontstaan tijdens de celdeling, bij het verdelen van het mtDNA over de dochtercellen, het algemene energiedefect tot uiting komt in een specifiek orgaan. De andere variant gaat uit van specifieke signaalroutes die ervoor zorgen dat in de ene cel, bijvoorbeeld een insulineproducerende cel in de alvleesklier, effect optreedt en in andere cellen niet.

Voor de eerste variant is het van belang om te weten hoe de verdeling van het mtDNA over de dochtercellen is georganiseerd. Voor alsnog werd ervan uitgegaan dat de mtDNA moleculen los in de cel liggen en dat de verdeling een willekeurige kansverdeling volgt. In hoofdstuk 2 en 3 wordt beschreven dat dit een erg onwaarschijnlijk model is en dat de mtDNA moleculen voornamelijk voorkomen in clusters die ook tijdens de celdeling blijven bestaan. In hoofdstuk 4 en 5 wordt de tweede variant bekeken door middel van een techniek die de invloed van mitochondriëel DNA op de werking van het kern DNA aan het licht brengt. Het lijkt erop dat als er op dit niveau een effect is dit te ingewikkeld is om een signaalroute te definiëren. Wel blijkt er op een ander niveau duidelijk effect te zijn, namelijk in de route voor het maken van eiwitten. Aangezien heel veel taken van de cel door eiwitten worden uitgevoerd is hiermee een aangrijpingspunt bloot gelegd voor het verklaren van ziekten veroorzaakt door mtDNA mutatie.





## Curriculum Vitae

The author of this thesis was born on the 30th of September 1974 in Heemstede, the Netherlands. She attended secondary school at College Hageveld in Heemstede where she received her diploma in 1994 and started her Chemistry study at the Free University in Amsterdam in 1995. For her biochemistry master she did an internship dedicated to Ribosomal RNA processing in yeast, partly in Amsterdam (Drs. Noor Eppens and Dr. Jaap Venema) and partly in Toulouse, France (Dr. Pierre-Emmanuel Gleizes). Additionally she did an internship in neuroscience at the VU Medical Center with Dr. Freek van Muiswinkel. Her master thesis was on the breast cancer susceptibility genes *BRCA1* and *2*, guided by Dr. Jos Jonkers of the Netherlands Cancer Institute. She worked as student-assistant to the Public Relations Department of the Free University and was treasurer to the board of the students association VCSVU. Beginning of 2002 she finished her masters and started her PhD study at the department of Molecular Cell Biology of the LUMC with Prof. Ton Raap and Prof. Ton Maassen. She attended the Affymetrix meeting 2002 in Amsterdam, the Human Genome Organisation Meeting 2003 in Mexico, the Euromit 2004 in Nijmegen and a course on the Padlock/Rolling Circle Amplification technique in Uppsala, Sweden. In 2005 she gave birth to her daughter Jasmijn and in 2007 her son Quinten was born. She returned to College Hageveld to teach chemistry.

## List of publication

1. Eppens, N.A., Faber, A.W., Rondaij, M., Jahangir, R.S., van Hemert, S., Vos, J.C., Venema, J. and Raue, H.A. (2002) Deletions in the S1 domain of Rrp5p cause processing at a novel site in ITS1 of yeast pre-rRNA that depends on Rex4p. *Nucleic Acids Res.*, 30, 4222-4231.
2. Maassen, J.A., 't Hart, L.M., Van Essen, E., Heine, R.J., Nijpels, G., Jahangir Tafrechi, R.S., Raap, A.K., Janssen, G.M. and Lemkes, H.H. (2004) Mitochondrial diabetes: molecular mechanisms and clinical presentation. *Diabetes*, 53 Suppl 1, S103-S109.
3. Bazuine, M., Carlotti, F., Tafrechi, R.S., Hoeber, R.C. and Maassen, J.A. (2004) Mitogen-activated protein kinase (MAPK) phosphatase-1 and -4 attenuate p38 MAPK during dexamethasone-induced insulin resistance in 3T3-L1 adipocytes. *Mol. Endocrinol.*, 18, 1697-1707.
4. Jahangir Tafrechi, R.S., Svensson, P.J., Janssen, G.M., Szuhai, K., Maassen, J.A. and Raap, A.K. (2005) Distinct nuclear gene expression profiles in cells with mtDNA depletion and homoplasmic A3243G mutation. *Mutat. Res.*, 578, 43-52.
5. Maassen, J.A., Jahangir Tafrechi, R.S., Janssen, G.M., Raap, A.K., Lemkes, H.H. and 't Hart, L.M. (2006) New insights in the molecular pathogenesis of the maternally inherited diabetes and deafness syndrome. *Endocrinol. Metab. Clin. North Am.*, 35, 385-3xi.
6. Allalou, A., van de Rijke, F.M., Jahangir Tafrechi, R.S., Raap, A.K. and Wahlby, C. (2007) Image based measurements of single cell mtDNA mutation load. In: *Image Analysis; Lecture Notes in Computer Science Vol 4522* pp 631-640. Springer Berlin/Heidelberg
7. Jahangir Tafrechi, R.S., van de Rijke, F.M., Allalou, A., Larsson, C., Sloos, W.C., van de, S.M., Wahlby, C., Janssen, G.M. and Raap, A.K. (2007) Single-cell A3243G mitochondrial DNA mutation load assays for segregation analysis. *J. Histochem. Cytochem.*, 55, 1159-1166.